



**REPORT**

# Updated Hydrogeology Modelling

*Meliadine Mine*

Submitted to:

**Agnico Eagle Mines Limited**

Submitted by:

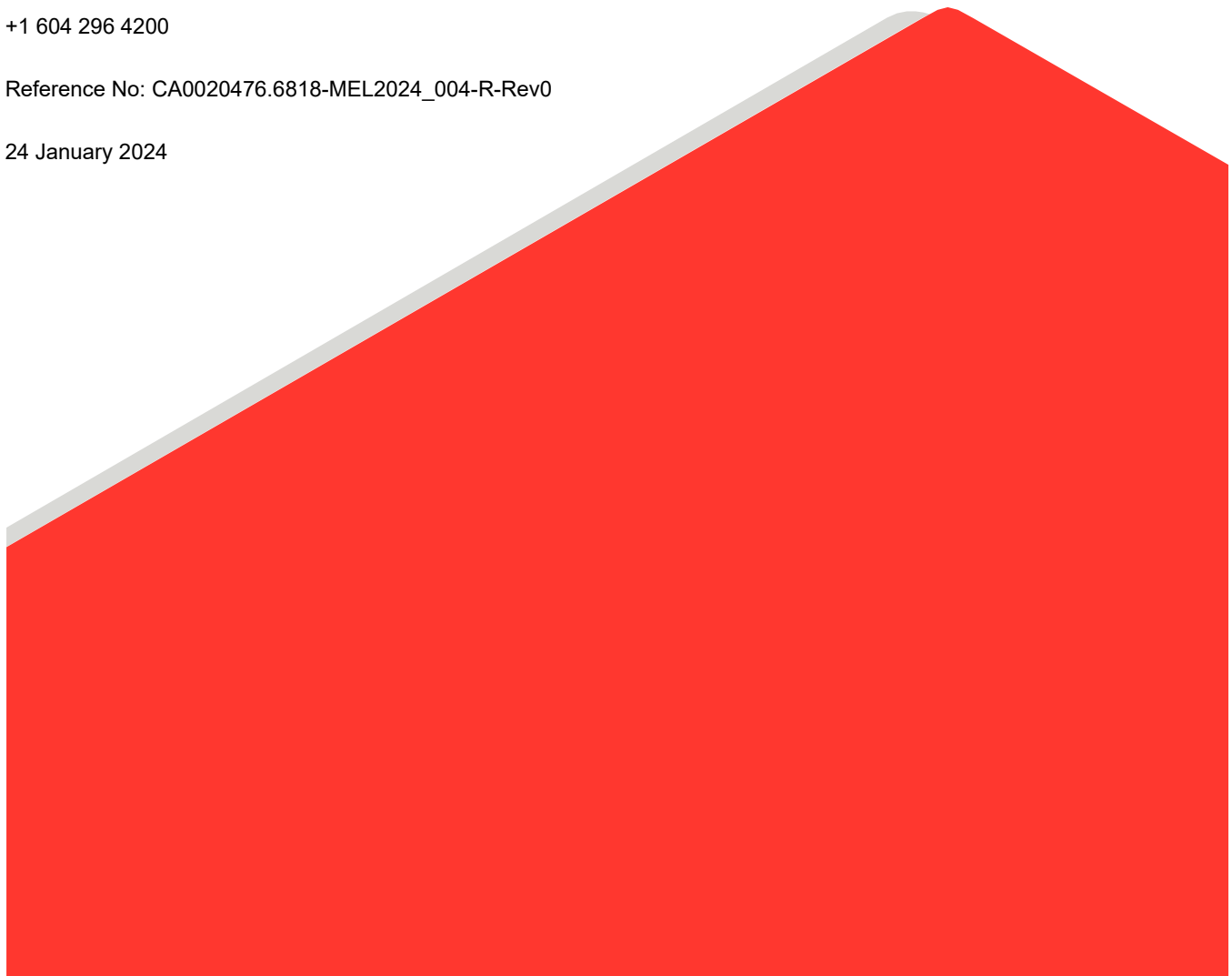
**WSP Canada Inc.**

Suite 200 - 2920 Virtual Way, Vancouver, British Columbia, V5M 0C4, Canada

+1 604 296 4200

Reference No: CA0020476.6818-MEL2024\_004-R-Rev0

24 January 2024



## Distribution List

Electronic Copy - Agnico Eagle Mines Limited

Electronic Copy - WSP Canada Inc..

Electronic Copy - Nuqsana Golder

# Table of Contents

<b>1.0 INTRODUCTION .....</b>	<b>1</b>
<b>2.0 CONCEPTUAL HYDROGEOLOGICAL MODEL .....</b>	<b>2</b>
2.1 Permafrost Depth .....	2
2.2 Hydrostratigraphy .....	4
2.3 Conceptual Groundwater Flow – Pre-Mining .....	7
2.4 Conceptual Groundwater Flow – Existing Conditions .....	14
2.5 Groundwater Flow – Mining .....	14
<b>3.0 NUMERICAL HYDROGEOLOGICAL MODEL .....</b>	<b>16</b>
3.1 Code Selection .....	16
3.2 Model Domain and Discretization .....	17
3.3 Hydrostratigraphy and Initial Model Parameters .....	17
3.4 Mine Schedule .....	21
3.5 Model Boundary Conditions – Flow .....	22
3.6 Model Boundary Conditions – Transport .....	24
<b>4.0 MODEL CALIBRATION .....</b>	<b>26</b>
4.1 Calibration Approach .....	26
4.2 Calibration Targets .....	26
4.3 Calibration Results .....	28
4.3.1 Post-Calibration Hydraulic Parameters .....	28
4.3.2 Measured versus Predicted Hydraulic Head .....	30
4.3.2.1 Flow Recession Test .....	30
4.3.2.2 Long-term Hydraulic Head Monitoring .....	40
4.3.3 Measured versus Predicted Groundwater Inflow .....	40
<b>5.0 BASE CASE MODEL PREDICTIONS .....</b>	<b>45</b>
5.1 Base Case – Predicted Groundwater Inflow .....	45
5.2 Base Case – Predicted Surface Water – Groundwater Interaction .....	49
5.3 Sensitivity Analysis .....	51

5.3.1	Sensitivity Scenarios .....	51
5.3.2	Sensitivity Results and Selection of Upper Bound Scenario .....	51
<b>6.0</b>	<b>UPPER BOUND PREDICTIONS OF GROUNDWATER INFLOW .....</b>	<b>56</b>
<b>7.0</b>	<b>SUMMARY AND CONCLUSIONS .....</b>	<b>58</b>
<b>8.0</b>	<b>CLOSURE .....</b>	<b>59</b>

## TABLES

Table 1: Estimated Hydraulic Properties – Competent Bedrock .....	5
Table 2: Estimated Hydraulic Properties – Enhanced Permeability Zones .....	6
Table 3: Lowest Elevation of Tiriganiaq Underground Mine Development .....	21
Table 4: Post-Calibration Hydraulic Properties – Competent Bedrock .....	28
Table 5: Post-Calibration Hydraulic Properties – Enhanced Permeability Zones .....	29
Table 6: Predicted Groundwater Inflow and TDS Quality to Tiriganiaq Underground Mine – Base Case .....	48
Table 7: Predicted Groundwater-Surface Water Interaction .....	50
Table 8: Comparison of Predicted Inflow to Tiriganiaq Underground Mine Year 2027 .....	52
Table 9: Predicted Upper Bound Groundwater Inflows – Groundwater Inflow, TDS Quality and Lake Water Contributions .....	57

## FIGURES

Figure 1: Groundwater Salinity Profile with Depth .....	3
Figure 2: Hydrogeology Model Extents and Conceptual Regional Groundwater Flow Directions .....	8
Figure 3: Schematic of Conceptual Permafrost and Groundwater Flow Conditions in Areas of Continuous Permafrost .....	9
Figure 4: Pre-Mining Conceptual Groundwater Flow Directions and Distribution of Hydrostratigraphic Units .....	10
Figure 5: Cross-Section View of Pre-Mining Conceptual Groundwater Flow Directions near Tiriganiaq Underground Mine .....	11
Figure 6: Cross-Section View of Pre-Mining Conceptual TDS Concentrations Near Tiriganiaq .....	12
Figure 7: Borehole Locations for Hydraulic Testing and Groundwater Sampling – Main Area .....	13
Figure 8: Cross-Section View of Conceptual Groundwater Flow Directions near Tiriganiaq Underground Mine – Year 2020 (Existing Conditions) .....	15
Figure 9: Finite Element Mesh and Active Model Domain .....	18
Figure 10: Structures of Enhanced Permeability – Main Area and Tiriganiaq-Wolf .....	19
Figure 11: Structures of Enhanced Permeability – Discovery .....	20

Figure 12: Model Boundary Conditions for Groundwater Flow .....	23
Figure 13: Model Boundary Conditions for Transport .....	25
Figure 14: Groundwater Inflow Measurements for the Tiriganiaq Underground Mine .....	27
Figure 15: Borehole Locations for Hydraulic Testing and Groundwater Sampling – KMS Corridor .....	32
Figure 16: Pressure Monitoring Data - Tiriganiaq Underground Mine – Part 1 .....	33
Figure 17: Pressure Monitoring Data - Tiriganiaq Underground Mine – Part 2 .....	34
Figure 18: Pressure Monitoring Data – Tiriganiaq Underground Mine – Part 3 .....	35
Figure 19: Pressure Monitoring Data – Tiriganiaq Underground Mine – Part 4 .....	36
Figure 20: Recession Test Calibration Results PZ-RF-200-01 and PZ-ES225-02 .....	37
Figure 21: Recession Test Calibration Results PZ-ML177-350-161 and PZ-ML375-164 .....	38
Figure 22: Recession Test Calibration Results PZ-ML350-171 and PZ-WH350-152 .....	39
Figure 23: Hydraulic Head Monitoring Calibration Results PZ-RF-200-01 and PZ-ES225-02 .....	41
Figure 24: Hydraulic Head Monitoring Calibration Results PZ-ML177-350-161 and PZ-ML375-164 .....	42
Figure 25: Hydraulic Head Monitoring Calibration Results PZ-ML350-171 and PZ-WH350-152 .....	43
Figure 26: Measured versus Predicted Groundwater Inflow to Tiriganiaq Underground Mine .....	44
Figure 27: Predicted Hydraulic Heads End of Year 2031 Final Year of Mining at Tiriganiaq Underground Mine .....	46
Figure 28: Cross-Section View of Predicted TDS Concentrations – End of 2031 – Final Year of Mining at Tiriganiaq Underground Mine .....	47
Figure 29: Sensitivity Analysis Results – Part 1 .....	53
Figure 30: Sensitivity Analysis Results – Part 2 .....	54
Figure 31: Measured versus Predicted Inflow to Tiriganiaq Underground Mine – Sensitivity Scenarios .....	55

## 1.0 INTRODUCTION

The Meliadine Gold Project (herein referred to as the Meliadine Mine or Project) is located approximately 25 km north from Rankin Inlet and 80 km southwest from Chesterfield Inlet in the Kivalliq Region of Nunavut. The Project includes open-pits and the Tiriganiaq Underground Mine (TM), which were components of the 2014 FEIS (Agnico Eagle 2014a).

Since the completion of the 2014 FEIS, supplemental hydrogeological data has been collected to enhance the understanding of hydrogeological conditions, which is presented in an updated existing conditions report (WSP 2024b). This report presents the results of a hydrogeological assessment of groundwater conditions that are present now and that are expected to develop in the Project area during mining. Specifically, it addresses the approaches and assumptions adopted in the estimate of the potential groundwater inflow quantity and groundwater quality (total dissolved solids [TDS] only) associated with the development of the open pits and TM. In this assessment, an updated three-dimensional numerical groundwater model was developed using FEFLOW (V8). This model incorporates the mine plan provided by Agnico Eagle for the Project.

## 2.0 CONCEPTUAL HYDROGEOLOGICAL MODEL

Prior to model development for the Project, a conceptual hydrogeological model was developed to aid in the construction of the numerical groundwater model. A conceptual hydrogeological model is a pictorial and descriptive representation of the groundwater regime that organizes and simplifies the site conditions so they can be readily modelled. The conceptual model must retain sufficient complexity so that the analytical or numerical models developed from it adequately reproduce or simulate the actual components of the groundwater flow system to the degree necessary to satisfy the objectives of the modelling study.

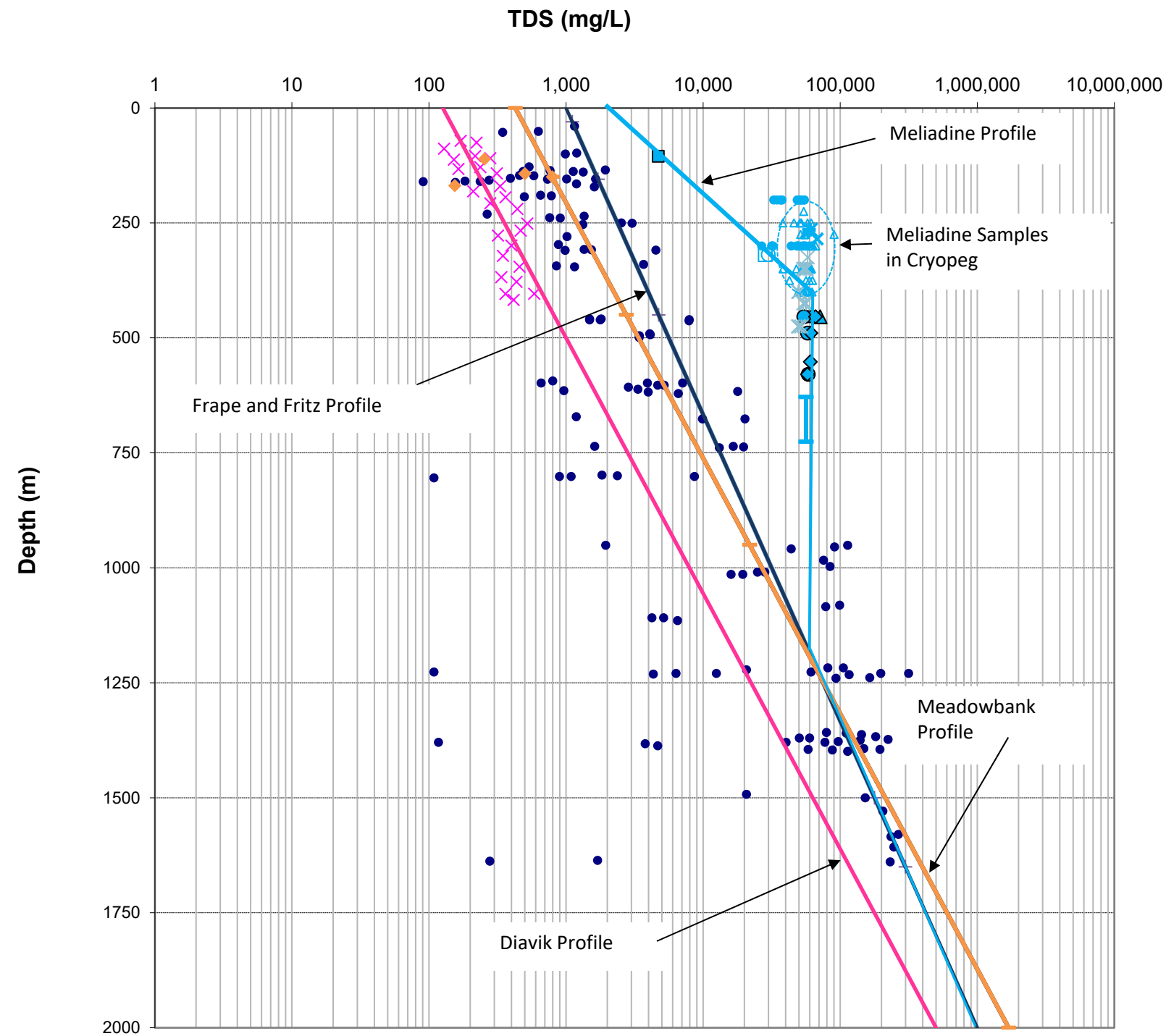
This conceptual model developed to describe key features of the pre-mining hydrogeological regime in the environmental study area is discussed in the Updated Summary of Hydrogeology Existing Conditions (WSP 2024b). The key features included in this conceptual model are the hydrostratigraphy, groundwater flow quantity and quality, and dominant groundwater flow directions. The following section summarizes the conceptual hydrogeological models for each stage of mining: predevelopment, mining, and closure. For further detail on the data used to develop the conceptual model components, including the hydrogeological data, the reader is referred to the Updated Summary of Hydrogeology Existing Conditions Report (WSP 2024b).

### 2.1 Permafrost Depth

The Meliadine Project is located within the zone of continuous permafrost (AEM 2014a). Thermal modelling indicates the depth to permafrost varies between 320 and 490 m depth, with the interpreted depth dependent on the proximity to nearby lakes (WSP 2024a). Based on the groundwater quality (salinity) data for the Project (Figure 1), and the results of thermal modelling, cryopeg conditions are assumed between the 0-degree and -3-degree isotherm. Near Tiriganiaq, this results in the depth to the basal cryopeg of approximately 280 to 290 m bgs (depth where unfrozen groundwater may first be encountered).

Open taliks (defined by the 0-degree isotherm) are predicted to be present beneath portions of each of the following lakes near the proposed open pits and TM: Lake B4, B5, B7, A6, A8, and CH6. The model results expand the list of lakes with potential open talik compared to what was estimated in the 2014 Freshwater Environment FEIS, where only the Meliadine lake, and Lakes A8, B7 and D7 were considered large enough to support open talik.

Closed talik is interpreted below Lake D4 based on the 0-degree isotherm. Predicted temperatures, however, suggest that the ground below the lake may not be fully frozen in consideration of the groundwater salinity, and that the lake may be connected to the regional groundwater flow system through the cryopeg zone.



- Multiple Sites (Frape and Fritz 1987)
- × Diavik (Kuchling et al. 2000)
- ◆ Meadowbank Data (Cumberland 2005)
- Meliadine GT09-19 - 2009 and M11-1257 - 2011 Samples
- ▲ Meliadine M11-1257 - 2012 Sample
- Meliadine M11-1257 - 2013 Sample
- ◆ Meliadine M11-1257 - 2014 Sample
- Meliadine 2015 - Underground Program
- × Meliadine 2015 Ramp Sample 1
- + Meliadine 2015 Ramp Sample 2
- × Meliadine 2015 Ramp Sample 3
- △ Meliadine 2016 and 2017 - DDH Holes Tiriganiaq
- Meliadine M20-3071 - 2020 Sample
- Meliadine M20-3071 - 2021 Sample
- ▲ Meliadine 2020 - DDH Holes Tiriganiaq
- × Meliadine 2021 - DDH Holes Tiriganiaq
- Meliadine 2021 Level 200 and 300 Sample

CLIENT



CONSULTANT



YYYY-MM-DD 2024-01-24

PREPARED JL

DESIGNED HG

REVIEWED JL

APPROVED DC

PROJECT

AGNICO EAGLE MINES LIMITED  
MELIADINE MINE  
NUNAVUT

TITLE

GROUNDWATER SALINITY PROFILE WITH DEPTH

PROJECT NO. CA0020476.6818

PHASE

REV. 0

FIGURE 1



## 2.2 Hydrostratigraphy

Table 1 and Table 2 present a summary of the hydrostratigraphic units defined for the Project Area and their estimated hydraulic properties based on hydraulic testing and observations made in the underground mine workings. Where test data was unavailable, the properties were defined based on published data for similar lithologies.

The shallow bedrock at the site is primarily within the frozen permafrost except in areas of taliks underlying lakes. The deeper competent bedrock has been subdivided into two separate units: Mafic Volcanic Rock formations and Sedimentary Rock formations. The Mafic Volcanic Rock formations are present between the Lower Fault and Pyke Fault and are inferred to transition to Sedimentary Rock formations to the east. Sedimentary Rock formations are present to the North of the Lower Fault, and South of Pyke Fault. Synthesis of the hydraulic testing results up to the end of 2021, indicates that the hydraulic conductivity of the bedrock decreases with depth.

In crystalline rocks, fault zones may act as groundwater flow conduits, barriers, or a combination of the two in different regions of the fault depending on the direction of groundwater flow and the fault zone architecture (Gleeson and Novakowski 2009). Within the Project area, three regional faults (North, Lower and Pyke) are present. In addition, review of structures in the Project area by Agnico Eagle identified 17 additional faults that have been incorporated into the conceptual hydrostratigraphy near the TM and open pit developments. Each of these faults have been assumed to have enhanced permeability relative to the surrounding competent bedrock. The additional structures are generally located between the Lower Fault and Pyke Fault within the Mafic Volcanic Rock formations and range in thickness from 2 to 6 m. An exception is the KMS Fault corridor, located in the sedimentary rock formations to the north of the Lower Fault at the TM. This corridor is a wider zone of rock located between the KMS Fault and Lower Fault that is associated with poor rock quality. The continuity of this corridor is unknown but based on rock quality is interpreted to thin to the east and west.

The hydraulic conductivity of the competent bedrock and faults is assumed to be linearly reduced by an order of magnitude between the top of the cryopeg and base of permafrost (zero-degree isotherm). This assumption reflects that this portion of the permafrost, which will contain partially unfrozen groundwater due to freezing point depression, is expected to have reduced hydraulic conductivity relative to the unfrozen bedrock reflecting the presence of isolated pockets of frozen groundwater within this zone. These frozen zones will result in a decrease in the hydraulic conductivity of the rock compared to that of the entirely unfrozen rock.

**Table 1: Estimated Hydraulic Properties – Competent Bedrock**

Hydrostratigraphic Unit	Depth Interval (mbgs)	Hydraulic Conductivity <sup>(a)</sup> (m/s)	Specific Storage <sup>(b)</sup> (1/m)	Effective Porosity <sup>(c)</sup> (-)
Shallow Rock	0 to 55	$3 \times 10^{-6}$	$1 \times 10^{-6}$	0.001
Sedimentary Rock Formations	55 to 320	$2 \times 10^{-8}$	$1 \times 10^{-6}$	0.001
	320 to 500	$3 \times 10^{-9}$	$1 \times 10^{-6}$	0.001
	500 to 1500	$3 \times 10^{-9}$	$2 \times 10^{-6}$	0.001
Mafic Volcanic Rock Formations	55 to 320	$2 \times 10^{-8}$	$1 \times 10^{-6}$	0.001
	320 to 500	$3 \times 10^{-9}$	$1 \times 10^{-6}$	0.001
	500 to 1500	$3 \times 10^{-10}$	$2 \times 10^{-7}$	0.001

Note: Hydraulic conductivity within the unfrozen permafrost zone is assumed to be lower than in the deeper unfrozen rock. Linearly decreasing hydraulic conductivity with temperature is assumed within this zone with a full order of magnitude decrease assumed at the top of the basal cryopeg, and hydraulic conductivity equivalent to unfrozen rock at the bottom of the basal cryopeg.

a) Parameter values based on in situ testing

b) Parameter values based on in situ testing and values documented in literature (Maidment 1992; Stober and Bucher 2007).

c) Values consistent with literature values (Guimerà J, Carrera J. 2000).

**Table 2: Estimated Hydraulic Properties – Enhanced Permeability Zones**

Hydrostratigraphic Unit	Depth Interval <sup>(e)</sup> (m)	Thickness <sup>(d)</sup> (m)	Packer Test Hydraulic Conductivity Estimates (m/s)	# of Tests	Assumed Hydraulic Conductivity <sup>(a)</sup> (m/s)	Specific Storage <sup>(b)</sup> (1/m)	Effective Porosity <sup>(c)</sup> (-)	Source of Assigned Hydraulic Conductivity
Lower Fault Zone	0 to 1000	5	$5 \times 10^{-8}$ to $1 \times 10^{-7}$	4	$1 \times 10^{-7}$	$2 \times 10^{-7}$	0.005	2020 Model Calibration and In Situ Testing
RM-175	0 to 1000	5	$2 \times 10^{-8}$	1	$5 \times 10^{-8}$	$2 \times 10^{-7}$	0.005	2020 Model Calibration and In Situ Testing
KMS Fault Corridor	0 to 1000	100	$4 \times 10^{-7}$	1*	$4 \times 10^{-7}$	$2 \times 10^{-7}$	0.005	2020 Model Calibration and In Situ Testing
North Fault	0 to 1000	5	-	-	$1 \times 10^{-7}$	$2 \times 10^{-7}$	0.005	Unchanged from FEIS Assumption
A	0 to 1000	6	$2 \times 10^{-8}$ to $2 \times 10^{-7}$	6	$1 \times 10^{-6}$	$2 \times 10^{-7}$	0.005	Assumed T Equal to Fault 2 and In Situ Testing
B	0 to 1000	5	-	-	$1 \times 10^{-6}$	$2 \times 10^{-7}$	0.005	Assumed T Equal to Fault 2
C	0 to 1000	3	$4 \times 10^{-9}$	1	$2 \times 10^{-6}$	$2 \times 10^{-7}$	0.005	Assumed T Equal to Fault 2
D	0 to 1000	5	-	-	$1 \times 10^{-6}$	$2 \times 10^{-7}$	0.005	Assumed T Equal to Fault 2
Pyke Fault	0 to 1000	15	$7 \times 10^{-9}$ to $3 \times 10^{-7}$	3	$3 \times 10^{-7}$	$2 \times 10^{-7}$	0.005	Maximum from In Situ Testing
AP0	0 to 1000	3	-	-	$2 \times 10^{-6}$	$2 \times 10^{-7}$	0.005	Assumed T Equal to Fault 2
ENE1/ENE2	0 to 1000	5	$3 \times 10^{-8}$	1	$1 \times 10^{-6}$	$2 \times 10^{-7}$	0.005	Assumed T Equal to Fault 2
ENE3	0 to 1000	3	-	-	$2 \times 10^{-6}$	$2 \times 10^{-7}$	0.005	Assumed T Equal to Fault 2
UM2	0 to 1000	6	-	-	$1 \times 10^{-6}$	$2 \times 10^{-7}$	0.005	Assumed T Equal to Fault 2
NW1	0 to 1000	5	$2 \times 10^{-10}$ to $2 \times 10^{-9}$	3	$5 \times 10^{-7}$	$1 \times 10^{-7}$	0.005	Assumed T Equal to Fault 2
WNW1	0 to 1000	3	-	-	$2 \times 10^{-6}$	$2 \times 10^{-7}$	0.005	Assumed T Equal to Fault 2
WNW2	0 to 1000	3	-	-	$2 \times 10^{-6}$	$2 \times 10^{-7}$	0.005	Assumed T Equal to Fault 2
UAU2	0 to 1000	2	-	-	$3 \times 10^{-6}$	$2 \times 10^{-7}$	0.005	Assumed T Equal to Fault 2
Fault 1	0 to 1000	5	$8 \times 10^{-7}$	1	$1 \times 10^{-6}$	$2 \times 10^{-7}$	0.005	Assumed T Equal to Fault 2
Fault 2	0 to 1000	5	$3 \times 10^{-7}$ m/s and $5 \times 10^{-7}$	4	$1 \times 10^{-6}$	$2 \times 10^{-7}$	0.005	In Situ Testing
Fault 3	0 to 1000	5	-	-	$1 \times 10^{-6}$	$2 \times 10^{-7}$	0.005	Assumed T Equal to Fault 2

a) Hydraulic conductivity within the unfrozen permafrost zone is assumed to be lower than in the deeper unfrozen rock. Linearly decreasing hydraulic conductivity with temperature is assumed within this zone with a full order of magnitude decrease assumed at the top of the basal cryopeg, and hydraulic conductivity equivalent to unfrozen rock at the bottom of the basal cryopeg.

b) Assumed parameter in consideration of competent bedrock testing.

c) Values consistent with literature values (Guimerà J, Carrera J. 2000).

d) Width of structures estimated by Agnico Eagle from review of borehole records.

e) Where fault hydraulic conductivity is less than shallow rock, the fault was excluded from 0 to 60 m depth interval. Where fault hydraulic conductivity is greater than shallow rock, fault was included within 0 to 60 m depth interval.

## 2.3 Conceptual Groundwater Flow – Pre-Mining

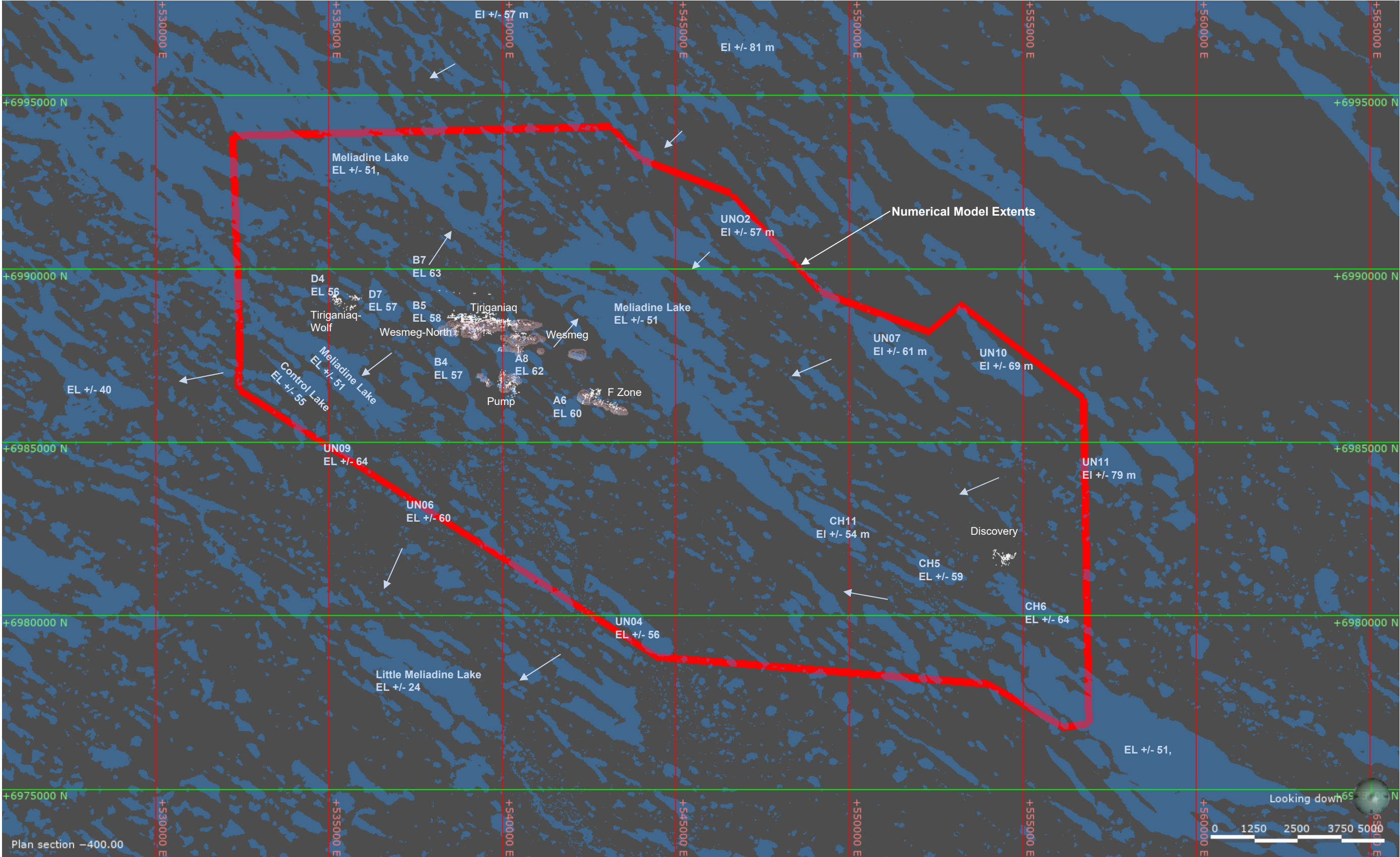
The conceptual hydrogeological model for pre-disturbance conditions is presented on Figure 2 through Figure 6.

In areas of continuous permafrost there are generally two groundwater flow regimes; a deep groundwater flow regime beneath the base of the permafrost and a shallow flow regime located in an active (seasonally thawed) layer near ground surface (Figure 3). Permafrost reduces the hydraulic conductivity of the rock by several orders of magnitude (McCauley et al. 2002; Burt and Williams 1976), therefore the shallow groundwater flow regime has little to no hydraulic connection with the groundwater regime located below the permafrost. Taliks (areas of unfrozen ground surrounded by permafrost) may be present in the permafrost in areas underlying lakes. Depending on lake size, depth, and thermal storage capacity, the taliks beneath lakes may fully penetrate the permafrost layer resulting in an open talik providing a hydraulic connection between surface water and the deep groundwater flow regime.

The elevations of the lakes underlain by open taliks provide the driving force for deep groundwater flow (Figure 2). The presence of thick permafrost beneath land masses results in negligible recharge to the deep groundwater flow regime from these areas. Consequently, recharge to the deep groundwater flow regime is predominantly limited to areas of taliks beneath large, surface water bodies. Generally, deep groundwater will flow from higher-elevation lakes to lower-elevation lakes. Groundwater beneath the permafrost is also influenced by density differences due to the upward diffusion of deep-seated brines (density-driven flow).

The Westbay multi-level monitoring system that was installed in borehole M11-1257 (Figure 7) is situated between Lake B7 and D7, and directly underneath Lake B5. Each of these lakes are predicted to be connected to the deep groundwater flow regime through open taliks. Relative to Lake B5, a variable vertical groundwater flow direction was observed at M11-1257. This may reflect that Lake B5 is both a recharge and discharge boundary given the relative elevation of the surrounding lakes.

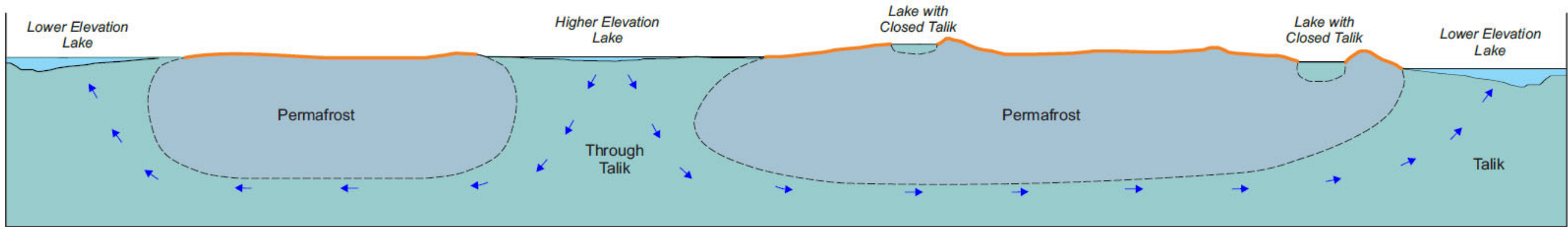
The Westbay multi-level monitoring system that was installed in borehole M20-3071 is situated below Lake CH6. The overall groundwater flow direction below Lake CH6 appears to be upwards based on pressure measurements at M20-3071 corrected for buoyancy effects. At deeper depths the interpreted gradient reverses, potentially because of the higher salinity groundwater at depth. The calculated directions of groundwater flow are approximate and sensitive to the assumed TDS versus depth profile, which is presented conceptually on Figure 1 and Figure 6. For example, if the TDS at depth is assumed to trend to a lower value at depth (approximately 54,000 mg/L), a consistent upward gradient would be measured between each of the M20-3071 ports and Lake CH6.



CLIENT  
**AGNICO EAGLE**

CONSULTANT	YYYY-MM-DD	2024-01-24
	PREPARED	JL
	DESIGNED	HG
	REVIEWED	JL
	APPROVED	DC

PROJECT	AGNICO EAGLE MINES LIMITED MELIADINE MINE NUNAVUT
TITLE	HYDROGEOLOGY MODEL EXTENTS AND CONCEPTUAL REGIONAL GROUNDWATER FLOW DIRECTIONS
PROJECT NO.	CA0020476.6818
PHASE	
REV.	0
FIGURE	2





CROSS SECTION

Schematic Only  
Not to Scale

LEGEND

- Conceptual Groundwater Flow Direction
- Active Layer

CLIENT			PROJECT		
			AGNICO EAGLE MINES LIMITED		
CONSULTANT			MELIADINE MINE		
			NUNAVUT		
			TITLE		
			SCHEMATIC OF CONCEPTUAL PERMAFROST AND		
			GROUNDWATER FLOW CONDITIONS IN AREAS OF		
			CONTINUOUS PERMAFROST		
			PROJECT NO.	PHASE	REV.
			CA0020476.6818		0
			FIGURE		
			3		



Volcanic Rock Formation (Cryopeg)

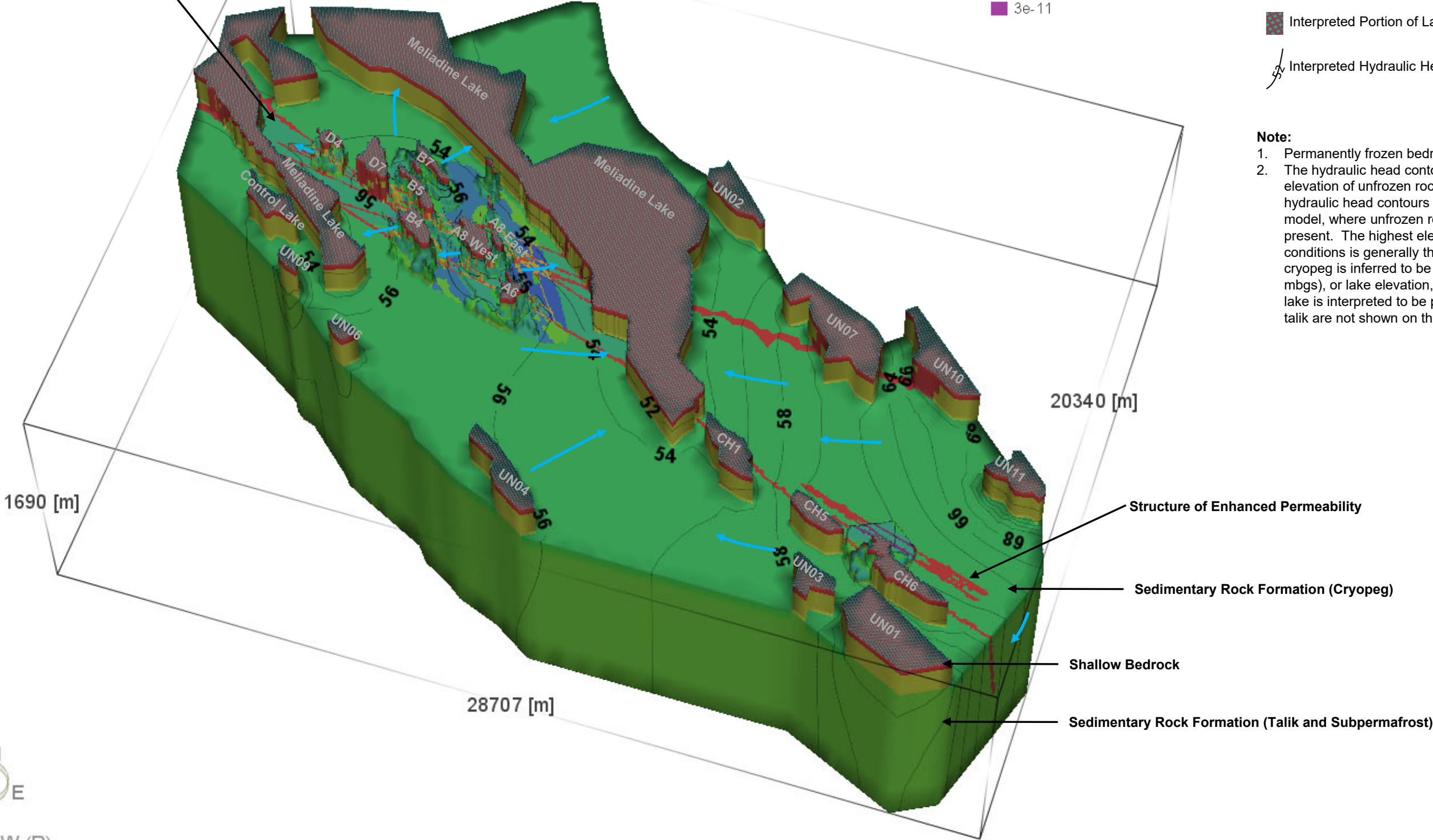
Conductivity: K<sub>xx</sub>  
- Patches -  
[m/s]  
3e-08  
3e-09  
3e-10  
3e-11

Legend

- Inferred Groundwater Flow Direction in Sub-permafrost
- Interpreted Portion of Lake Footprint with Open Talik
- Interpreted Hydraulic Head Contour (masl)

**Note:**

1. Permanently frozen bedrock not shown.
2. The hydraulic head contours are shown for the highest elevation of unfrozen rock conditions, along with the hydraulic head contours on the perimeter of the model, where unfrozen rock conditions are present. The highest elevation of unfrozen rock conditions is generally the top of cryopeg where cryopeg is inferred to be present (approximately 280 mbgs), or lake elevation, where open talik below the lake is interpreted to be present. Lakes without open talik are not shown on these figures.



5x Vertical Exaggeration

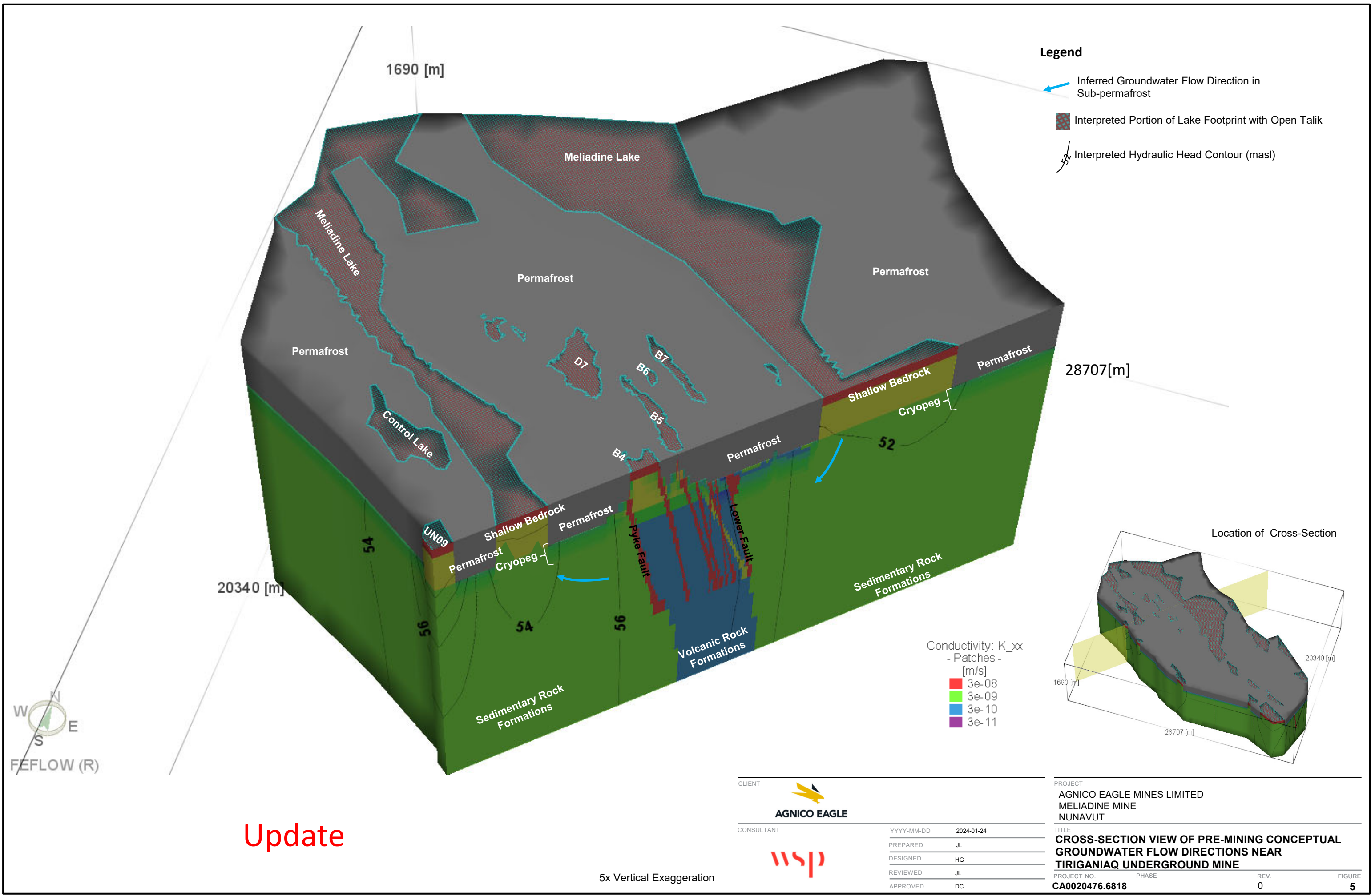
CLIENT  
**AGNICO EAGLE**

CONSULTANT	YYYY-MM-DD	2024-01-24
PREPARED	JL	
DESIGNED	HG	
REVIEWED	JL	
APPROVED	DC	

PROJECT  
AGNICO EAGLE MINES LIMITED  
MELIADINE MINE  
NUNAVUT

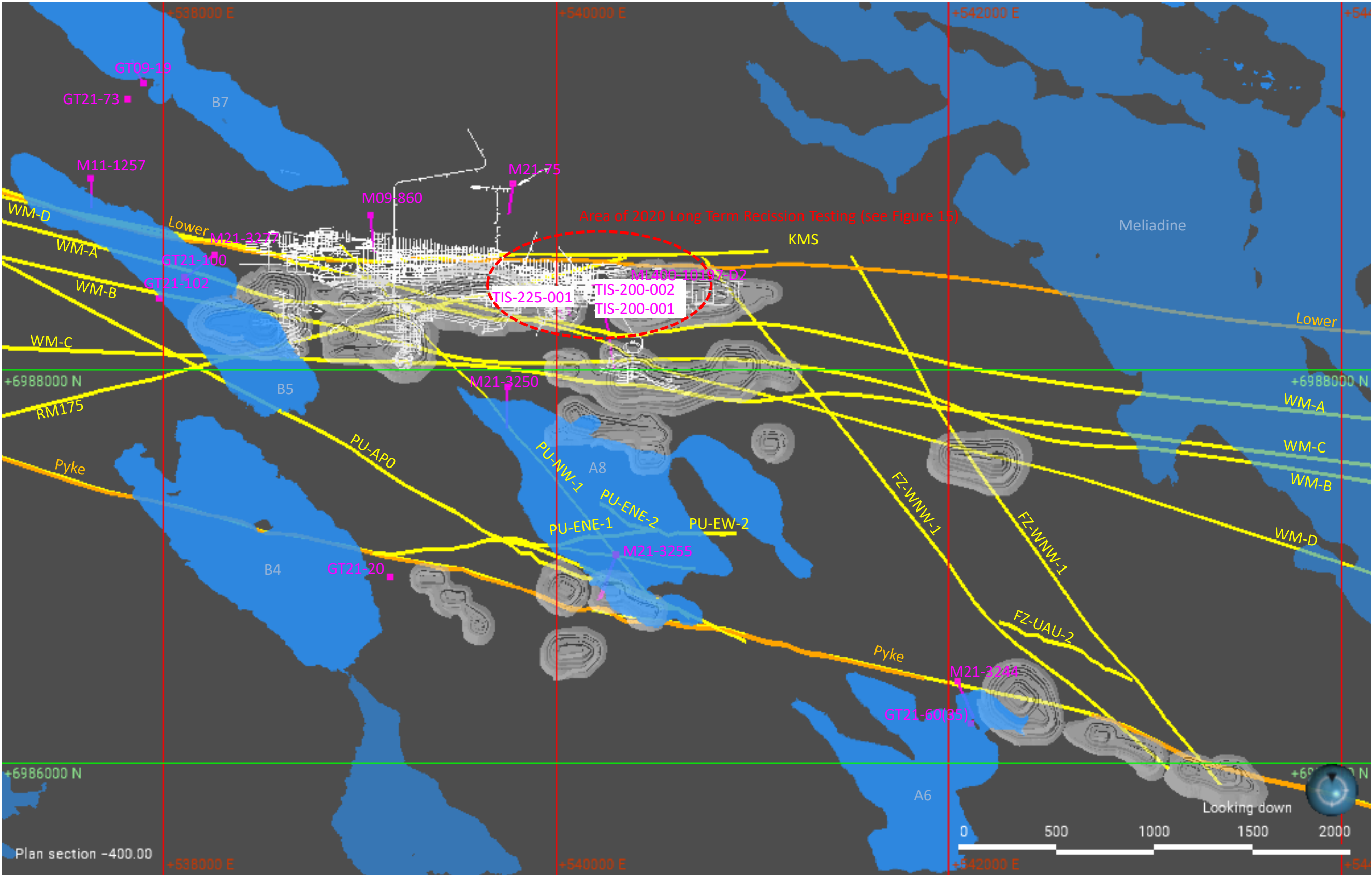
TITLE  
**PRE-MINING CONCEPTUAL GROUNDWATER FLOW DIRECTIONS AND DISTRIBUTION OF HYDROSTRATIGRAPHIC UNITS**

PROJECT NO.	PHASE	REV.	FIGURE
CA0020476.6818		0	4









**LEGEND**

- Inferred Lake with Open Talik
- Regional Fault
- Supplemental Faults Based on 2020 Agnico Eagle Review
- Borehole Collar / Borehole Trace

Fault traces are shown for an elevation of -400 masl.

CLIENT  
 **AGNICO EAGLE**

CONSULTANT	YYYY-MM-DD	2024-01-24
	PREPARED	JL
	DESIGNED	HG
	REVIEWED	JL
	APPROVED	DC

**wsp**

PROJECT  
AGNICO EAGLE MINES LIMITED  
MELIADINE MINE  
NUNAVUT

TITLE  
**BOREHOLE LOCATIONS FOR HYDRAULIC TESTING  
AND GROUNDWATER SAMPLING – MAIN AREA**

PROJECT NO.	PHASE	REV.	FIGURE
CA0020476.6818		0	7

0 25mm IF THIS MEASUREMENT DOES NOT MATCH WHAT IS SHOWN, THE SHEET SIZE HAS BEEN MODIFIED FROM A3S-B

## 2.4 Conceptual Groundwater Flow – Existing Conditions

Groundwater inflows are presently intercepted at the TM, where mining has extended into the cryopeg and sub-permafrost groundwater flow system. In September of 2015, the mine development extended to the estimated depth of basal cryopeg and groundwater inflow was observed to the underground. Groundwater inflows were low (approximately 15 m<sup>3</sup>/day in the fourth quarter of 2015) but have since increased on an average of between 220 and 340 m<sup>3</sup>/day in 2021/2022. Groundwater inflows are mitigated by active grouting which locally reduces the effective hydraulic conductivity of structures adjacent to the development.

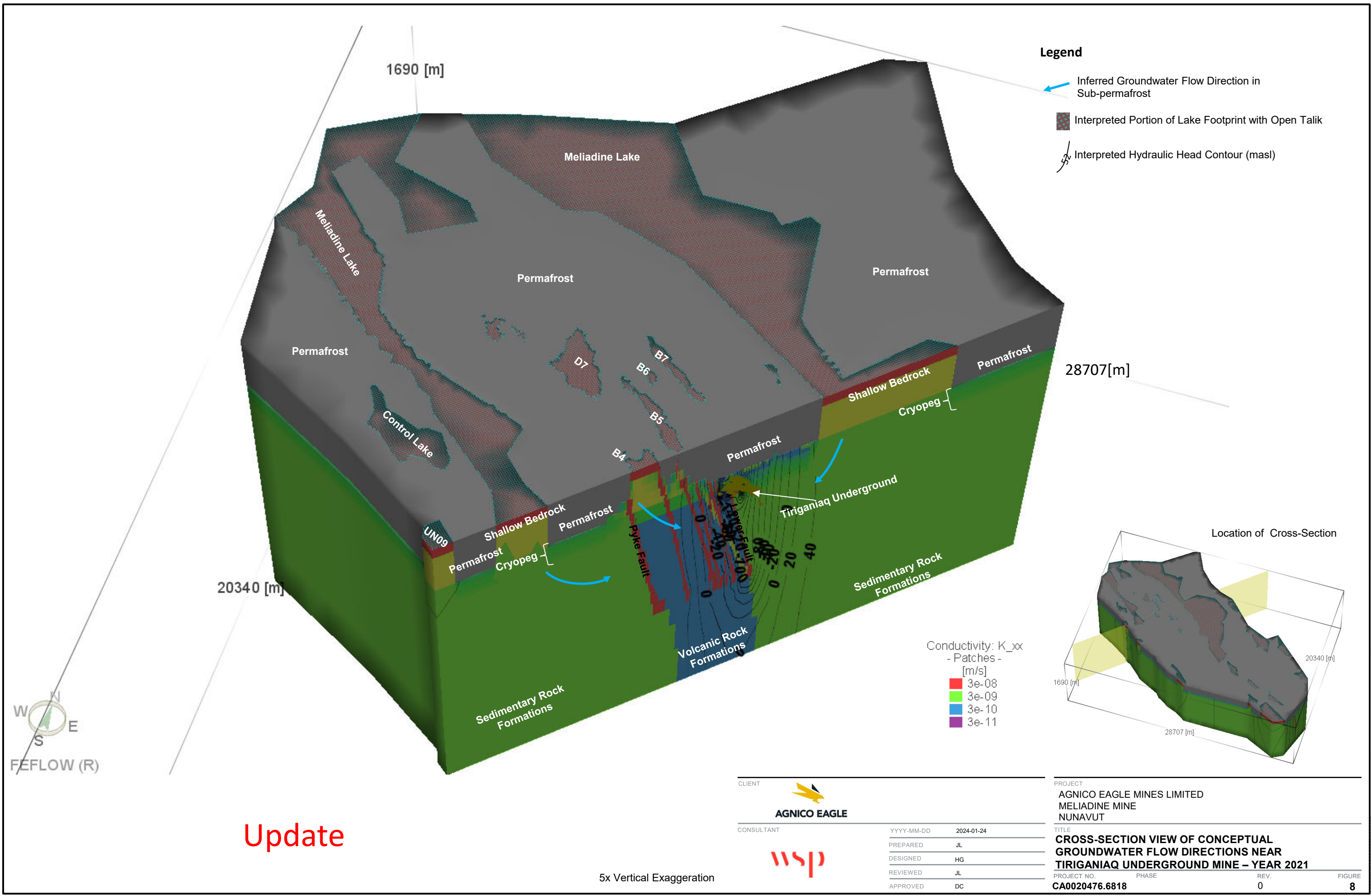
At Tiriganiaq, local depressurization of over 450 m has been observed at piezometers installed near the underground (Figure 8). Further depressurization is expected at TM and open pits as they develop. To date, no open pit mining in bedrock connected to open taliks has occurred. Tir02 pit is located at the south end of CP5. A shallow closed talik may be present below the pond resulting in some seepage to the open pit. This seepage, if present, would not be expected to significantly increase given the pit depth is likely already past the base of the closed talik.

## 2.5 Groundwater Flow – Mining

TM and open pits in connection with open taliks or the sub-permafrost groundwater flow system will act a sink for groundwater flow. Excavation will induce the water to flow through the bedrock to the mine workings once the mine has advanced below the base of the permafrost or into open talik.

Except for NOR01, WES03, and PUM04, none of the other open pits are interpreted to intersect the cryopeg or the deep groundwater regime below the permafrost. Portions of the pits may intersect small lakes that may have limited unfrozen groundwater within closed taliks. Lake dewatering is planned for each pit that may have such a hydraulic connection. This may result in freeze-back of the pit slopes, limiting the seepage of local groundwater from closed taliks into the open pits.





## 3.0 NUMERICAL HYDROGEOLOGICAL MODEL

### 3.1 Code Selection

The numerical groundwater model was constructed using FEFLOW (Version 7.5). This numerical code was selected because it is capable of simulating transient, saturated-unsaturated groundwater flow, and density-coupled solute transport in heterogeneous and anisotropic porous media under a variety of hydrogeologic boundaries and stresses. FEFLOW is well suited for development of the site model because it allows for simultaneous predictions of groundwater flow and solute transport and has been successfully used for simulated groundwater inflow to TM as part of past assessments.

Specific assumptions and limitations adopted in the model are summarized below, with additional detail presented in Section 4.2 to 3.6 and the model calibration is described in Section 5.0:

- The model predictions assumed fully saturated confined conditions. Hydraulic head measurements between 2015 and 2020 indicate saturated conditions are present near TM, and with respect to the future inflow predictions this assumption will likely bias predictions high because if unconfined conditions are encountered later in the mine life, these conditions would tend to reduce inflows. However, under continuous permafrost conditions the seepage from above is already very small and unconfined conditions may not reduce inflows much from what are predicted with confined conditions.
- The model treats the bedrock as an equivalent porous medium (EPM), although flexibility exists to introduce discrete structures as warranted to evaluate potential preferential flow paths along discrete faults. Flow in bedrock is assumed to be laminar, steady, and governed by Darcy's Law.
- Horizontal and vertical mesh discretization of approximately 10 to 25 m was considered to provide sufficient spatial resolution for simulation of groundwater flow and transport near TM and open pits.
- Initial values of model input parameters were based on the results of permeability testing across the Project and previous modelling in the area of Tiriganiaq. Where testing results were not available, initial model properties were based on typical values published in the literature.
- Surface waterbodies were simulated using specified head boundaries. It was assumed that the permeability of lake bed sediments beneath these waterbodies is the same as those of the underlying geologic strata. Thus, no restriction of flow between the surface water and individual hydrostratigraphic units was simulated.
- Groundwater flow deeper than approximately 1.7 km below ground surface (800 m deeper than the deepest mine) was assumed to be negligible and to have negligible influence on model predictions.

## 3.2 Model Domain and Discretization

The extent of the numerical hydrogeological model was based on the understanding of groundwater flow conditions, with model boundaries set sufficiently distant from the mine workings to allow adequate representation of groundwater conditions near the open pits and TM. As part of the prediction scenarios, checks were completed to verify that the predicted extent of depressurization from the underground dewatering did not extend to the lateral model boundaries.

The model domain is approximately 305 km<sup>2</sup> and consisted of over 2.8 million triangular elements (Figure 9). The element size is refined in the areas of the underground development and open pits, ranging between 10 to 25 m, and increases in size towards the periphery of the model where elements are approximately 500 m. The model domain encompasses potential areas where open pits and underground development may influence the sub-permafrost groundwater flow system.

Vertically, the model domain is discretized into 32 layers. The top of Layer 1 is generally set to approximately 55 masl, the ground surface elevation in the Tiriganiaq area, with local adjustment under lakes with open talik in consideration of lake elevations. The bottom of layer 32 was set to a constant elevation of -1,635 masl (approximately 1.7 km below ground surface and approximately 800 m below the TM).

## 3.3 Hydrostratigraphy and Initial Model Parameters

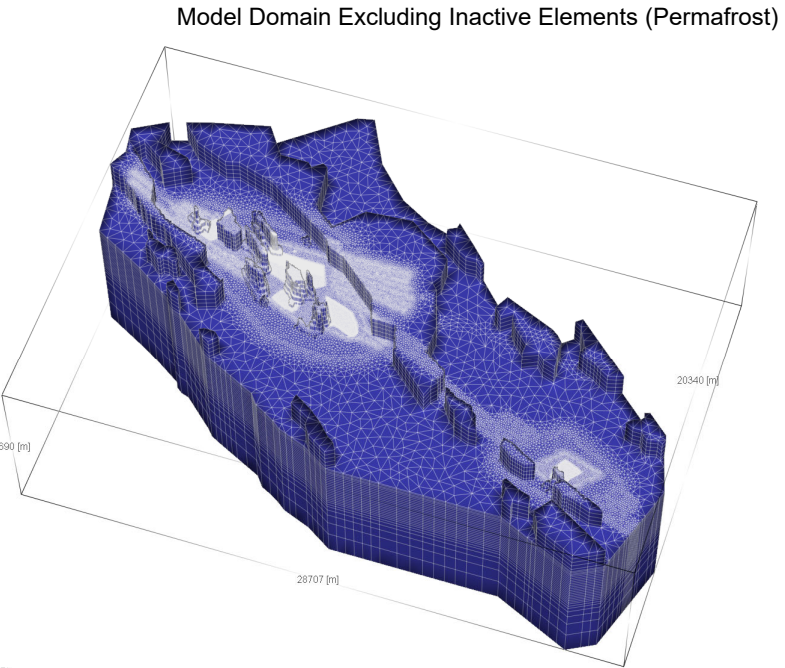
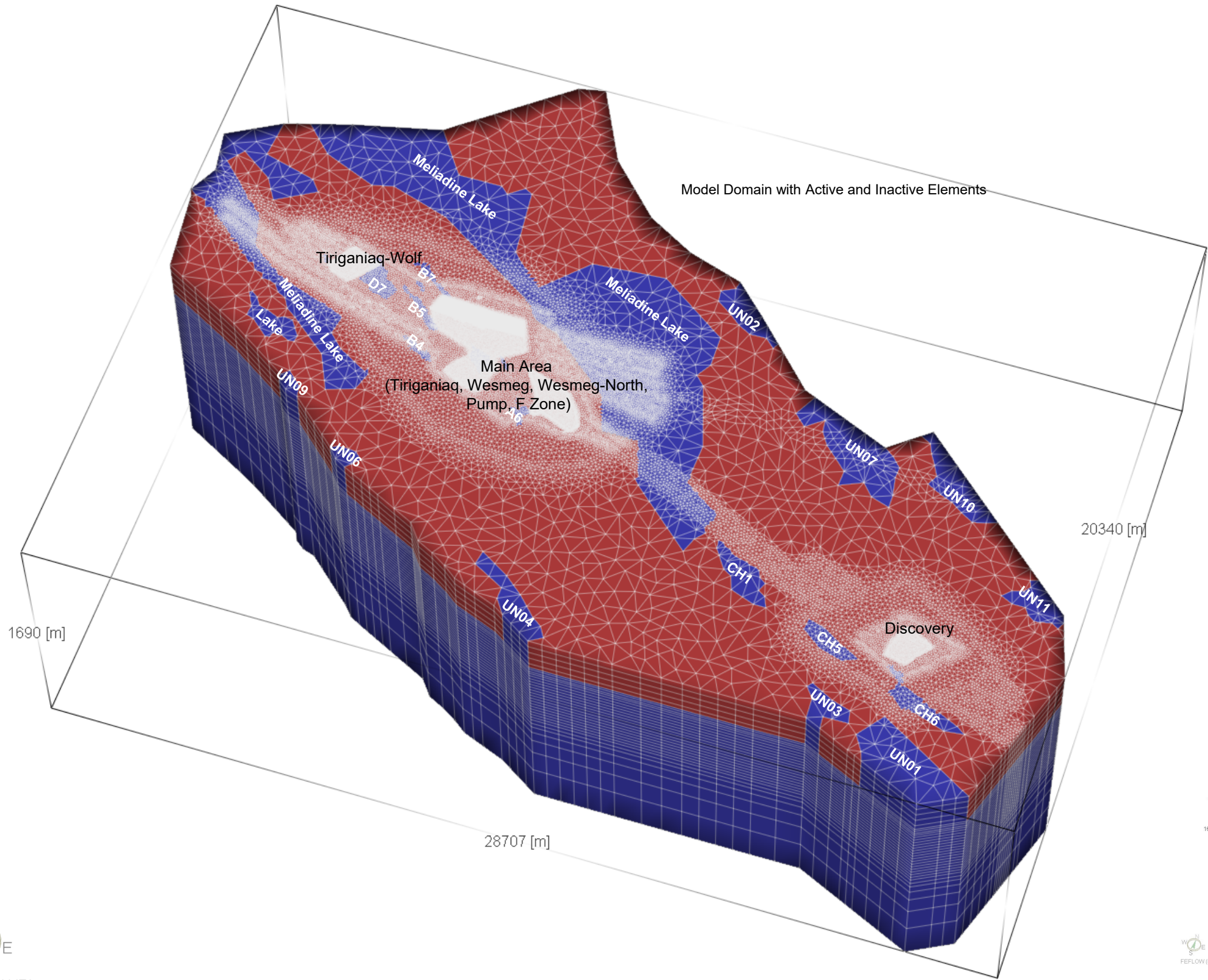
Table 1 and Table 2 of Section 2.2 present a summary of the hydrostratigraphic units and their estimated hydraulic properties. These parameters were later adjusted as part of model calibration, as described in Section 4.0. Figure 4 presents the relative location of the hydrostratigraphic units, with more detail on the fault locations presented on Figure 10 and Figure 11.

Faults within the Project area generally range from 2 to 6 m thick, which is less than the element size near the TM and open pits (10 to 25 m). An exception of the Pyke Fault and KMS corridor that have larger interpreted widths (15 to 100 m). Faults were simulated in model by assigning an effective hydraulic conductivity representative of the combined transmissivity of the fault and competent bedrock to elements parallel to the fault alignment, with the fault set to be approximately two elements wide. The faults have been conservatively assumed to extend several kilometres away from TM and open pit developments and to extend to a depth of approximately one kilometre (-1,025 m elevation).

To mitigate groundwater inflows, Agnico Eagle actively grouts faults, joints and other structures within the rock that contribute to inflow to the underground. To simulate this grouting, elements representative of the faults within 30 m of the underground were assigned an effective hydraulic conductivity of  $1 \times 10^{-8}$  m/s. This parameter was then iteratively adjusted in the model to improve the match between measured and predicted inflows to the underground.



- Legend**
- Active Model Elements  
(Cryopeg and Unfrozen Bedrock)
  - Inactive Model Elements  
(Permafrost Excluding Cryopeg)



CLIENT



CONSULTANT



YYYY-MM-DD 2024-01-24

PREPARED JL

DESIGNED HG

REVIEWED JL

APPROVED DC

PROJECT

AGNICO EAGLE MINES LIMITED  
MELIADINE MINE  
NUNAVUT

TITLE

**FINITE ELEMENT MESH AND ACTIVE MODEL  
DOMAIN**

PROJECT NO.  
**CA0020476.6818**

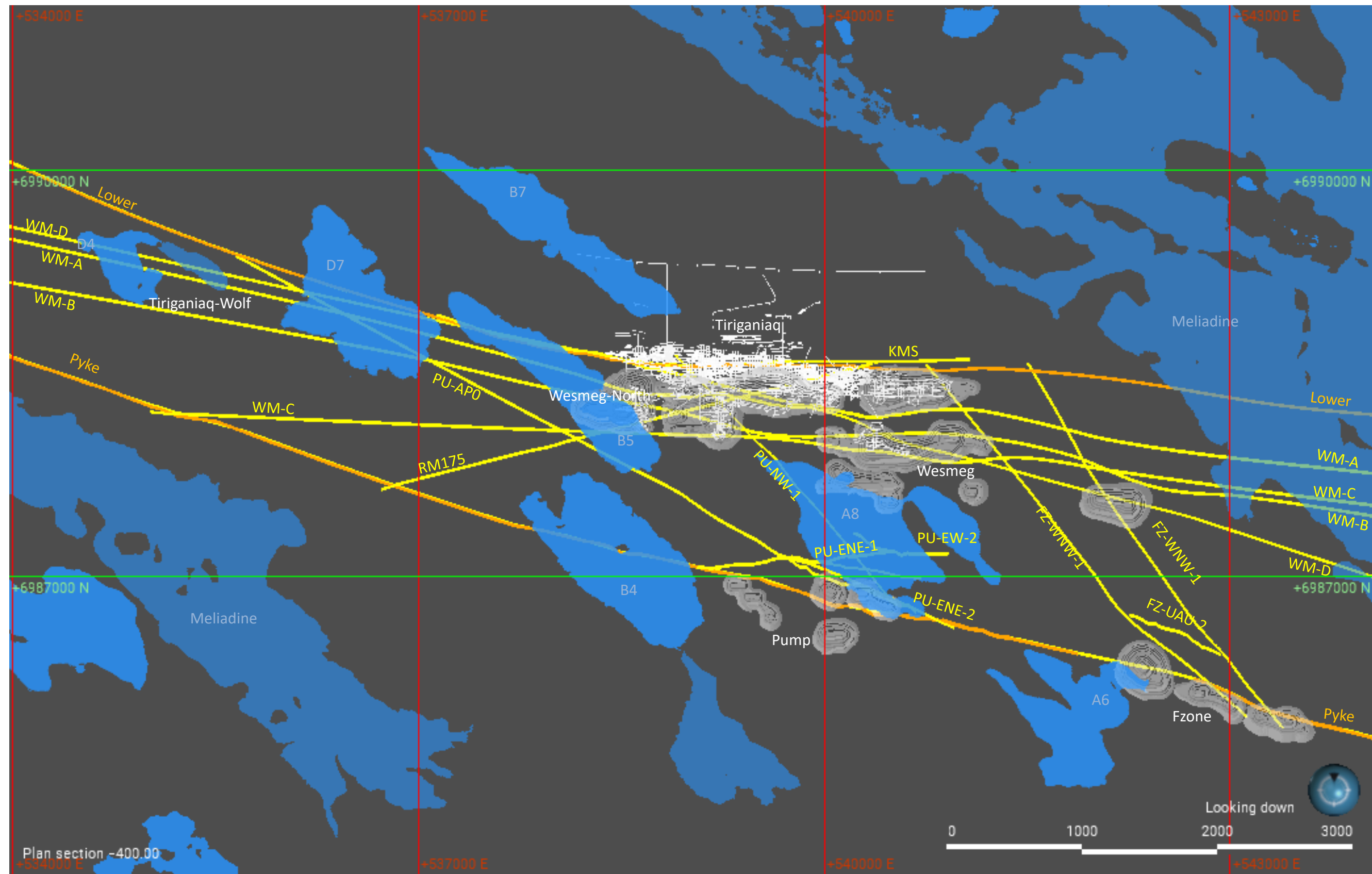
PHASE

REV.  
**0**

FIGURE  
**9**

5x Vertical Exaggeration

IF THIS MEASUREMENT DOES NOT MATCH WHAT IS SHOWN, THE SHEET SIZE HAS BEEN MODIFIED FROM A3S B



**LEGEND**

- Inferred Lake with Open Talik
  - Regional Fault
  - Supplemental Faults Based on 2020 Agnico Eagle Review
- Fault traces are shown for an elevation of -400 masl.

CLIENT



CONSULTANT



YYYY-MM-DD	2024-01-24
PREPARED	JL
DESIGNED	HG
REVIEWED	JL
APPROVED	DC

PROJECT

AGNICO EAGLE MINES LIMITED  
MELIADINE MINE  
NUNAVUT

TITLE

**STRUCTURES OF ENHANCED PERMEABILITY – MAIN  
AREA AND TIRIGANIAQ-WOLF**

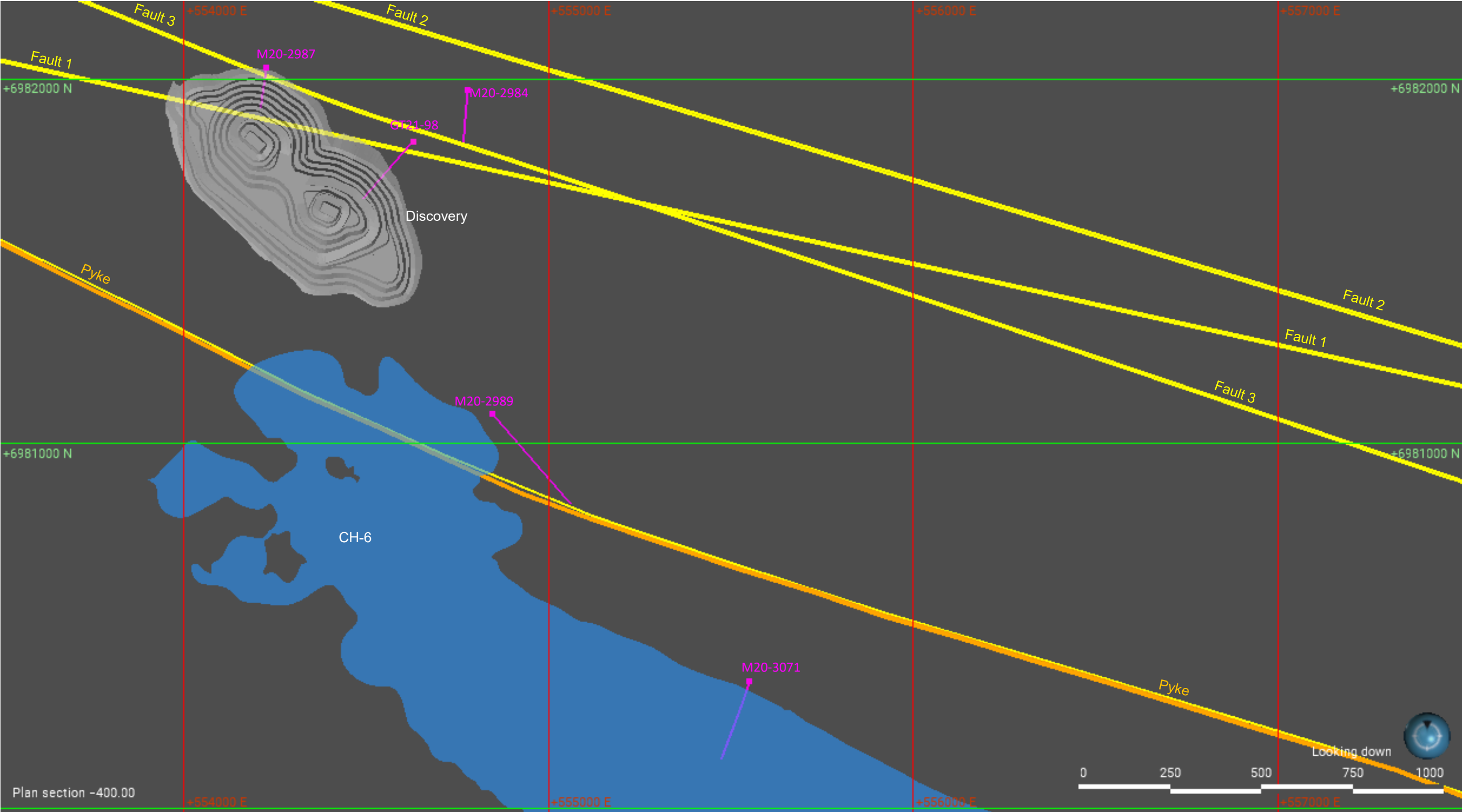
PROJECT NO.  
**CA0020476.6818**

PHASE





REV.  
0

FIGURE  
**10**





Fault traces are shown for an elevation of -400 masl.

-  Inferred Lake with Open Talik
-  Regional Fault
-  Supplemental Faults Based on 2020 Agnico Eagle Review
-  Borehole Location

CLIENT



CONSULTANT



YYYY-MM-DD	2024-01-24
PREPARED	JL
DESIGNED	HG
REVIEWED	JL
APPROVED	DC

PROJECT

AGNICO EAGLE MINES LIMITED  
MELIADINE MINE  
NUNAVUT

TITLE

**STRUCTURES OF ENHANCED PERMEABILITY –  
DISCOVERY**

PROJECT NO.  
**CA0020476.6818**

PHASE

REV.  
0

FIGURE  
**11**

25 mm IF THIS MEASUREMENT DOES NOT MATCH WHAT IS SHOWN, THE SHEET SIZE HAS BEEN MODIFIED FROM A3S-B

### 3.4 Mine Schedule

This model incorporates the mine plan provided by Agnico Eagle, as summarized in Table 3 for the lowest elevation of the TM development.

**Table 3: Lowest Elevation of Tiriganiaq Underground Mine Development**

Year	Lowest Elevation Tiriganiaq Underground Mine (m)
2021	-490
2022	-560
2023	-640
2024	-735
2025	-845
2026	-845
2027	-845
2028	-845
2029	-845
2030	-845
2031	-845

Based on permafrost limits (WSP 2024a), open pits in the F Zone, Pump and Discovery, which vary in depth between 70 and 140 mbgs, will be within permafrost and/or intersect shallow closed taliks in adjacent lakes. Where open pits in the F Zone, Pump and Discovery intersect lakes, these Lakes are planned to be dewatered in advance of mining.

Wesmeg-North Pit (WN-01) is planned to be about 130 m deep with the ultimate base of the pit at -65 masl and is under a portion of Lake B5 where thermal models predict the existence of an open talik (WSP 2024a).

Pump Pit 4 (PUM04) is planned to be about 40 m deep with the ultimate pit at -20 masl and is under the southern portion of Lake A8 West.

Wesmeg Pit 5 (Wes05) is planned to be about 120 m deep with the ultimate base of the pit at -55 masl and is partially under the north side of Lake A8 West, where thermal models predict the presence of an open talik (WSP 2024a). For purposes of this hydrogeological model, it was assumed that Lake B5 and Lake A8 West would be dewatered in advance of both underground and open-pit mining in these areas.

### 3.5 Model Boundary Conditions – Flow

Model boundary conditions provide a link between the model domain and the surrounding hydrologic and hydrogeologic systems. Two types of flow boundary conditions were used in the model: specified head and no-flow (zero-flux) boundaries. The locations of these boundaries are shown in Figure 12 and are summarized below.

Specified head boundaries were assigned to Layer 1 of the model to represent all lakes assumed to have open taliks connected to the deep groundwater flow regime. Each of these boundaries was set to the lake elevation derived from site topographic data. It was conservatively assumed that the surface water/groundwater interaction at all lakes is not impeded by lower-permeability lakebed sediments that may exist on the bottom of some of these lakes. Specified head boundaries were also assigned beneath the permafrost along the perimeter of the model along inferred flow lines for predictions during operations. Overall, model limits are set sufficient far enough from the mine developments to not influence model predicted inflow and were assessed as part of sensitivity analysis (Section 5.3).

During operations, time-variable specified head boundaries were assigned to Layer 1 of the model to represent dewatering of Lake A8 West, Lake B5 and Lake A6. Lake A8 West overlaps with open pits WES03 and PUM04. Lake B5 overlaps with open pit WN01. Lake A6 overlaps with open pit FZ001; however, the portion of Lake A6 that overlaps with FZ001 is not interpreted to have open talik below it. For one month of the year, it was assumed that dewatering outside of berm pit areas would not keep up with freshet inflows and standing water would be present in the lakes; the remaining 11 months it assumed that the lake is fully dewatered. It is assumed that any water reporting to the dewatered lake footprint and bermed pit area would report as runoff to the open pit or dewatering system, which is not a predicted component of the groundwater flow model.

Mine workings in unfrozen bedrock (open pits and TM) were simulated in the model using time-variable specific head boundaries. At each mesh node within the perimeter of the open pit and/or along the underground development, a specified head boundary was assigned and the head value at this boundary was varied over time to represent progressive expansion of the mine development according to the mine schedule provided by Agnico Eagle and generally described in Section 3.4. In addition, all boundaries representing mine workings during mining were constrained to allow only outflow from surrounding sediments/bedrock into the mine (i.e., these boundaries act as seepage faces).

A no-flow boundary applied along the bottom of the model at a depth of 1.7 km below ground surface (-1,635 masl). Flow at greater depth is expected to be negligible in comparison to lateral inflow above this elevation, and therefore is expected to have negligible impact on model predictions. No-flow boundaries were also assigned along the edges of the permafrost as the permafrost is essentially impermeable. Mesh elements representing permafrost (excluding the cryopeg) were deactivated in all model simulations (Figure 9). The permafrost zones were assigned to the model based on the updated thermal modelling results (WSP 2024a).

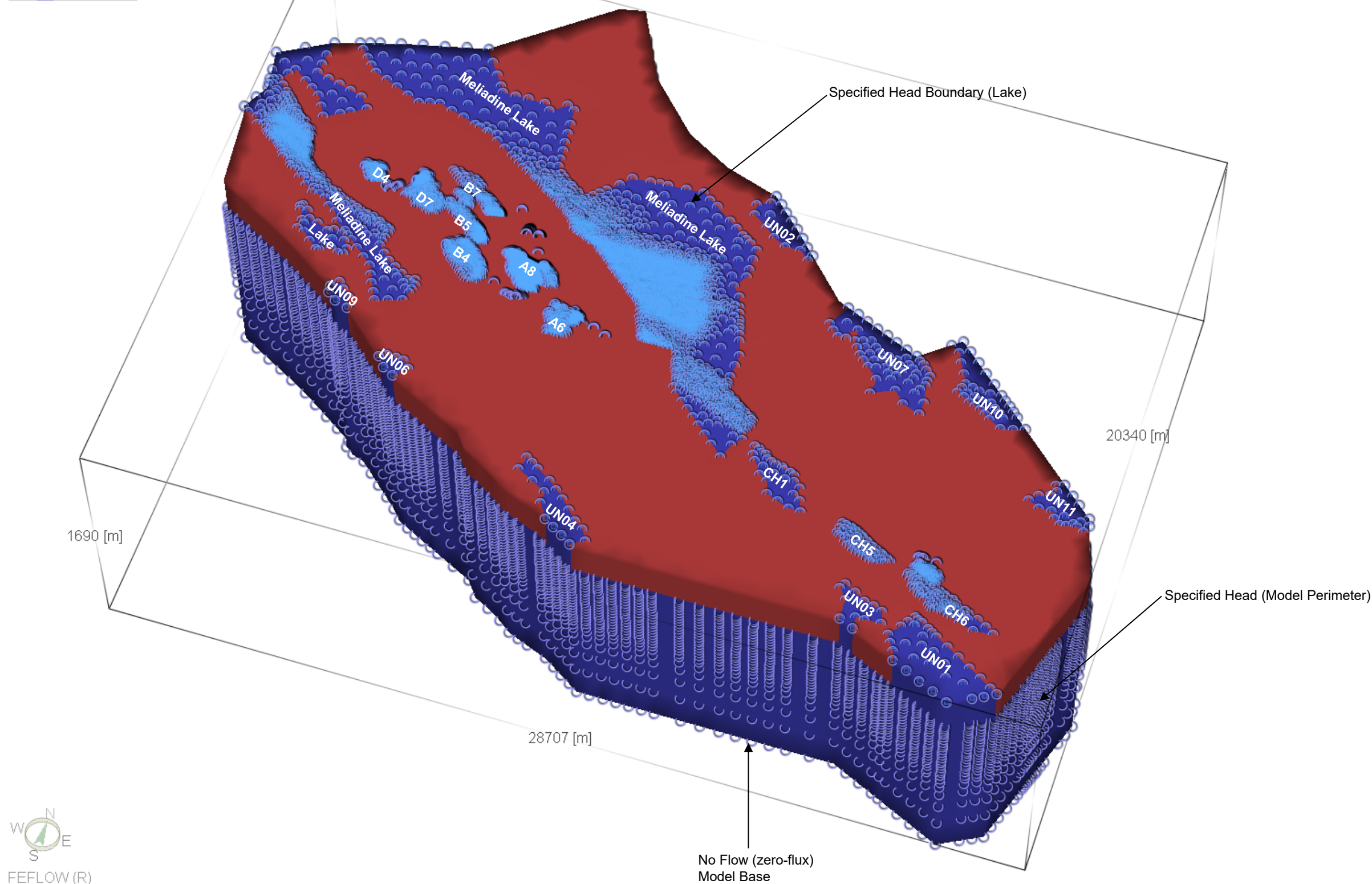
Initial groundwater flow conditions in the model were established by running the model in steady state with no active mine developments. This simulation represents the pre-mining flow regime described in the Updated Summary of Hydrogeology Existing Conditions (WSP 2024b), where the groundwater flow pattern is controlled by the water elevations of the large lakes (Figure 2). The predicted groundwater flow contours from this simulation are presented on the conceptual flow model shown on Figure 5 and is consistent with the interpreted flow pattern interpreted from Lake Elevations associated with open taliks (Figure 2).

In-/active Elements  
- Patches -  
□ inactive  
■ active

**Legend**

■ Active Model Elements  
(Cryopeg and Unfrozen  
Bedrock)

■ Inactive Model Elements  
(Permafrost Excluding Cryopeg)



CLIENT



CONSULTANT



YYYY-MM-DD 2024-01-24

PREPARED JL

DESIGNED HG

REVIEWED JL

APPROVED DC

PROJECT

AGNICO EAGLE MINES LIMITED  
MELIADINE MINE  
NUNAVUT

TITLE

**MODEL BOUNDARY CONDITIONS FOR  
GROUNDWATER FLOW**

PROJECT NO.  
**CA0020476.6818**

PHASE

REV.  
0

FIGURE  
**12**

5x Vertical Exaggeration

IF THIS MEASUREMENT DOES NOT MATCH WHAT IS SHOWN, THE SHEET SIZE HAS BEEN MODIFIED FROM A3S/B

### 3.6 Model Boundary Conditions – Transport

Initial TDS concentrations in each model layer were assigned based on the assumed concentrations of TDS versus depth shown on Figure 1.

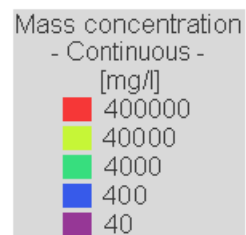
Three types of boundary conditions were used to simulate transport of TDS in groundwater: specified concentration boundaries, zero flux boundaries, and exit (Cauchy type) boundaries. The location of these boundaries is shown Figure 13.

Specified concentration boundaries of zero milligrams per litre (mg/L) (freshwater) were assigned along the bottom of all lakes assumed to have open taliks in connection with the deep groundwater flow regime. TDS predictions in the model do not account for changes in the TDS concentrations in these lakes; TDS from these sources will be accounted for in the Site Wide Water Quality Analysis. The numerical hydrogeologic model provides estimates of the groundwater flow from lakes over time to the TM or open pit for this purpose.

A specified concentration boundary of 500 mg/L was applied to Lake B4 starting in Year 2025 to represent that it will be dewatered and filled with contact water. A specified concentration boundary of 55,000 mg/L was applied to Lake B7 starting in Year 2025 to represent that it will be dewatered and then filled with saline water. The concentration of the saline water is an approximation and will need to be verified through surface water balance modelling. The saline concentration is likely to be variable given that it will mix with fresh water during freshet. Zero flux boundaries were assigned along the model bottom, which corresponds to the no flow boundaries described in Section 3.5.

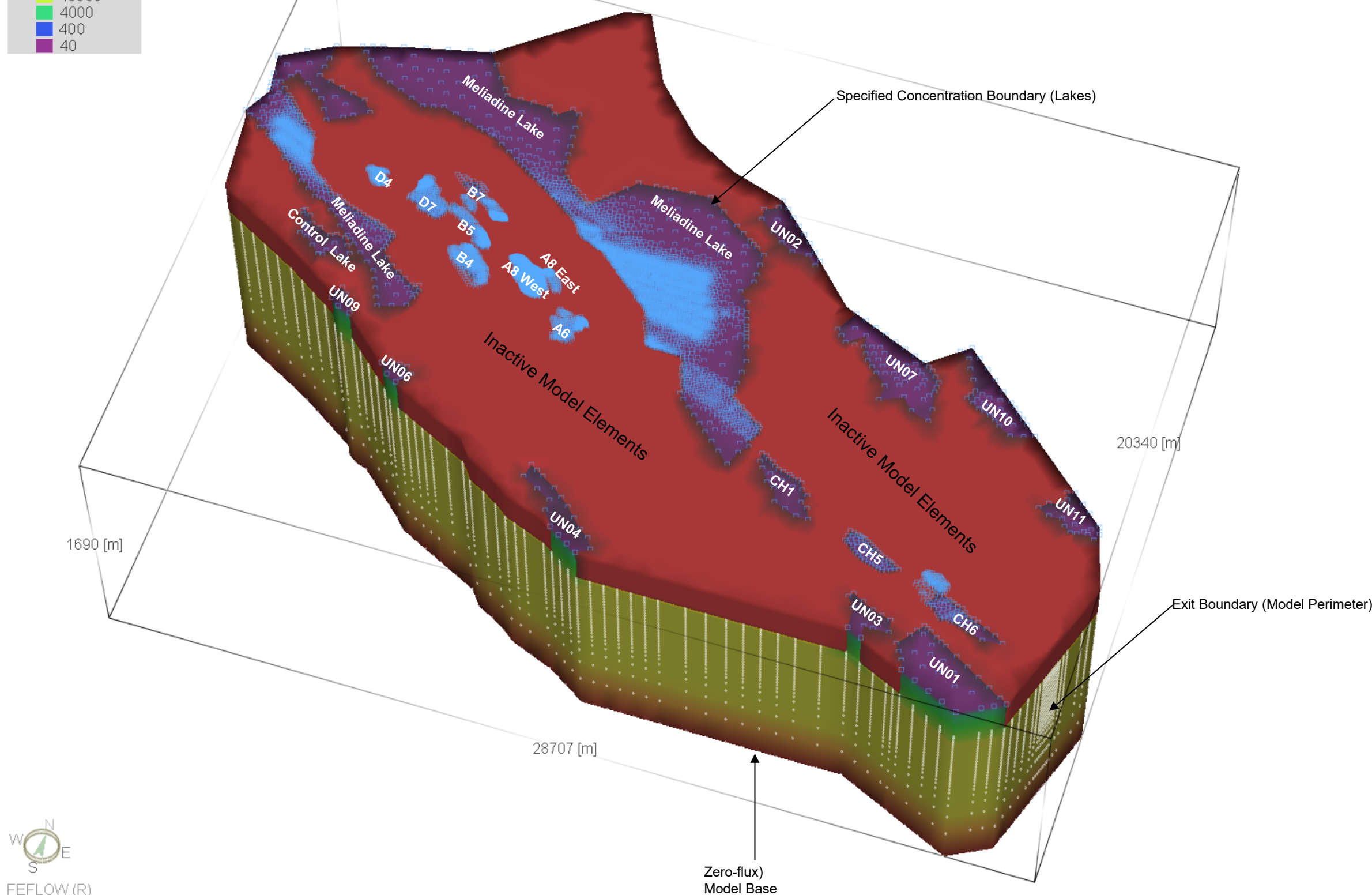
Exit (Cauchy type) boundaries were assigned to the nodes representing the pit walls and underground development. These boundaries simulated the movement of TDS mass out of the surrounding groundwater system and into the mine workings. Exit boundaries were also assigned to specified head boundaries along the perimeter of the model, allowing groundwater to enter or exit the model domain according to the predicted groundwater quality in the area of the specified head boundary.





# Legend

- Active Model Elements  
(Cryopeg and Unfrozen  
Bedrock)
- Inactive Model Elements  
(Permafrost Excluding Cryopeg)



CLIENT



CONSULTANT



YYYY-MM-DD 2024-01-24

PREPARED JL

DESIGNED HG

REVIEWED JL

APPROVED DC

PROJECT

AGNICO EAGLE MINES LIMITED  
MELIADINE MINE  
NUNAVUT

TITLE

**MODEL BOUNDARY CONDITIONS FOR  
TRANSPORT**

PROJECT NO.  
**CA0020476.6818**

PHASE

REV.  
0

FIGURE  
**13**

## 4.0 MODEL CALIBRATION

The calibration process involves refining the numerical model parameters to achieve the desired degree of correspondence between the model simulation results and the observations of the groundwater flow system, while reasonably representing the conceptual groundwater model. It consists of adjustments to hydraulic parameters within a reasonable range of values. If the hydraulic property adjustment fails to provide adequate calibration results, the conceptual model may be reviewed and refined, and the iterative adjustments of model parameters repeated.

The following sub-sections presents the calibration approach, targets and results of calibration. As documented in these sub-sections, a reasonable calibration is achieved to measured inflow and hydraulic heads, increasing model prediction confidence for predictions of groundwater inflow.

### 4.1 Calibration Approach

Due to the size of the model mesh and complexity of hydrostratigraphic units and boundary conditions, an automatic parameter estimation method was not appropriate for the model calibration, and calibration was carried out manually using professional judgement and observation to guide the trial-and-error changes to successive iterations during model calibration. During the calibration, the model was run repeatedly in transient model to simulate the development of the TM between 2015 (first year where groundwater inflow was observed) and 2020 (the most recent full year of mining) available prior to initiating this modelling study, and the model parameters (hydraulic conductivity and specific storage) were iteratively adjusted until a reasonable agreement between predicted and observed hydraulic heads and groundwater inflow rates near TM were achieved. Model parameter adjustments were limited to values considered reasonable for a given hydrostratigraphic unit in consideration of the measured data.

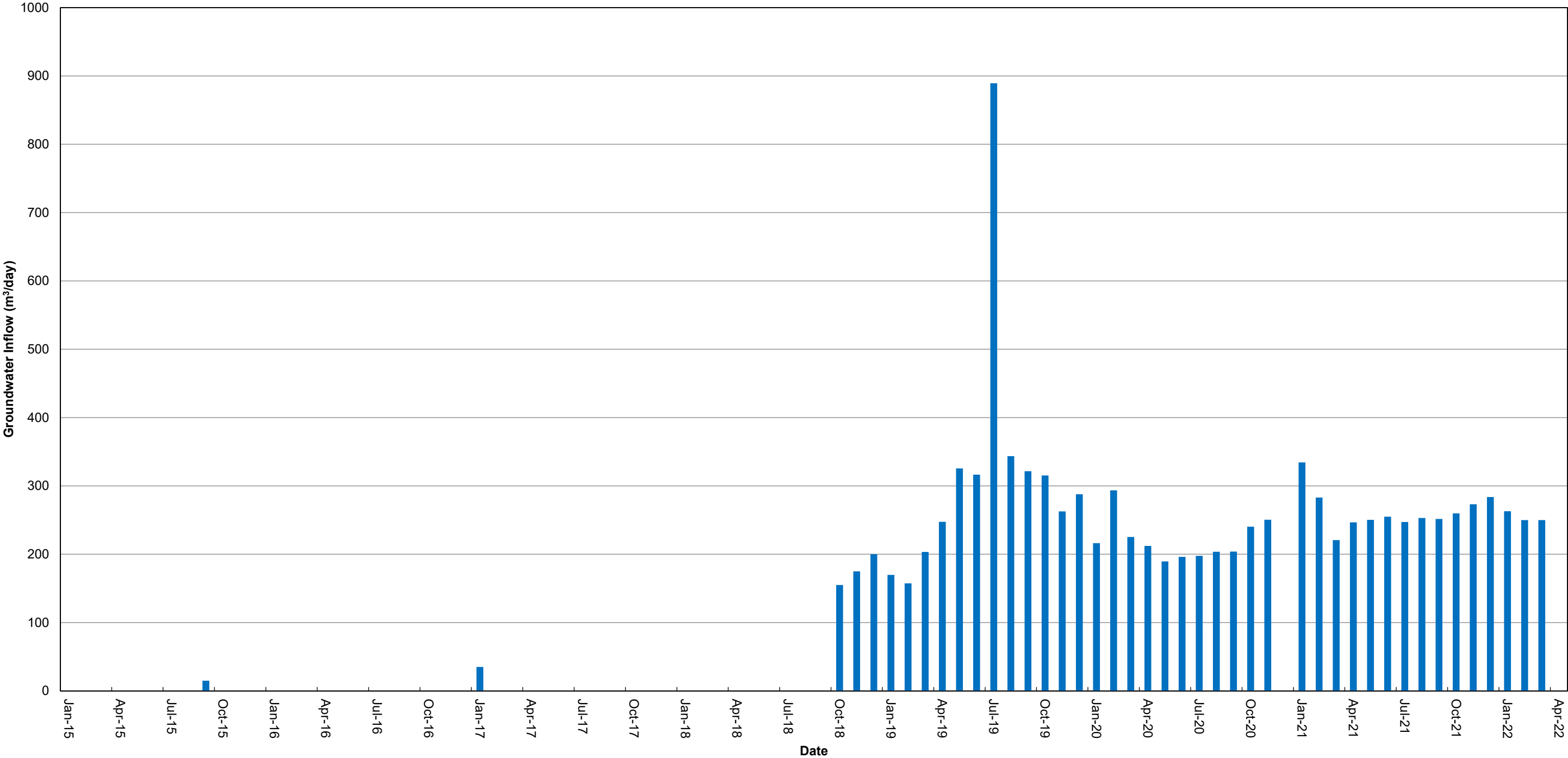
For the transient run, it is not practical to simulate the continual daily expansion of the underground development. Instead, the model boundaries were set to reflect ten development stages provided by Agnico Eagle for which calibration data is available. These stages included:

- Q4 2015, June 2016 and June 2017
- November 2018 and January 2019
- April and December 2020
- June and December 2021
- March 2022

### 4.2 Calibration Targets

Three data sets were used to assess the overall quality of calibration, as follows:

- Changes in hydraulic head observed in response to mining between 2015 and early 2022 at piezometers installed from TM.
- Changes in hydraulic head observed in response to the long-term recession test in the KMS Corridor at piezometers installed from TM.
- Estimated groundwater inflow to the TM between 2015 and early 2022 (Figure 14).



CLIENT



CONSULTANT



YYYY-MM-DD	2024-01-24
PREPARED	JL
DESIGNED	HG
REVIEWED	JL
APPROVED	DC

PROJECT

AGNICO EAGLE MINES LIMITED  
MELIADINE MINE  
NUNAVUT

TITLE

**GROUNDWATER INFLOW MEASUREMENTS  
FOR THE TIRIGANIAQ UNDERGROUND MINE**

PROJECT NO.  
**CA0020476.6818**

PHASE

REV.

0

FIGURE

14



## 4.3 Calibration Results

### 4.3.1 Post-Calibration Hydraulic Parameters

As described in Section 5.1, hydraulic parameters (hydraulic conductivity, specific storage, and grouting properties) were adjusted from the initial values presented on Table 1 to achieve a suitable match between predicted and observed hydraulic heads and TM inflows. Table 4 and Table 5 summarizes the final parameters for hydraulic conductivity and storage that provide the best fit to the measured data.

**Table 4: Post-Calibration Hydraulic Properties – Competent Bedrock**

Hydrostratigraphic Unit	Depth Interval (mbgs)	Hydraulic Conductivity <sup>(a)</sup> (m/s)	Specific Storage (1/m)	Effective Porosity (-)
Shallow Sedimentary Rock Formations	0 to 55	$3 \times 10^{-6}$	$1 \times 10^{-6}$	0.001
Sedimentary Rock Formations <sup>(b)</sup>	55 to <u>280</u>	<u><math>7 \times 10^{-9}</math></u>	$1 \times 10^{-6}$	0.001
	<u>280</u> to <u>370</u>	$3 \times 10^{-9}$	$1 \times 10^{-6}$	0.001
	<u>370</u> to 1500	$3 \times 10^{-9}$	<u><math>1 \times 10^{-6}</math></u>	0.001
Shallow Sedimentary Rock Formations	0 to 55	$3 \times 10^{-6}$	<u><math>1 \times 10^{-7}</math></u>	0.001
Mafic Volcanic Rock Formations <sup>(b)</sup>	55 to <u>280</u>	<u><math>7 \times 10^{-9}</math></u>	<u><math>1 \times 10^{-7}</math></u>	0.001
	<u>280</u> to <u>370</u>	<u><math>2 \times 10^{-9}</math></u>	<u><math>1 \times 10^{-7}</math></u>	0.001
	<u>370</u> to 1500	$3 \times 10^{-10}$	<u><math>1 \times 10^{-7}</math></u>	0.001

(a) Linearly decreasing hydraulic conductivity with temperature is assumed within the cryopeg zone with a full order of magnitude decrease assumed at the top of the basal cryopeg, and hydraulic conductivity equivalent to unfrozen rock at the bottom of the basal cryopeg.

(b) Underline value indicates parameter value changed from pre-calibration value (Table 1).

**Table 5: Post-Calibration Hydraulic Properties – Enhanced Permeability Zones**

Hydrostratigraphic Unit	Primary Deposit Area	Depth Interval (m) <sup>(b)</sup>	Thickness (m)	Hydraulic Conductivity (m <sup>2</sup> /s) <sup>(a)</sup>	Specific Storage (1/m)	Effective Porosity (-)
Lower Fault Zone (Outside of KMS Corridor)	Tiriganiaq	0 to 1000	20	$1 \times 10^{-7}$	$1 \times 10^{-7}$	0.005
Lower Fault Zone (in KMS Corridor)	Tiriganiaq	0 to 1000	5	$2 \times 10^{-7}$	$1 \times 10^{-7}$	0.005
RM-175	Tiriganiaq	0 to 1000	5	$5 \times 10^{-8}$	$1 \times 10^{-7}$	0.005
KMS Fault Corridor	Tiriganiaq	0 to 1000	100 (variable)	<u><math>5 \times 10^{-7}</math></u>	$1 \times 10^{-7}$	0.005
North Fault	Tiriganiaq	0 to 1000	5	$5 \times 10^{-7}$	$1 \times 10^{-7}$	0.005
A	Wesmeg	0 to 1000	6	<u><math>5 \times 10^{-7}</math></u>	$1 \times 10^{-7}$	0.005
B	Wesmeg	0 to 1000	5	<u><math>5 \times 10^{-7}</math></u>	$1 \times 10^{-7}$	0.005
C	Wesmeg	0 to 1000	3	<u><math>1 \times 10^{-6}</math></u>	$1 \times 10^{-7}$	0.005
D	Wesmeg	0 to 1000	5	<u><math>5 \times 10^{-7}</math></u>	$1 \times 10^{-7}$	0.005
Pyke Fault	Pump	0 to 1000	15	<u><math>2 \times 10^{-7}</math></u>	$1 \times 10^{-7}$	0.005
AP0	Pump	0 to 1000	3	<u><math>1 \times 10^{-6}</math></u>	$1 \times 10^{-7}$	0.005
ENE2	Pump	0 to 1000	5	<u><math>5 \times 10^{-7}</math></u>	$1 \times 10^{-7}$	0.005
ENE3	Pump	0 to 1000	3	<u><math>1 \times 10^{-6}</math></u>	$1 \times 10^{-7}$	0.005
UM2	Pump	0 to 1000	6	<u><math>5 \times 10^{-7}</math></u>	$1 \times 10^{-7}$	0.005
NW1	Pump	0 to 1000	5	$5 \times 10^{-7}$	$1 \times 10^{-7}$	0.005
WNW1	F Zone	0 to 1000	3	<u><math>1 \times 10^{-6}</math></u>	$1 \times 10^{-7}$	0.005
WNW2	F Zone	0 to 1000	3	<u><math>1 \times 10^{-6}</math></u>	$1 \times 10^{-7}$	0.005
UAU2	F Zone	0 to 1000	2	<u><math>2 \times 10^{-6}</math></u>	$1 \times 10^{-7}$	0.005
Fault 1	Discovery	0 to 1000	5	$1 \times 10^{-6}$	$1 \times 10^{-7}$	0.005
Fault 2	Discovery	0 to 1000	5	$1 \times 10^{-6}$	$1 \times 10^{-7}$	0.005
Fault 3	Discovery	0 to 1000	5	$1 \times 10^{-6}$	$1 \times 10^{-7}$	0.005

- (a) Hydraulic conductivity within the unfrozen permafrost zone is assumed to be lower than in the deeper unfrozen rock. Linearly decreasing hydraulic conductivity with temperature is assumed within this zone with a full order of magnitude decrease assumed at the top of the basal cryopeg, and hydraulic conductivity equivalent to unfrozen rock at the bottom of the basal cryopeg.
- (b) Where fault hydraulic conductivity is less than shallow rock, the fault was excluded from 0 to 60 m depth interval. Where fault hydraulic conductivity is greater than shallow rock, fault was included within 0 to 60 m depth interval.
- (c) Underline value indicates parameter value changed from pre-calibration value (Table 1).

The following changes were made to improve the match to mine inflow and hydraulic heads:

- The hydraulic conductivity of the competent bedrock between approximately 55 and 500 mbgs was lowered to improve the match between measured and predicted groundwater inflows. Prior to model calibration, the assigned hydraulic conductivity for this depth interval had generally been raised relative to the previous groundwater model to reflect supplemental data collection in 2021 (WSP 2024b). This change, however, was found to significantly over predict groundwater inflow and the hydraulic conductivity was therefore reduced. Assigned hydraulic conductivity values are within the range of measurements measured from packer testing (WSP 2024b).
- The hydraulic conductivity of the faults within the Project area were reduced by a factor of 2, except for the Lower Fault Zone, KMS Corridor and RM-175. This change improved the match between measured and predicted groundwater inflows and is supported by recent supplemental fault testing in 2021 (test results from supplemental testing were lower than the final values at the end of calibration).

The hydraulic conductivity of the KMS corridor was increased slightly from  $4 \times 10^{-7}$  to  $5 \times 10^{-7}$  m/s to improve the match to predicted changes in hydraulic head during the long-term recession test.

### 4.3.2 Measured versus Predicted Hydraulic Head

Figure 7 and Figure 15 show the locations of boreholes with vibrating wire sensors to monitor hydraulic heads. A summary of pressure monitoring data used in the calibration process is presented on Figure 16 to Figure 19. The pressure recorded at each vibrating wire sensor was converted to equivalent fresh water hydraulic head according to the following equation:

$$P = \rho_{fw} * g * H_{fw}$$

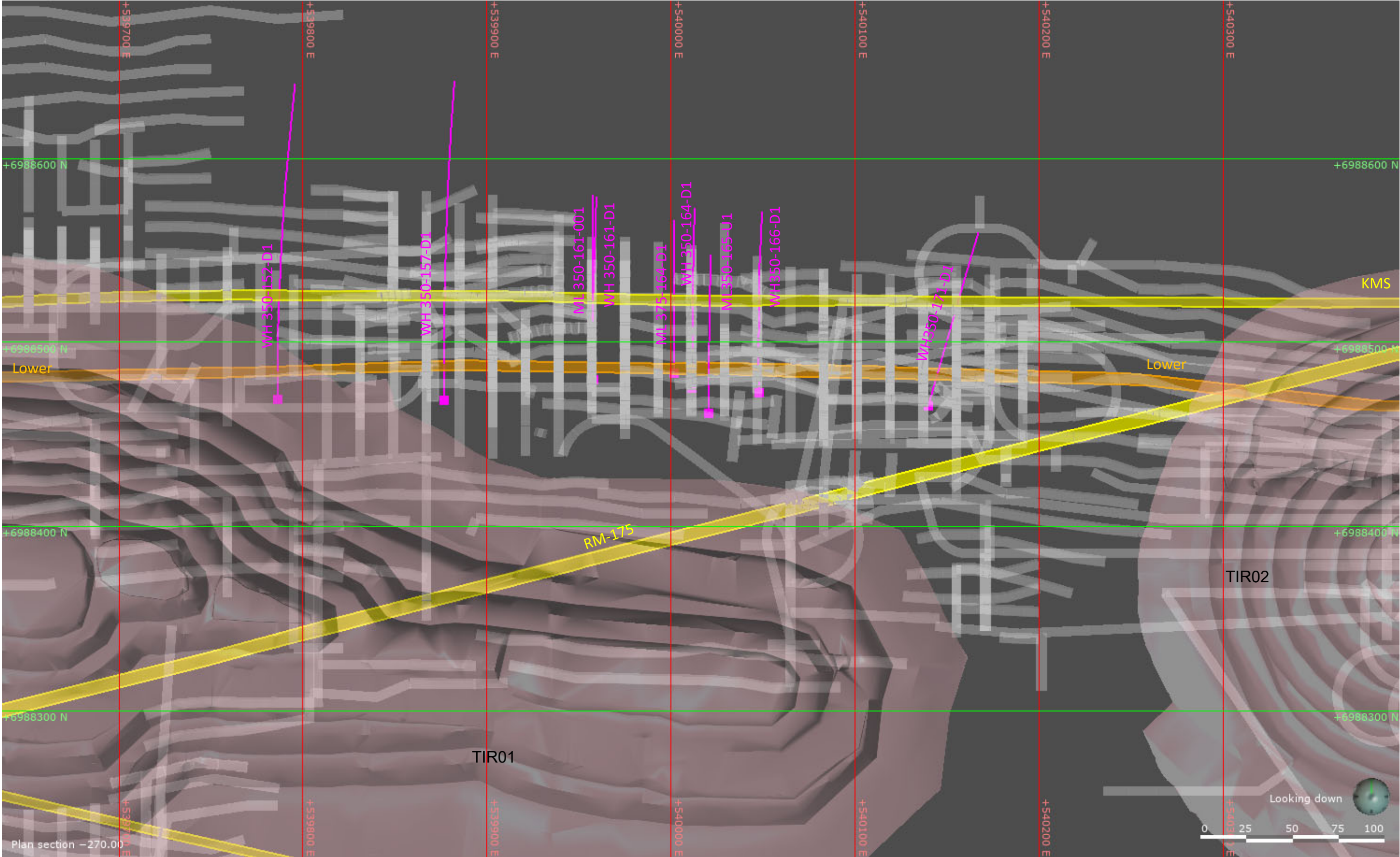
$$H_{fw} = \frac{P}{\rho_{fw} * g}$$

Where P is the pressure measured at the sensor,  $\rho_{fw}$  is density of freshwater ( $1000 \text{ kg/m}^3$ ), g is the gravitation constant ( $9.8 \text{ m/s}^2$ ) and  $H_{fw}$  is the equivalent freshwater hydraulic head. The long-term trends in the measured hydraulic head data (expressed as equivalent freshwater hydraulic head) were used to understand the extent of depressurization near the underground and the relative changes in that hydraulic head at different locations as mining progressed (the relative change in hydraulic head was a calibration target).

#### 4.3.2.1 Flow Recession Test

Figure 7 and Figure 15 show the locations of boreholes with vibrating wire sensors to monitor hydraulic heads. Figure 20 to Figure 22 presents a summary of the measured versus predicted hydraulic head during the flow recession test in 2020. During this test, a 'pumping well' was allowed to flow from an open borehole for approximately 72 hrs and the change in head recorded at piezometers installed nearby. The flowing borehole was simulated in FEFLOW using discrete features elements to represent the borehole, with a specified flux boundary assigned to the collar equal to the observed flow rate.

During the test, minimal response to testing was observed in piezometer sensors at PZ-RF-200-01 and PZ-ES225-02 within the Volcanic Rock Formations, which is consistent with model predictions. For the other piezometers, responses were observed that were also reasonably reproduced by the model predictions (Figure 21 and Figure 22) indicating a good fit to the observed data. Where a response was observed, the magnitude of the response varied from less than 10 m to just under 25 m. As discussed in the existing conditions report (WSP 2024b) the responses were variable, even for sensors equidistance to the pumping well, suggesting some compartmentalization within the corridor. Given that this compartmentalization can not be accurately defined nor practically simulated in a model of this scale, the objective of the calibration was to match the general trend of data, which would indicate the model can predict the influence of this corridor on groundwater flow to the underground. This objective is considered to have been achieved.



**LEGEND**

- Regional Fault
- Supplemental Faults Based on 2020 Agnico Eagle Review
- Borehole Collar / Borehole Trace

Fault traces are shown for an elevation of -270 masl.

CLIENT



CONSULTANT



YYYY-MM-DD	2024-01-24
PREPARED	JL
DESIGNED	HG
REVIEWED	JL
APPROVED	DC

PROJECT

AGNICO EAGLE MINES LIMITED  
MELIADINE MINE  
NUNAVUT

TITLE

**BOREHOLE LOCATIONS FOR HYDRAULIC TESTING AND  
GROUNDWATER SAMPLING – KMS CORRIDOR**

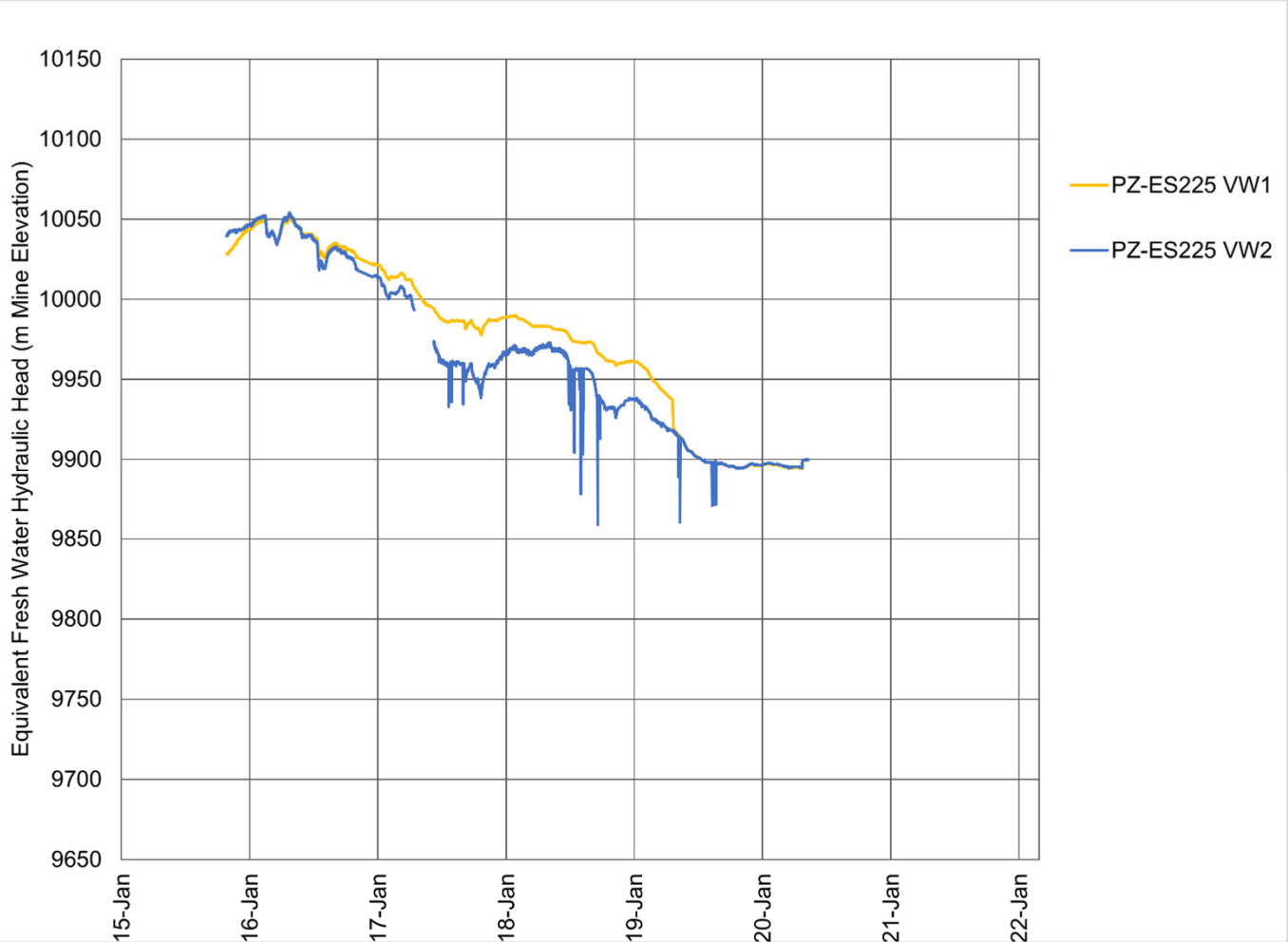
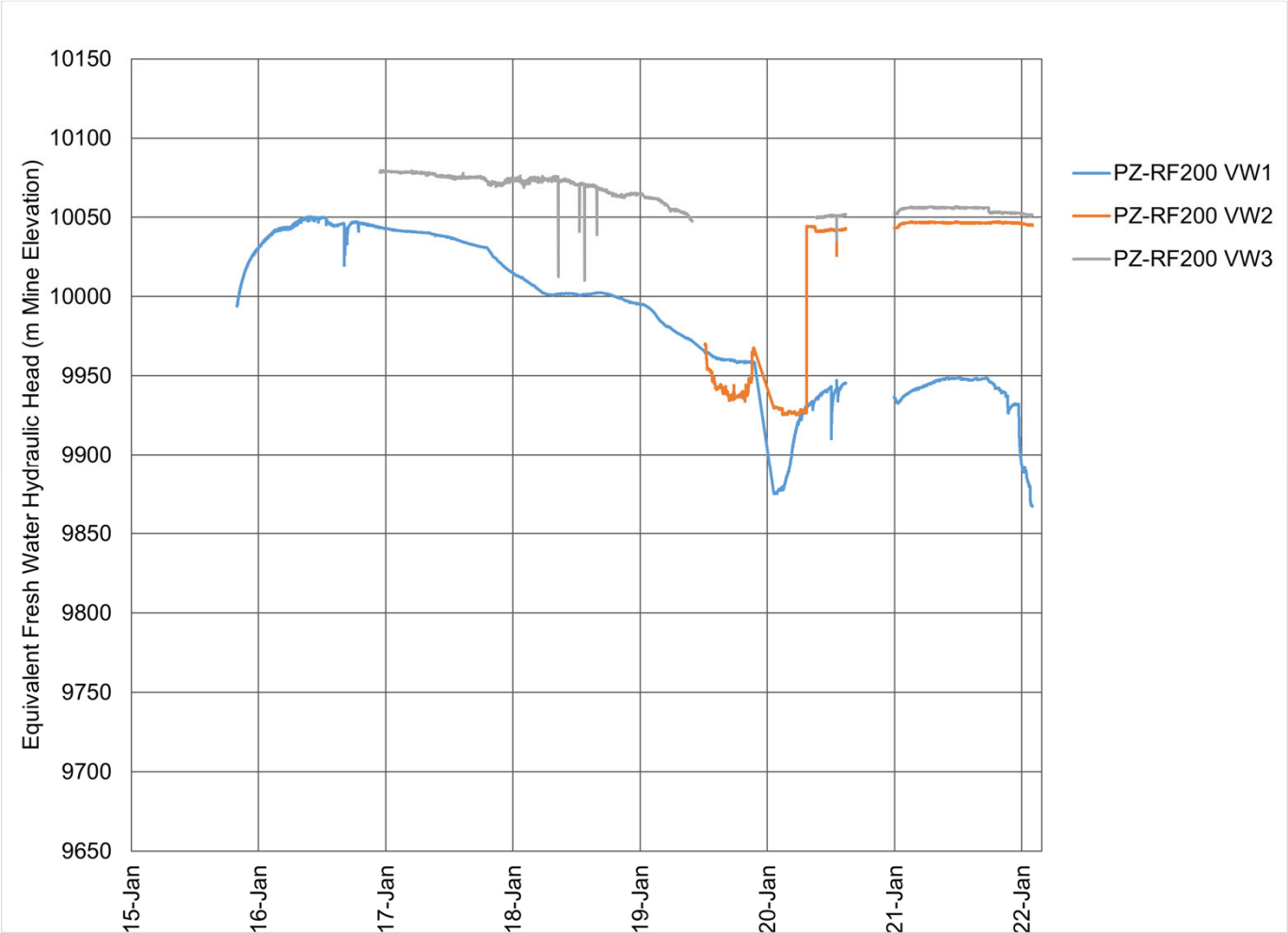
PROJECT NO.  
**CA0020476.6818**

PHASE

REV.  
0

FIGURE  
**15**

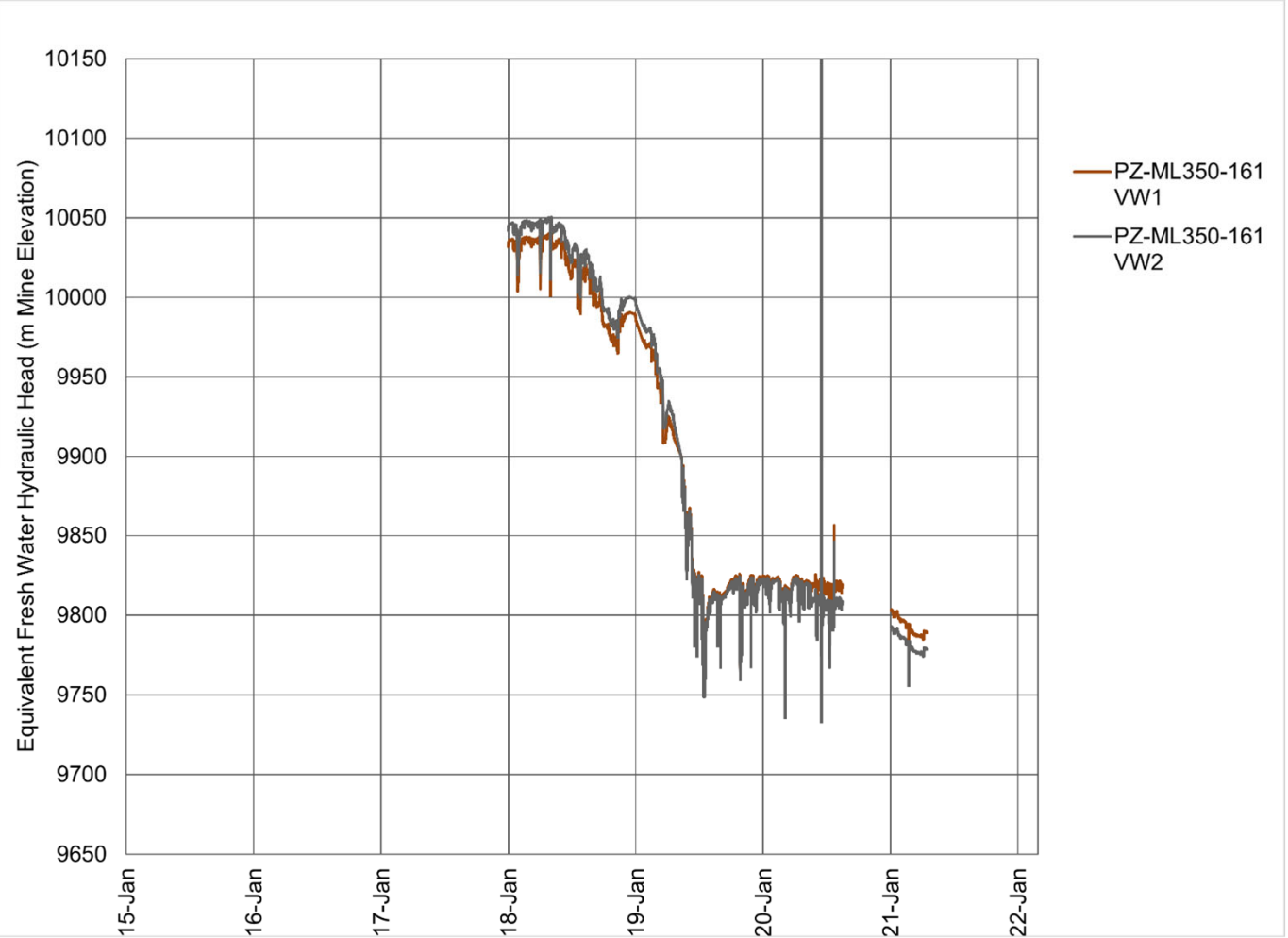
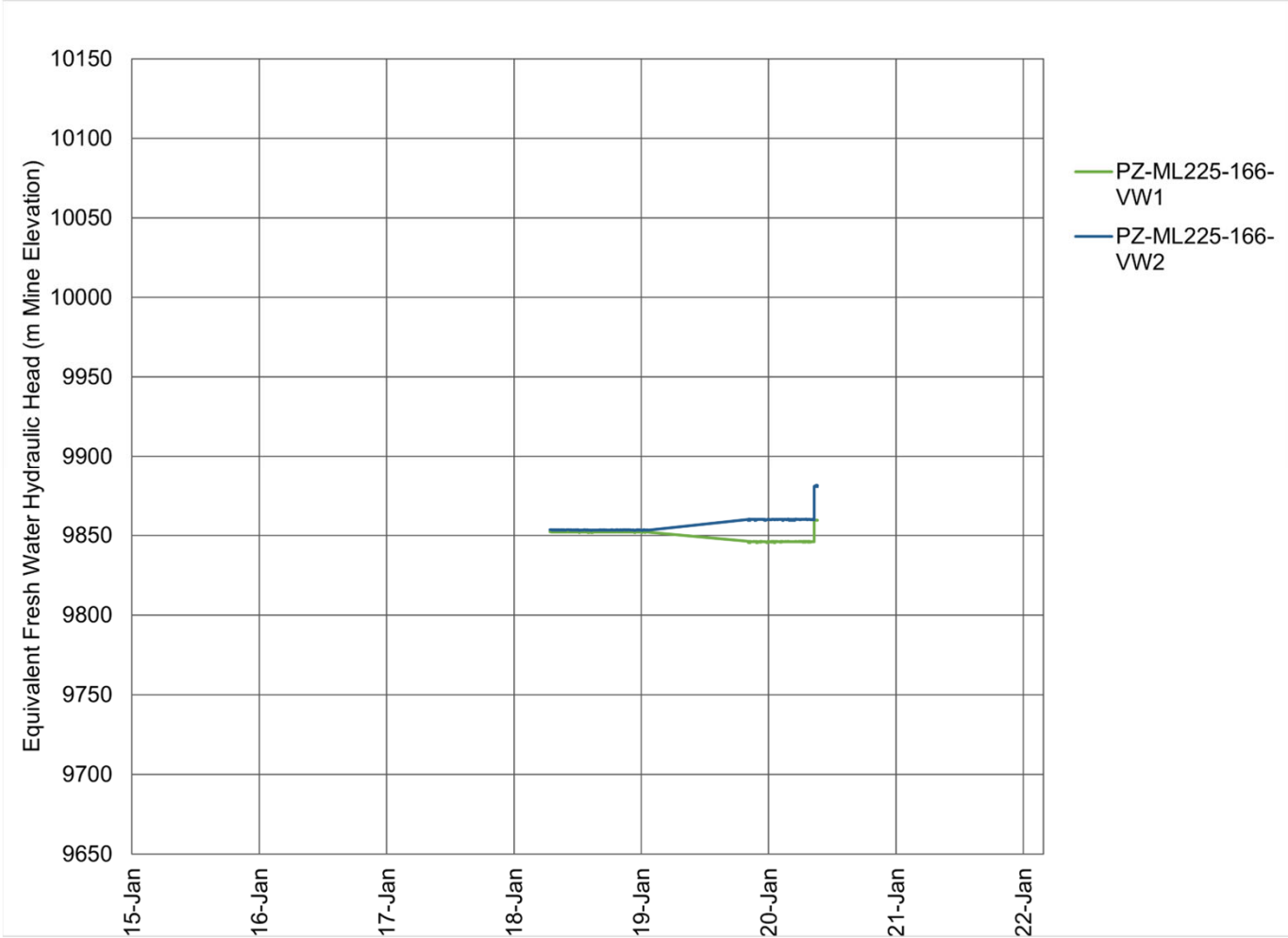




Piezometer	Borehole ID	Node	Sensor Elevation (m Mine Grid)	Sensor Elevation (masl)	Approximate Sensor Depth (mbgs)	Hydrostratigraphic Unit
PZ-RF200-01	TIS-200-001	VW1	9729.3	-270.7	325.7	Volcanic Rock Formations
		VW2	9680.9	-319.1	374.1	Volcanic Rock Formations
		VW3	9435.3	-564.7	619.7	Volcanic Rock Formations
PZ-ES225-02	TIS-225-001	VW1	9726.8	-273.2	328.2	Volcanic Rock Formations
		VW2	9678.5	-321.5	376.5	Volcanic Rock Formations

As-Built Stage	Deepest Elevation of Mine (masl)	Deepest Elevation of Mine (m Mine Grid)
Q4 2015	-235	9765
Jun-16	-280	9720
Jun-17	-325	9675
Nov-18	-355	9645
Jan-19	-355	9645
Apr-20	-375	9625
Mar-22	-430	9570

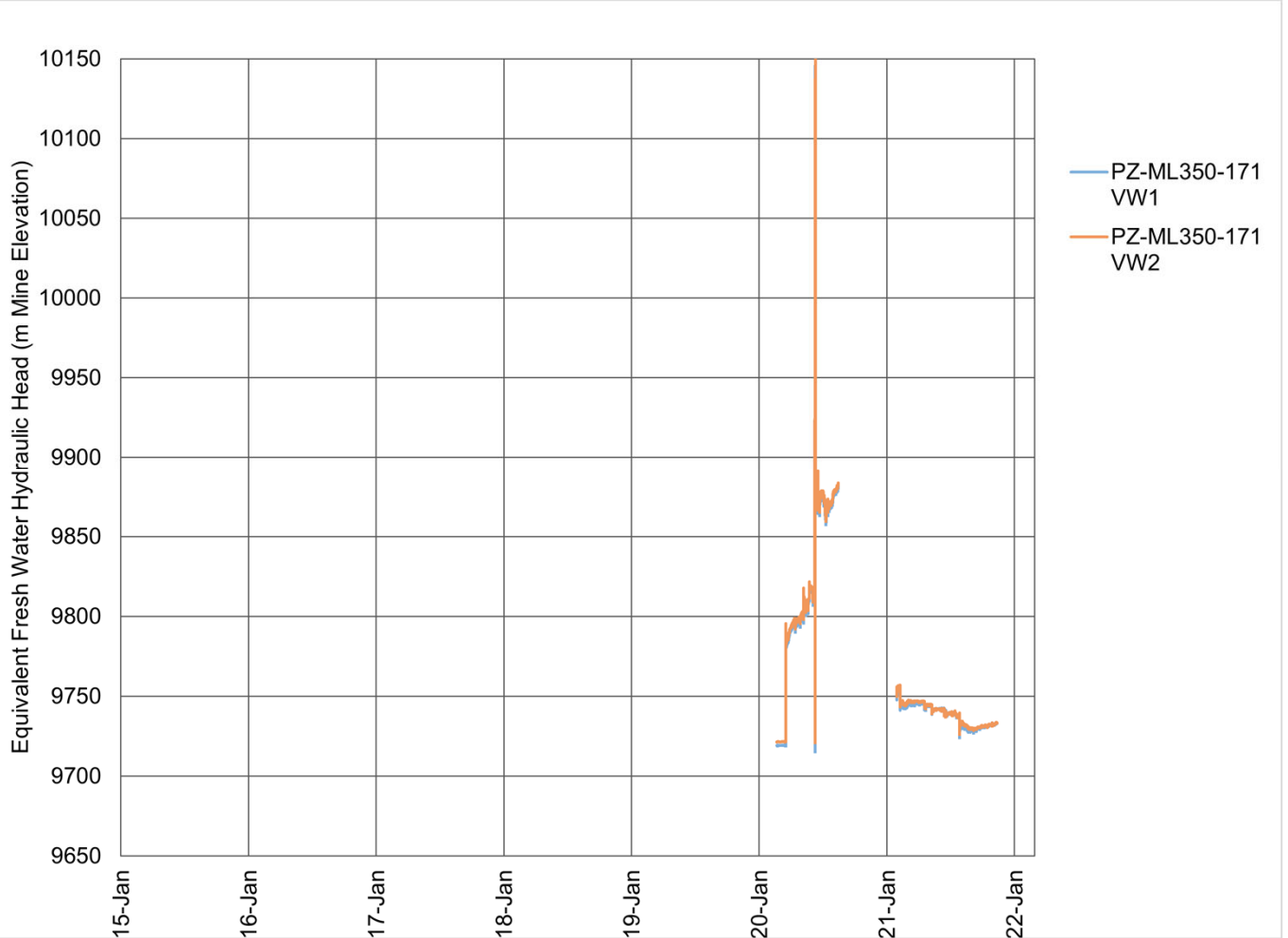
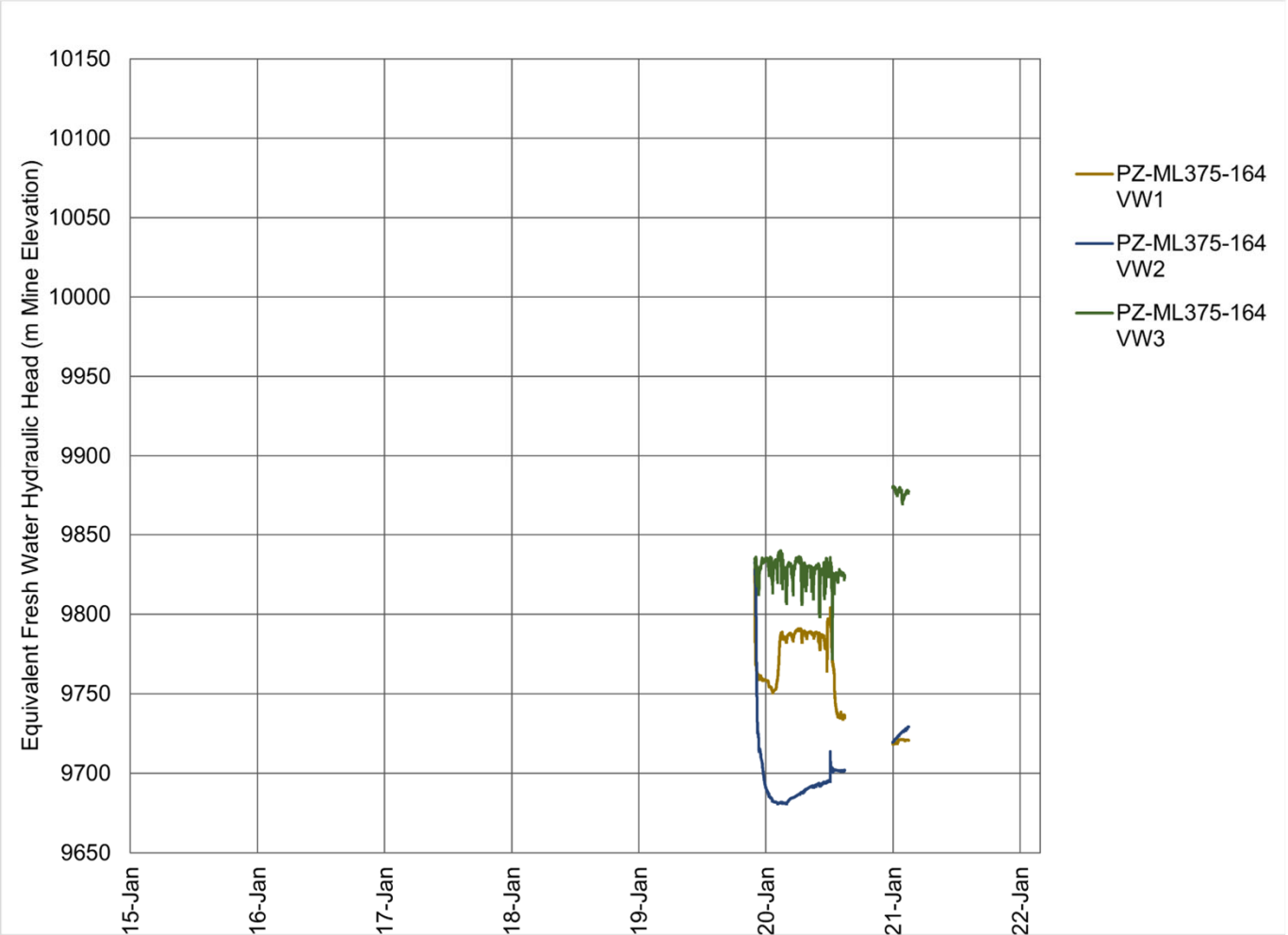
Note: Mine Grid Elevation is 10,000 m higher than Geodetic Elevation (masl).



Piezometer	Borehole ID	Node	Sensor Elevation (m Mine Grid)	Sensor Elevation (masl)	Approximate Sensor Depth (mbgs)	Hydrostratigraphic Unit
PZ-ML17-225-166	ML17-225-166-F1	VW1	9856.1	-143.9	198.9	Volcanic Rock Formations
		VW2	9856	-144	199.3	Lower Fault/KMS Corridor
PZ-ML17-350-161	ML17-350-161-001	VW1	9732	-268	323.4	Lower Fault/KMS Corridor
		VW2	9732	-268	323.2	Lower Fault/KMS Corridor

Note: Mine Grid Elevation is 10,000 m higher than Geodetic Elevation (masl).

As-Built Stage	Deepest Elevation of Mine (masl)	Deepest Elevation of Mine (m Mine Grid)
Q4 2015	-235	9765
Jun-16	-280	9720
Jun-17	-325	9675
Nov-18	-355	9645
Jan-19	-355	9645
Apr-20	-375	9625
Mar-22	-430	9570

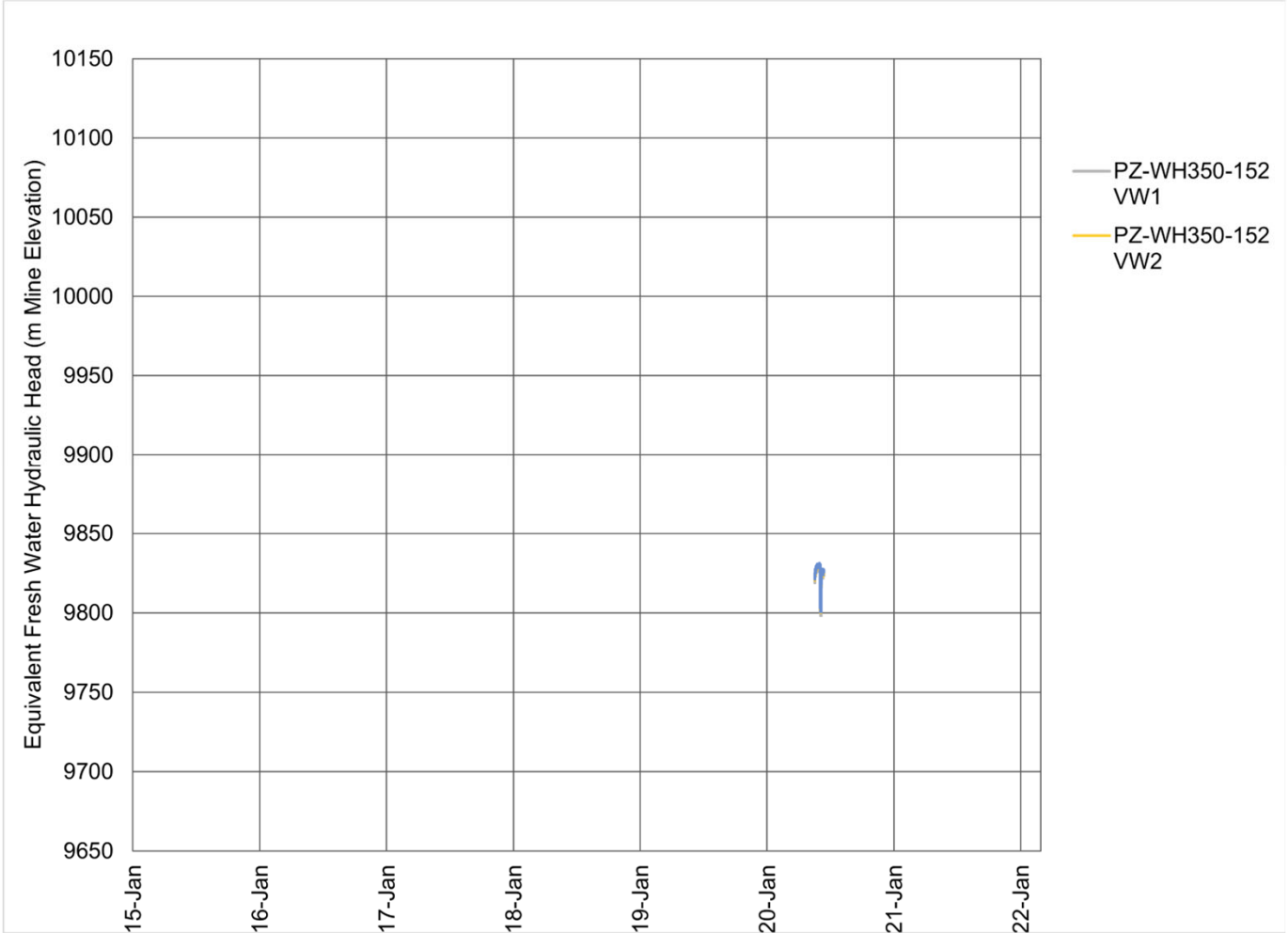


Piezometer	Borehole ID	Node	Sensor Elevation (m Mine Grid)	Sensor Elevation (masl)	Approximate Sensor Depth (mbgs)	Hydrostratigraphic Unit
PZ-ML375-164	ML376-164-D1	VW1	9694	-306	361	Lower Fault/KMS Corridor
		VW2	9683	-317	372	Lower Fault/KMS Corridor
		VW3	9681	-319	374	Lower Fault/KMS Corridor
PZ-ML350-171	ML350-171-D1	VW1	9714	-286	341	Lower Fault/KMS Corridor
		VW2	9712	-288	343	Lower Fault/KMS Corridor

Note: Mine Grid Elevation is 10,000 m higher than Geodetic Elevation (masl).

As-Built Stage	Deepest Elevation of Mine (masl)	Deepest Elevation of Mine (m Mine Grid)
Q4 2015	-235	9765
Jun-16	-280	9720
Jun-17	-325	9675
Nov-18	-355	9645
Jan-19	-355	9645
Apr-20	-375	9625
Mar-22	-430	9570

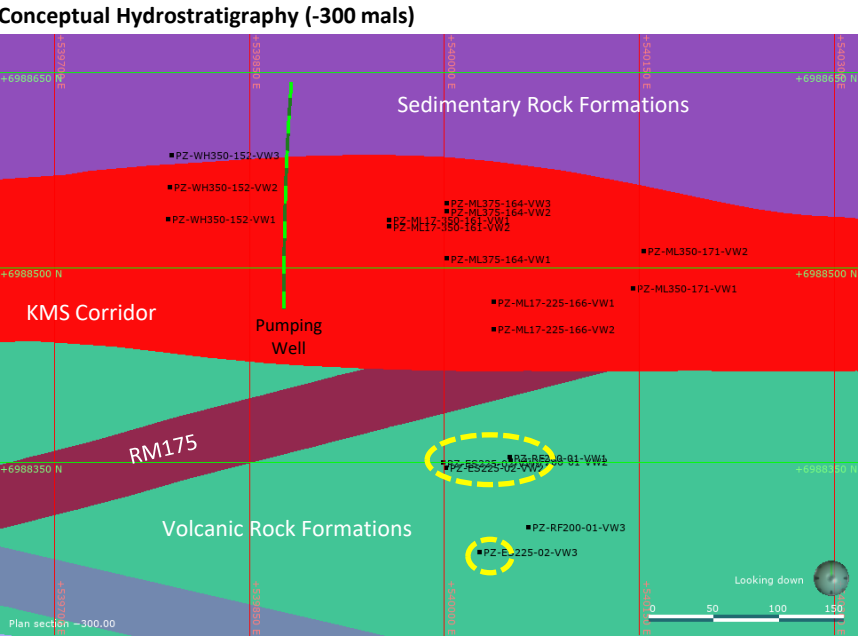
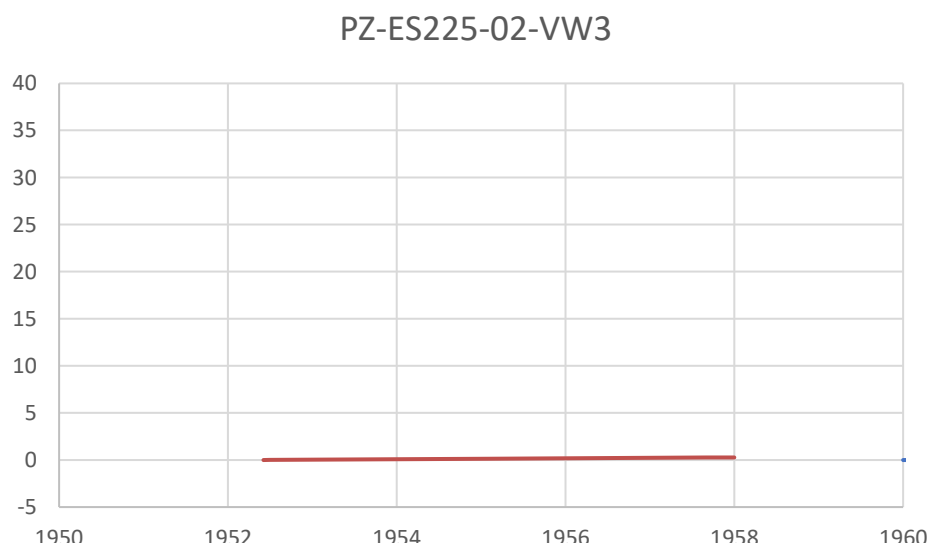
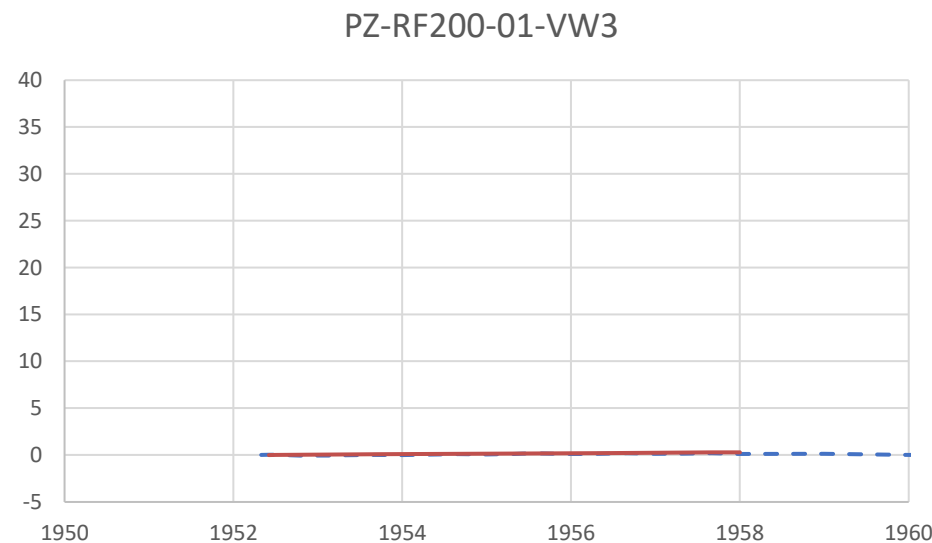
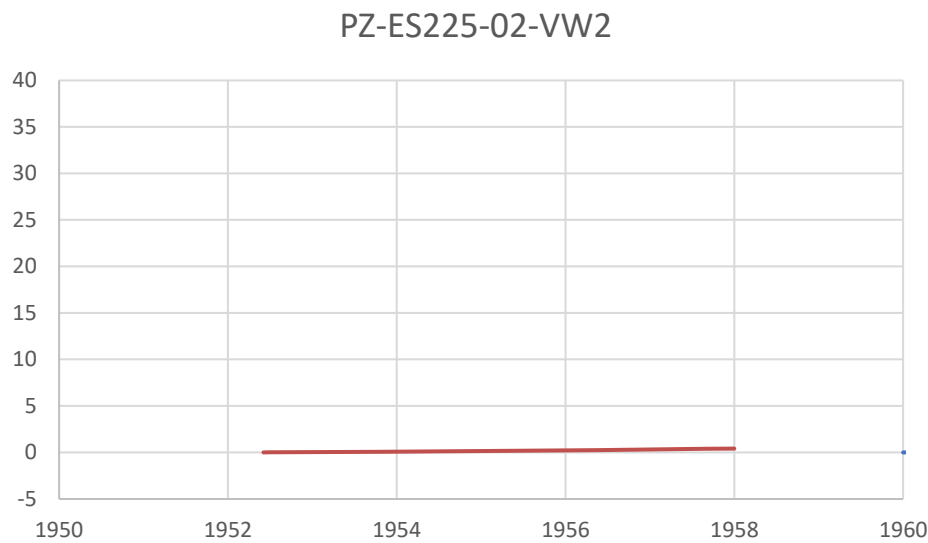
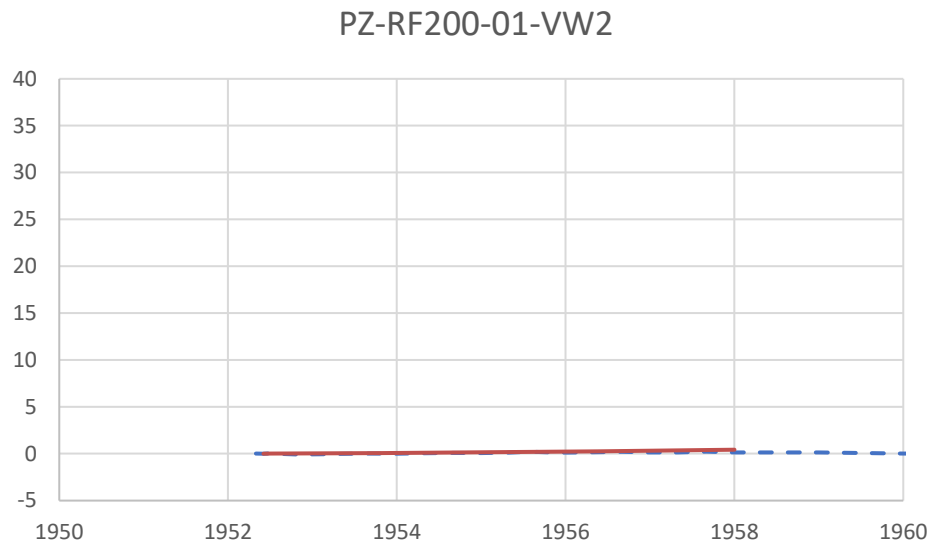
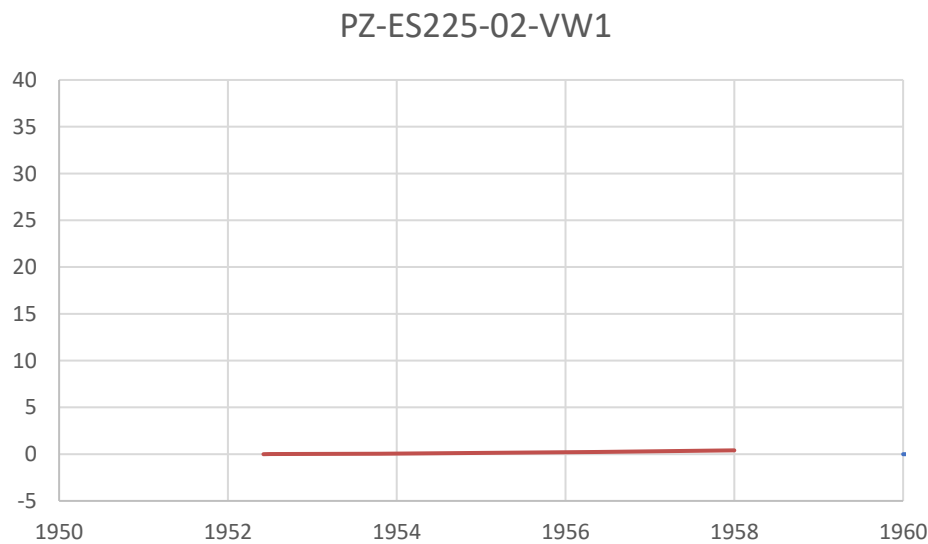
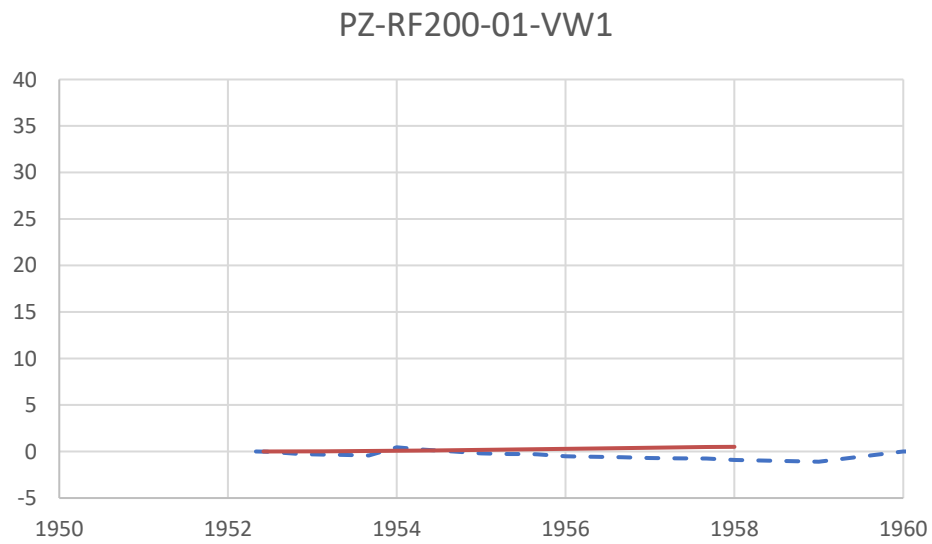




Piezometer	Borehole ID	Node	Sensor Elevation (m Mine Grid)	Sensor Elevation (masl)	Approximate Sensor Depth (mbgs)	Hydrostratigraphic Unit
PZ-WH350-152	WH350-152-D1	VW1	9724	-276	331	Lower Fault/KMS Corridor
		VW2	9720	-280	335	Lower Fault/KMS Corridor
		VW3	9715	-285	340	Sedimentary Rock Formations

Note: Mine Grid Elevation is 10,000 m higher than Geodetic Elevation (masl).

As-Built Stage	Deepest Elevation of Mine (masl)	Deepest Elevation of Mine (m Mine Grid)
Q4 2015	-235	9765
Jun-16	-280	9720
Jun-17	-325	9675
Nov-18	-355	9645
Jan-19	-355	9645
Apr-20	-375	9625
Mar-22	-430	9570



Legend

- Observed
- Predicted

Notes:  
X-axis on plots are model simulation time in days. Day zero corresponds to the start of Year 2015.  
Y-axis on plots are predicted / measured changed in hydraulic head (masl).

Piezometer	Borehole ID	Node	Sensor Elevatin (Mine Grid)	Sensor Elevation (masl)	Approximate Sensor Depth (mbgs)
PZ-RF200-01	TIS-200-001	VW1	9729.3	270.70	325.7
		VW2	9680.9	319.10	374.1
		VW3	9435.3	564.70	619.7
PZ-ES225-02	TIS-225-001	VW1	9726.8	273.20	328.2
		VW2	9678.5	321.50	376.5

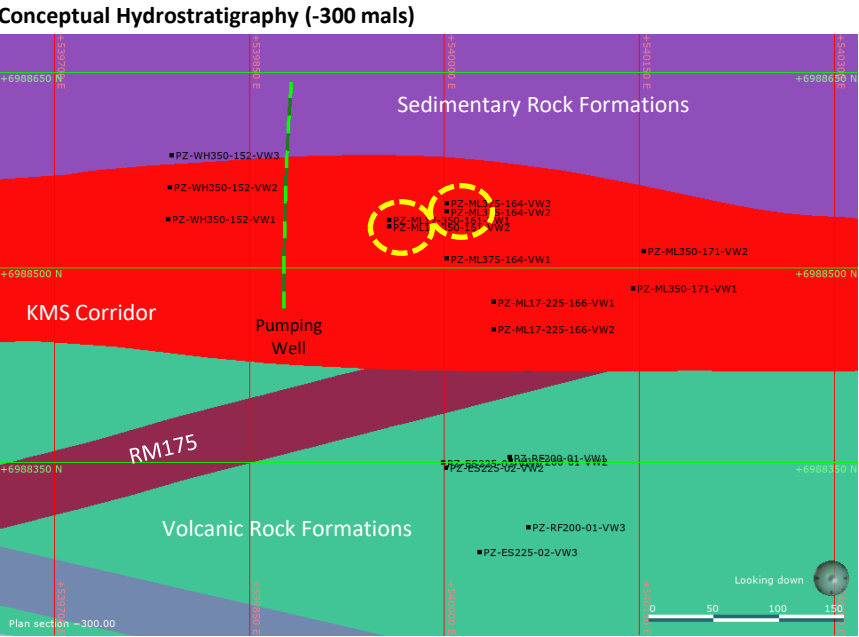
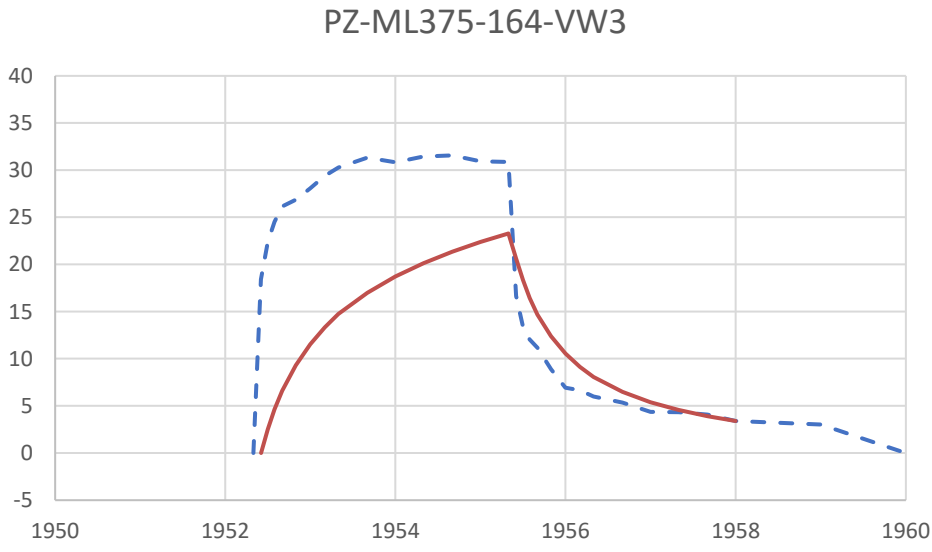
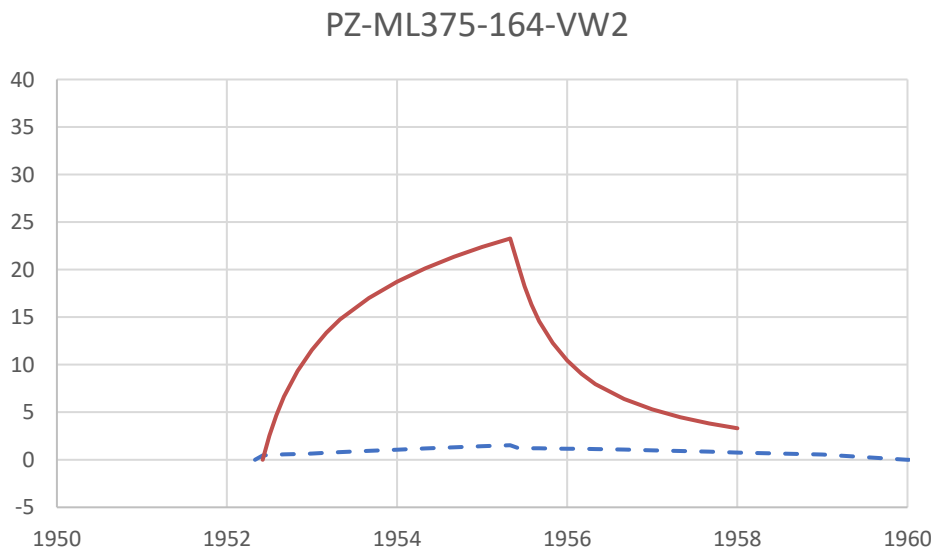
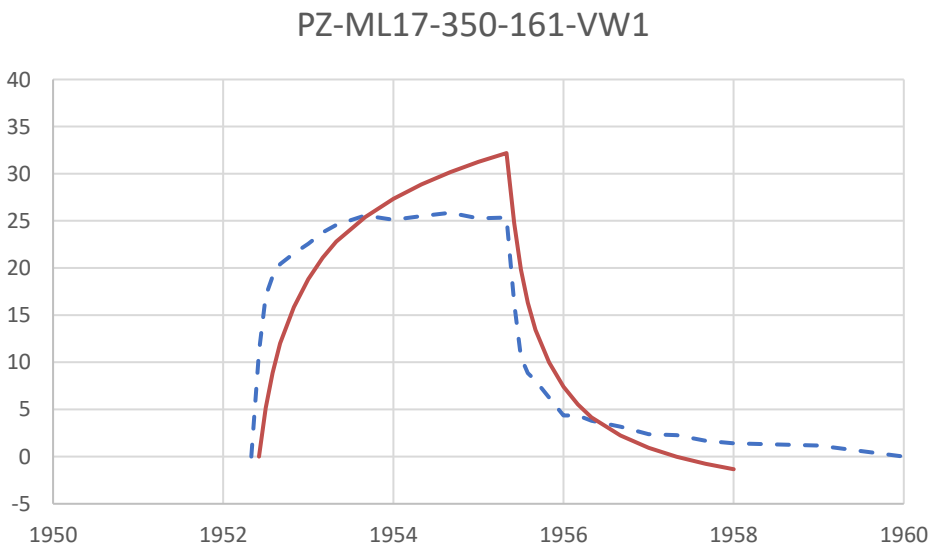
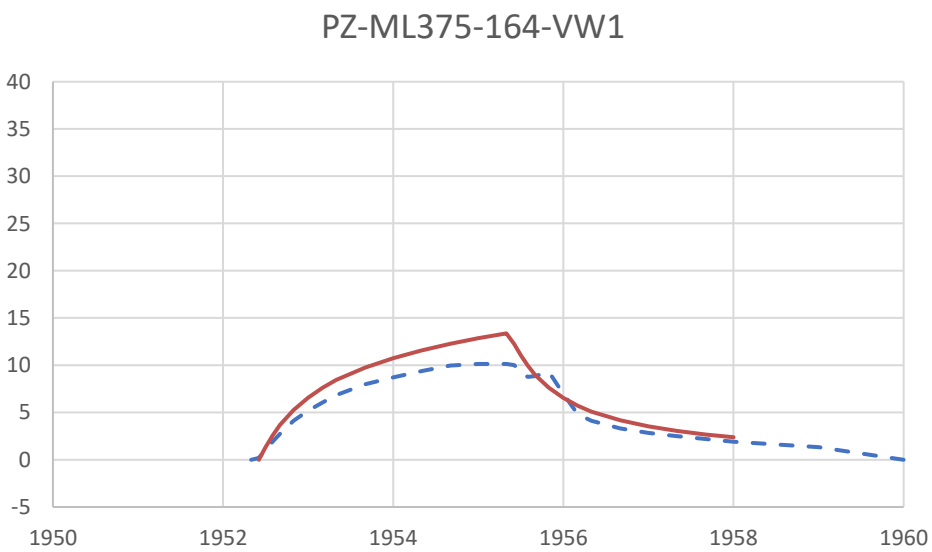
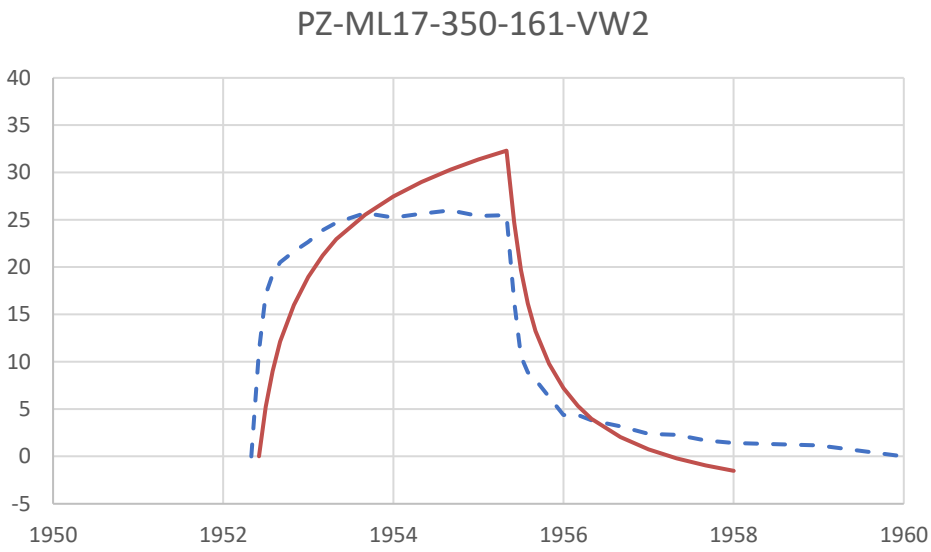


YYYY-MM-DD	2024-01-24
PREPARED	JL
DESIGNED	HG
REVIEWED	JL
APPROVED	DC

PROJECT  
AGNICO EAGLE MINES LIMITED  
MELIADINE MINE  
NUNAVUT

TITLE  
**RECESSION TEST CALIBRATION RESULTS  
PZ-RF200-01 AND PZ-ES225-02**

PROJECT NO.	PHASE	REV.	FIGURE
CA0020476.6818		0	20



Legend

- Observed
- Predicted

Notes:  
X-axis on plots are model simulation time in days. Day zero corresponds to the start of Year 2015.  
Y-axis on plots are predicted / measured change in hydraulic head (masl).

Piezometer	Borehole ID	Node	Sensor Elevatin (Mine Grid)	Sensor Elevation (masl)	Approximate Sensor Depth (mbgs)
PZ-ML17-350-161	ML17-350-161-001	VW1	9732	268.40	323.4
		VW2	9732	268.20	323.2
PZ-ML375-164	ML376-164-D1	VW1	9694	306.00	361.0
		VW2	9683	317.00	372.0
		VW3	9681	319.00	374.0

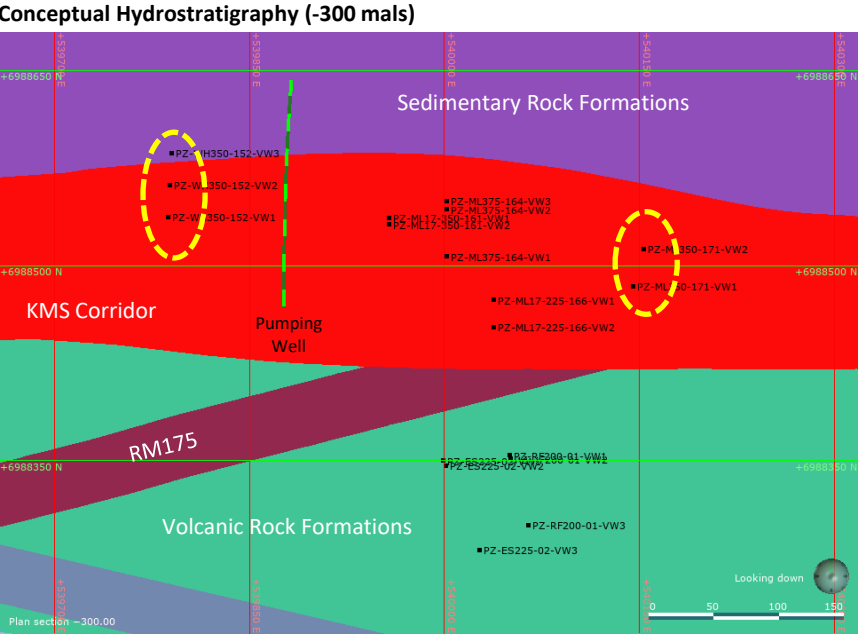
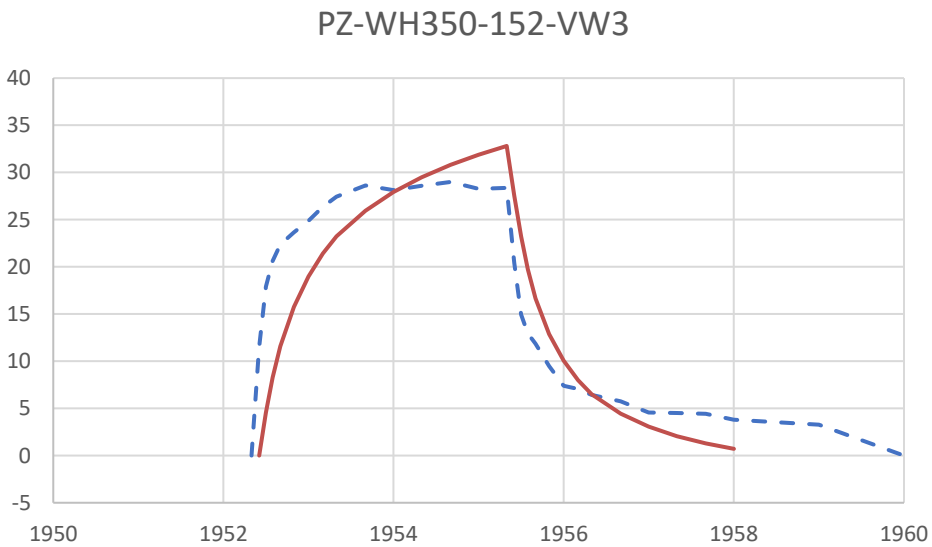
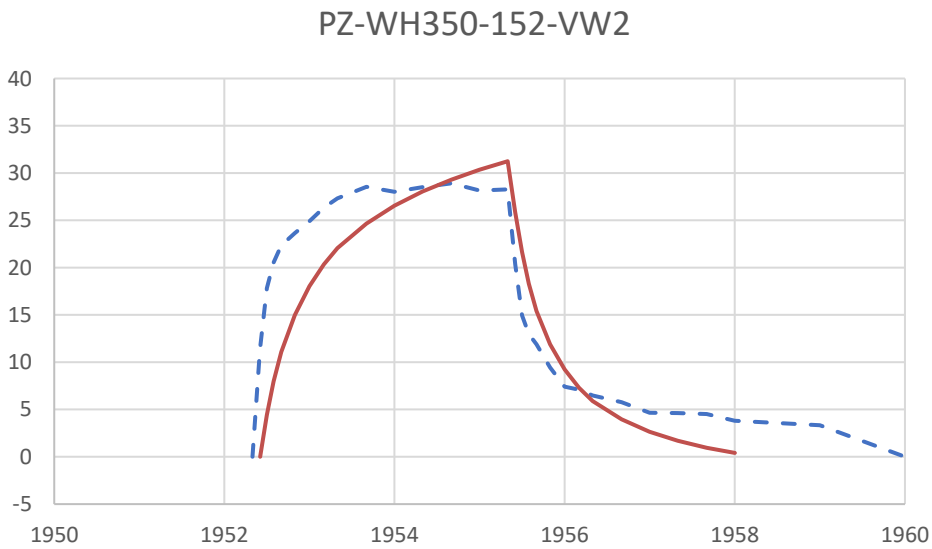
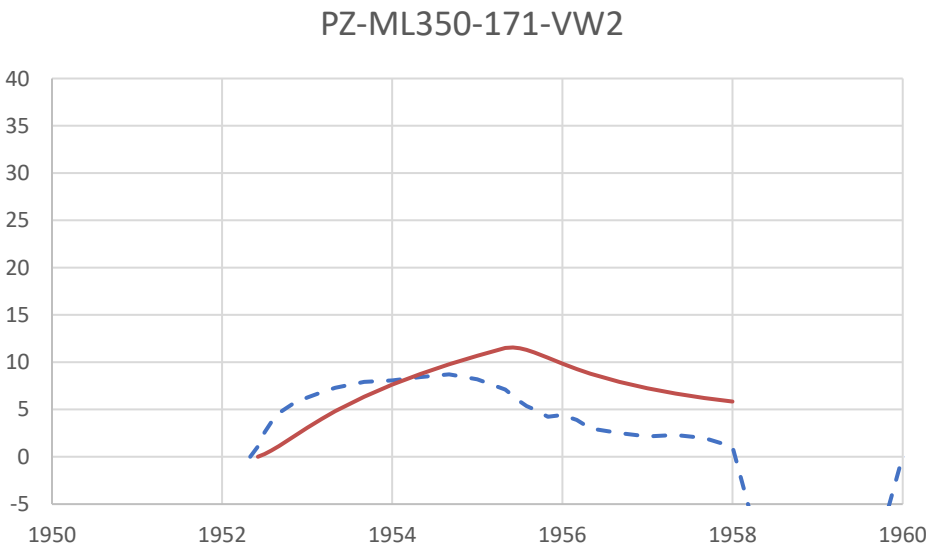
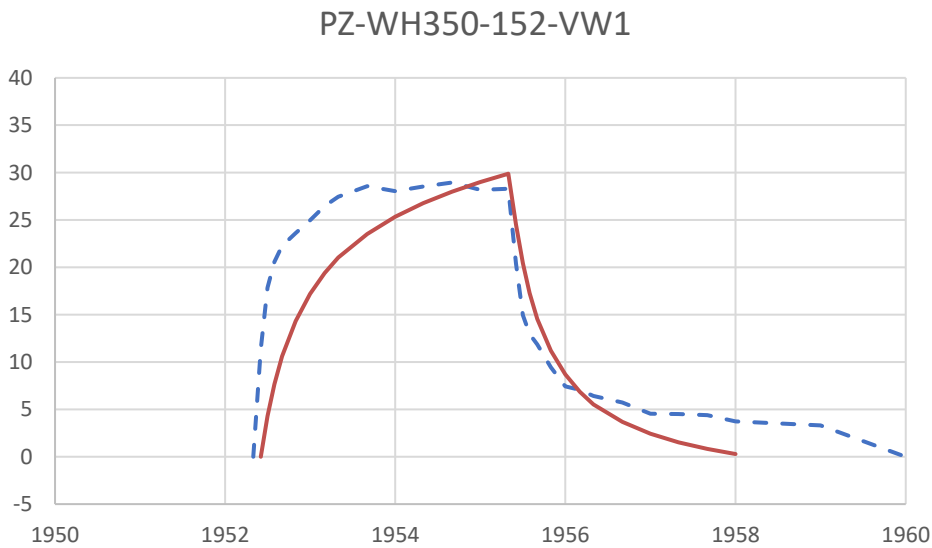
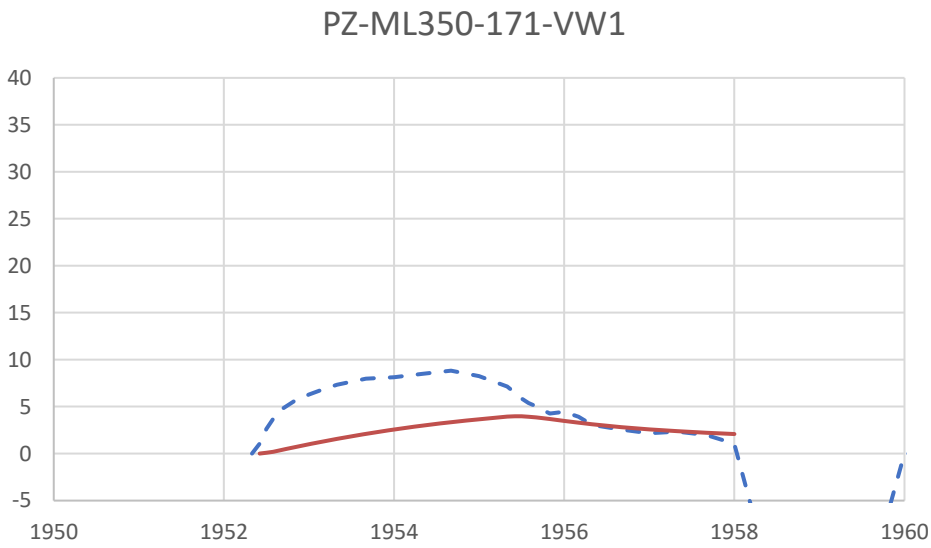


YYYY-MM-DD	2024-01-24
PREPARED	JL
DESIGNED	HG
REVIEWED	JL
APPROVED	DC

PROJECT  
AGNICO EAGLE MINES LIMITED  
MELIADINE MINE  
NUNAVUT

TITLE  
**RECESSION TEST CALIBRATION RESULTS  
PZ-ML177-350-161 AND PZ-ML375-164**

PROJECT NO.	PHASE	REV.	FIGURE
CA0020476.6818		0	21



Legend

- Observed
- Predicted

Notes:  
X-axis on plots are model simulation time in days. Day zero corresponds to the start of Year 2015.  
Y-axis on plots are predicted / measured change in hydraulic head (masl).

Piezometer	Borehole ID	Node	Sensor Elevatin (Mine Grid)	Sensor Elevation (masl)	Approximate Sensor Depth (mbgs)
PZ-ML350-171	ML350-171-D1	VW1	9714	286.00	341.0
		VW2	9712	288.00	343.0
PZ-WH350-152	WH350-152-D1	VW1	9724	276.00	331
		VW2	9720	280.00	335
		VW3	9715	285.00	340



YYYY-MM-DD	2024-01-24
PREPARED	JL
DESIGNED	HG
REVIEWED	JL
APPROVED	DC

PROJECT  
AGNICO EAGLE MINES LIMITED  
MELIADINE MINE  
NUNAVUT

TITLE  
**RECESSION TEST CALIBRATION RESULTS  
PZ-ML350-171 AND PZ-WH350-152**

PROJECT NO.	PHASE	REV.	FIGURE
CA0020476.6818		0	22

#### **4.3.2.2 Long-term Hydraulic Head Monitoring**

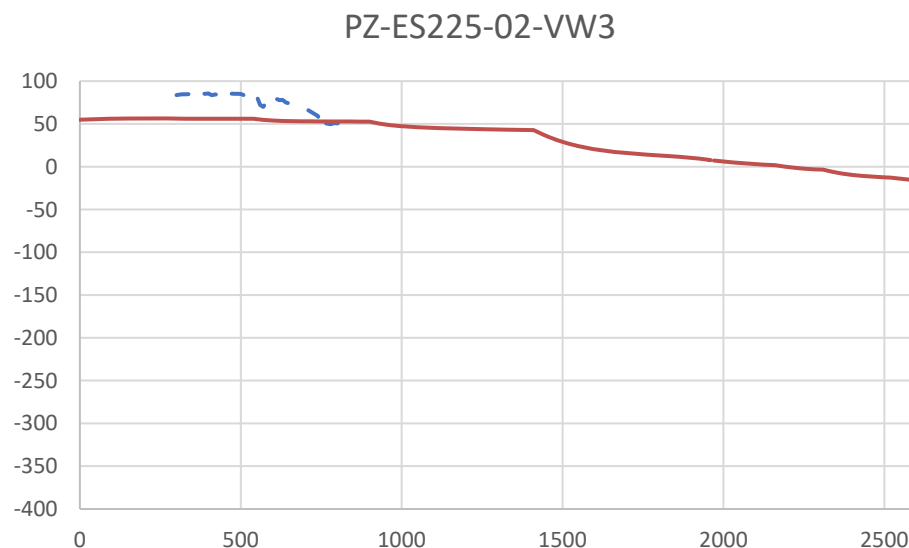
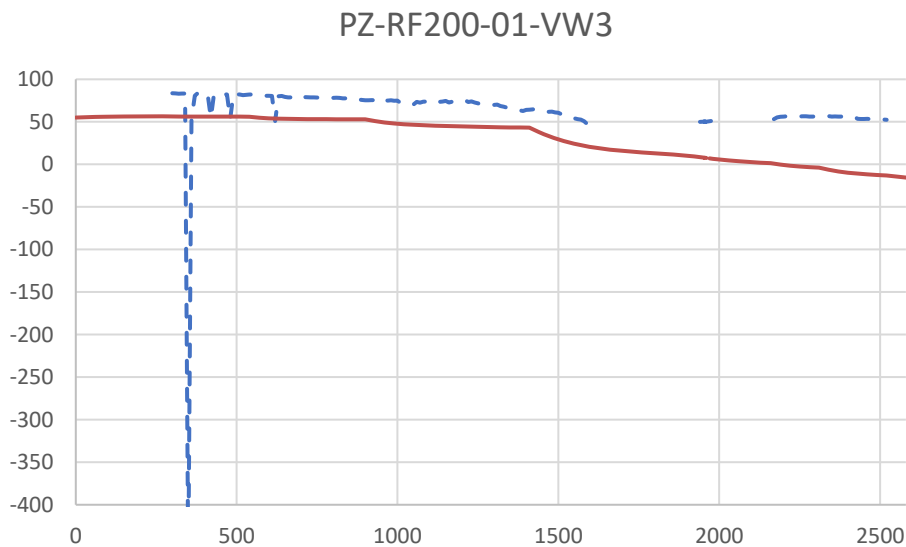
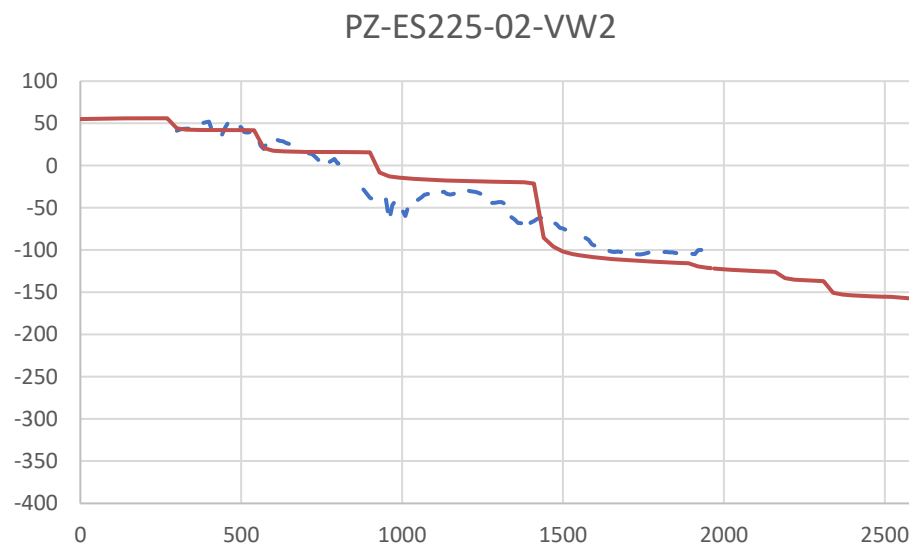
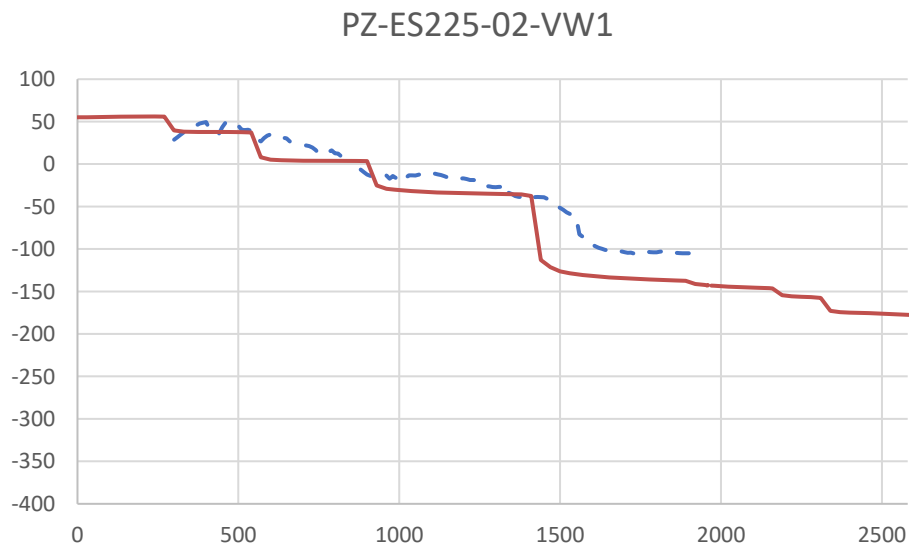
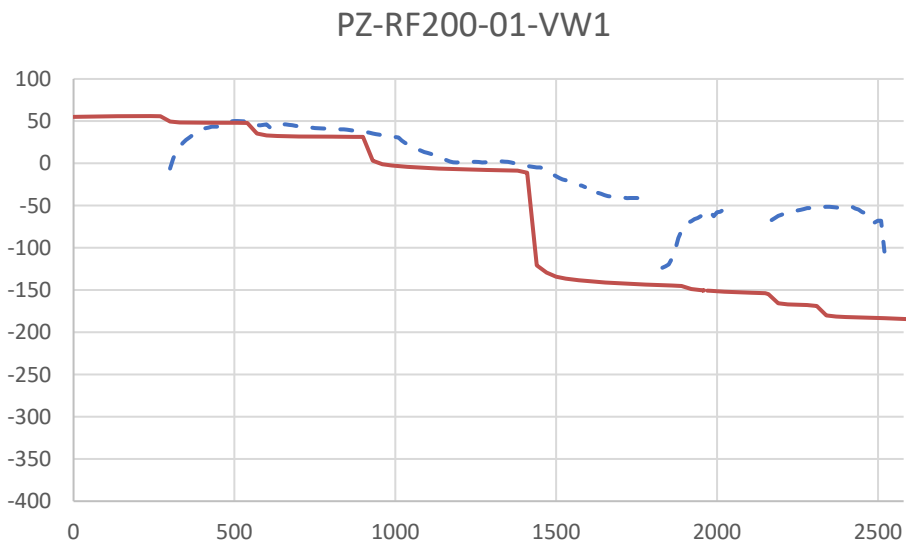
Figure 23 to Figure 25 presents the predicted versus observed hydraulic head in the piezometers installed near Tiriganiaq. The observed data in these figures has been smoothed to reflect the average trend of the data and to facilitate easier comparison to model predictions. The observed data is responsive to the actual progress of the TM for the period of record available for the transducers. The longest data set is available for the PZ-RF200-01 and PZ-ES225, followed by PZ-ML-360-161, which was installed in the 2015 Underground Program (Golder 2016). The remaining piezometers have shorter records, having been recently installed at the TM in support of the 2020 flow recession testing.

The predicted data presented on Figure 23 to Figure 25 is representative of the progression of the underground through the ten as-built development stages included in the transient calibration model. Despite this simplification of the mine plan, the trend of the predicted data reasonably matches the trend of the observed data, indicating a good calibration has been achieved. A precise fit was never considered reasonable to achieve given the simplifications of the mine plan, faults and representation of grouting in the model, however given the model reproduces the general trend of these data, the model is considered capable of reproducing groundwater flow conditions in the area of the underground for the objectives of the model.

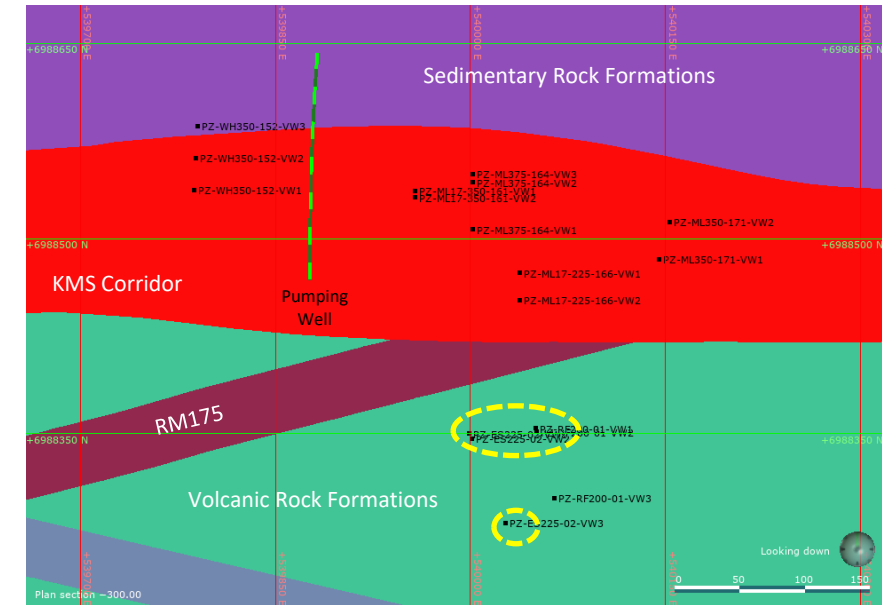
#### **4.3.3 Measured versus Predicted Groundwater Inflow**

Figure 26 presents a summary of measured versus predicted groundwater flow to the TM at the end of calibration. Predicted inflows are generally within a factor of 1.5 of measured inflows, and in general are similar to, or above the estimated inflows. Exceptions are the peak monthly flows measured in 2019 and 2020 during periods where boreholes were allowed to free drain into the underground as part of recession testing. Model calibration does not simulate this condition and therefore underestimates this period of flows.

Overall mass balance error in the model domain was less than 0.1%, indicating numerical stability in the predicted inflows. A mass balance error of less than 0.1% indicates the total inflow to the model domain was within 0.1% of outflow to the model domain.



Conceptual Hydrostratigraphy (-300 mals)



Legend

- Observed
- Predicted

Notes:  
X-axis on plots are model simulation time in days. Day zero corresponds to the start of Year 2015.  
Y-axis on plots are predicted / measured hydraulic head (masl).

Piezometer	Borehole ID	Node	Sensor Elevatin (Mine Grid)	Sensor Elevation (masl)	Approximate Sensor Depth (mbgs)
PZ-RF200-01	TIS-200-001	VW1	9729.3	270.70	325.7
		VW2	9680.9	319.10	374.1
		VW3	9435.3	564.70	619.7
PZ-ES225-02	TIS-225-001	VW1	9726.8	273.20	328.2
		VW2	9678.5	321.50	376.5



CONSULTANT

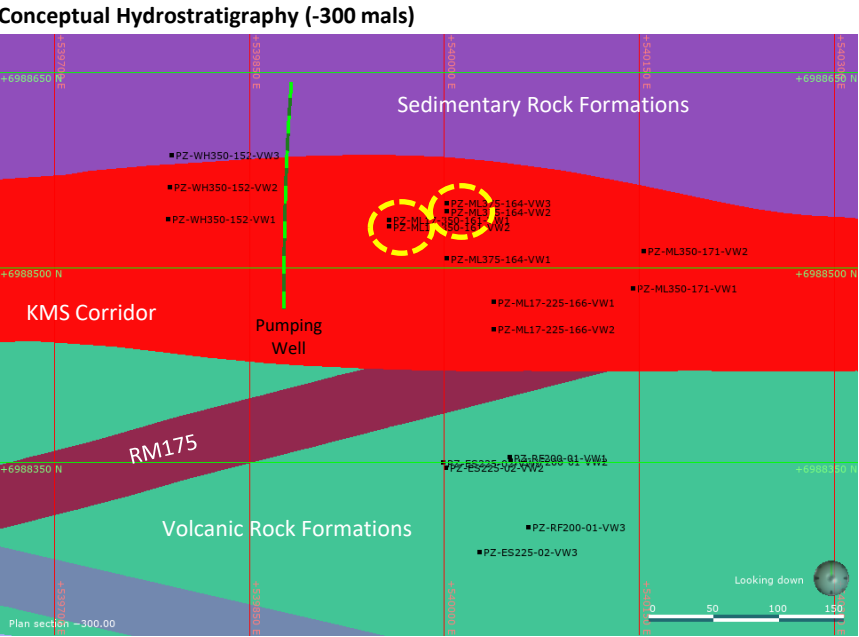
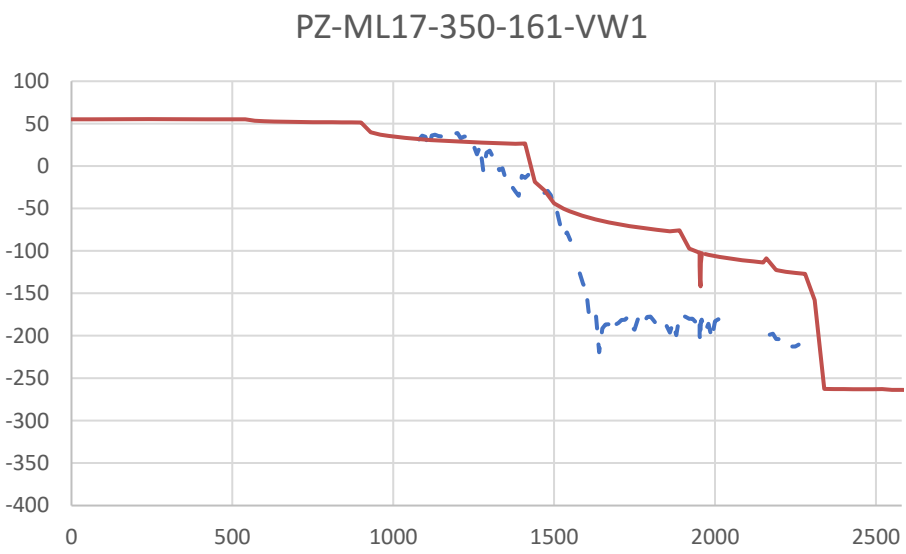
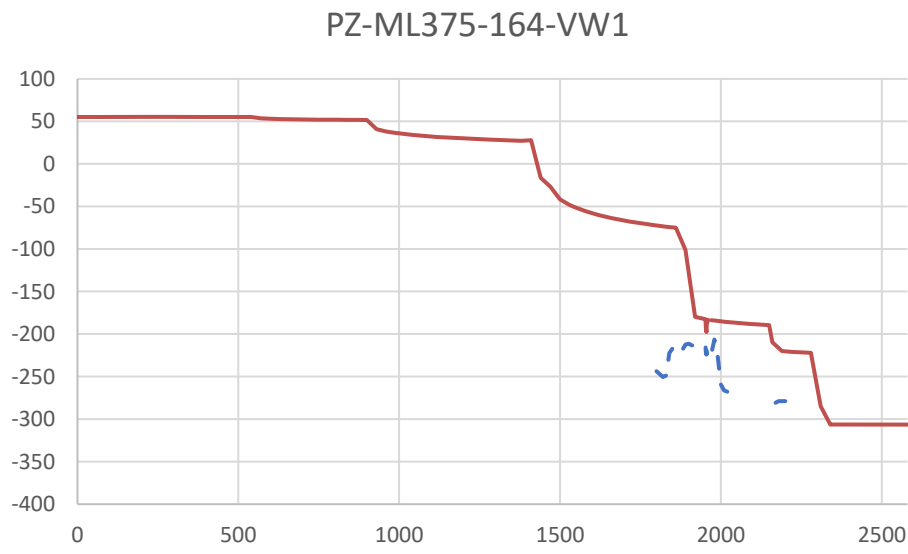
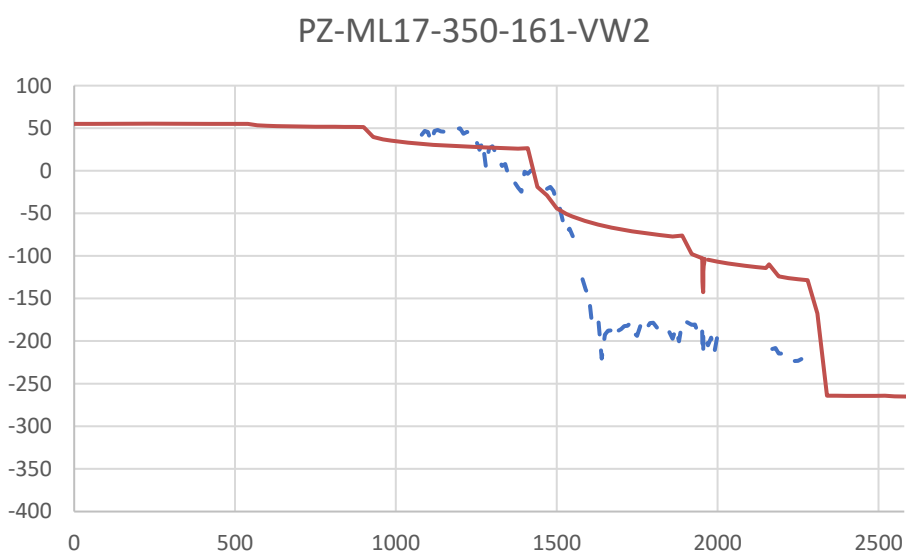


YYYY-MM-DD	2024-01-24
PREPARED	JL
DESIGNED	HG
REVIEWED	JL
APPROVED	DC

PROJECT  
AGNICO EAGLE MINES LIMITED  
MELIADINE MINE  
NUNAVUT

TITLE  
**HYDRAULIC HEAD MONITORING CALIBRATION  
RESULTS - PZ-RF200-01 AND PZ-ES225-02**

PROJECT NO.	PHASE	REV.	FIGURE
CA0020476.6818		0	23



Legend

- Observed
- Predicted

Notes:  
X-axis on plots are model simulation time in days. Day zero corresponds to the start of Year 2015.  
Y-axis on plots are predicted / measured hydraulic head (masl).

Piezometer	Borehole ID	Node	Sensor Elevatin (Mine Grid)	Sensor Elevation (masl)	Approximate Sensor Depth (mbgs)
PZ-ML17-350-161	ML17-350-161-001	VW1	9732	268.40	323.4
		VW2	9732	268.20	323.2
PZ-ML375-164	ML376-164-D1	VW1	9694	306.00	361.0
		VW2	9683	317.00	372.0
		VW3	9681	319.00	374.0

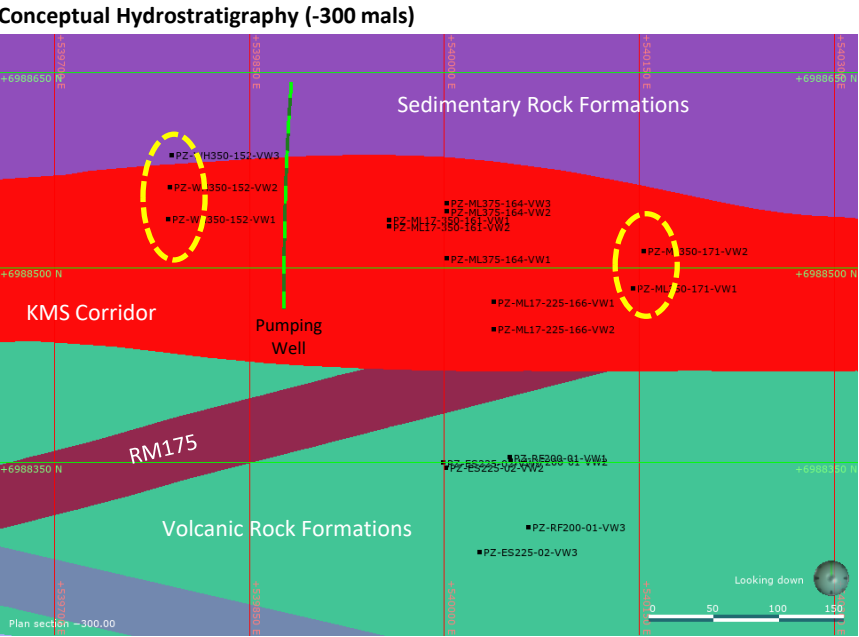
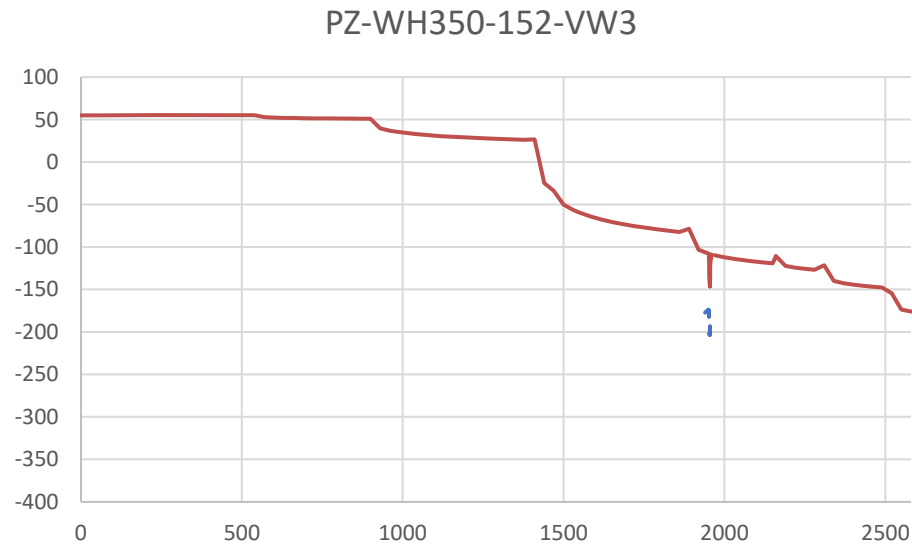
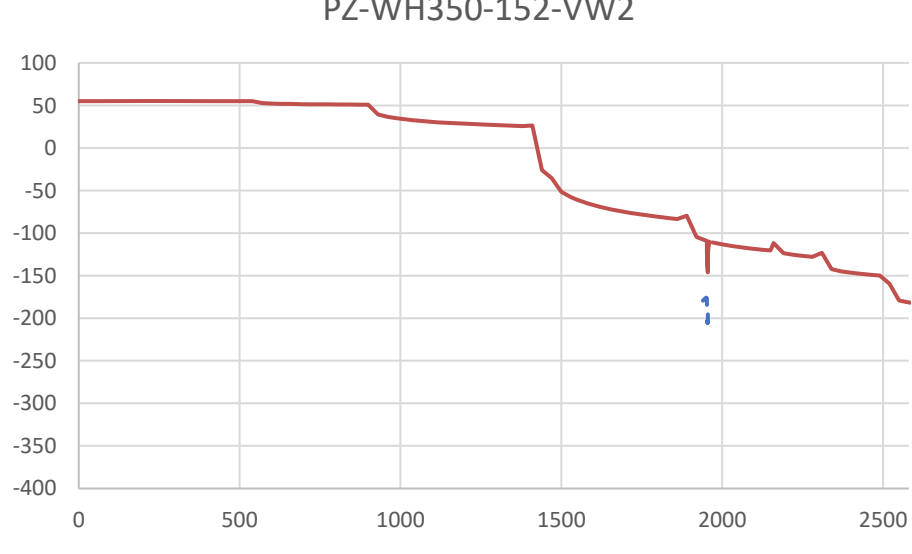
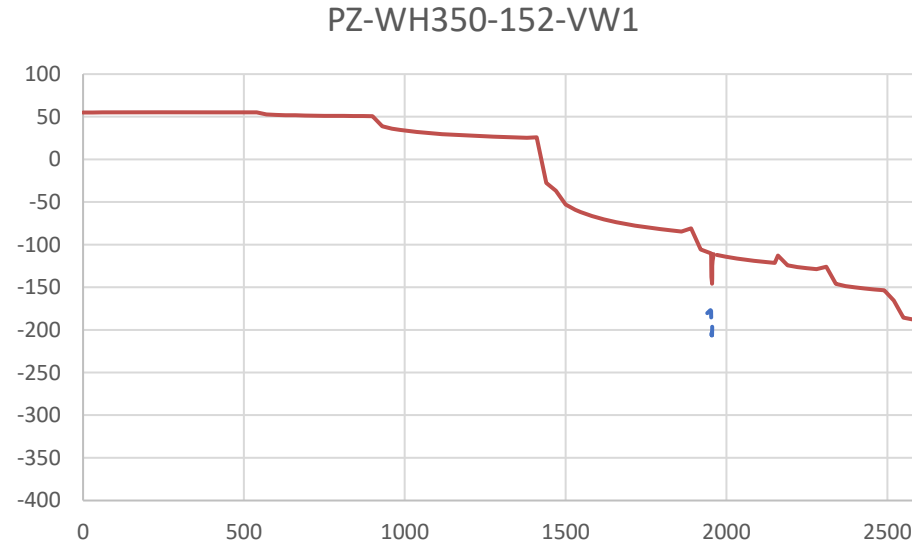
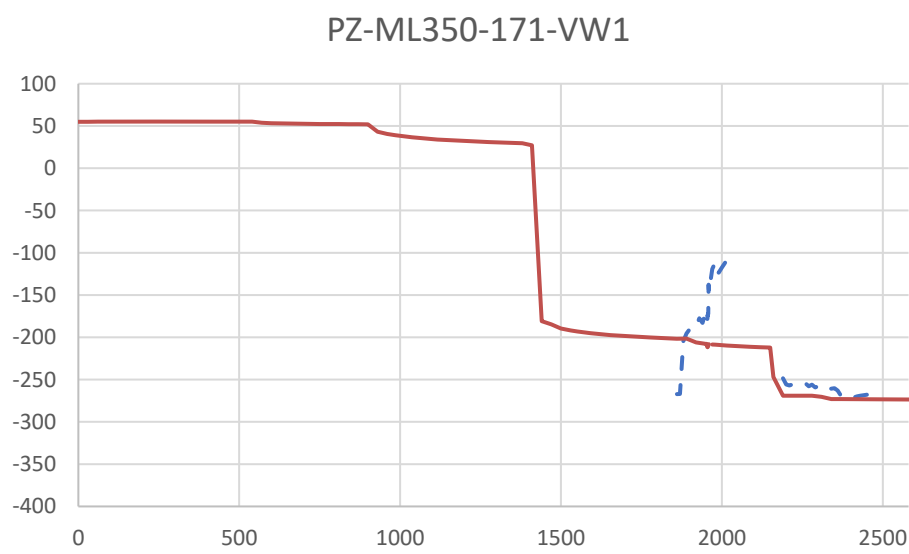


YYYY-MM-DD	2024-01-24
PREPARED	JL
DESIGNED	HG
REVIEWED	JL
APPROVED	DC

PROJECT  
AGNICO EAGLE MINES LIMITED  
MELIADINE MINE  
NUNAVUT

TITLE  
HYDRAULIC HEAD MONITORING CALIBRATION  
RESULTS - PZ-ML177-350-161 AND PZ-ML375-164

PROJECT NO.	PHASE	REV.	FIGURE
CA0020476.6818		0	24



- Legend
- Observed
  - Predicted

Notes:  
X-axis on plots are model simulation time in days. Day zero corresponds to the start of Year 2015.  
Y-axis on plots are predicted / measured hydraulic head (masl).

Piezometer	Borehole ID	Node	Sensor Elevatin (Mine Grid)	Sensor Elevation (masl)	Approximate Sensor Depth (mbgs)
PZ-ML350-171	ML350-171-D1	VW1	9714	286.00	341.0
		VW2	9712	288.00	343.0
PZ-WH350-152	WH350-152-D1	VW1	9724	276.00	331
		VW2	9720	280.00	335
		VW3	9715	285.00	340



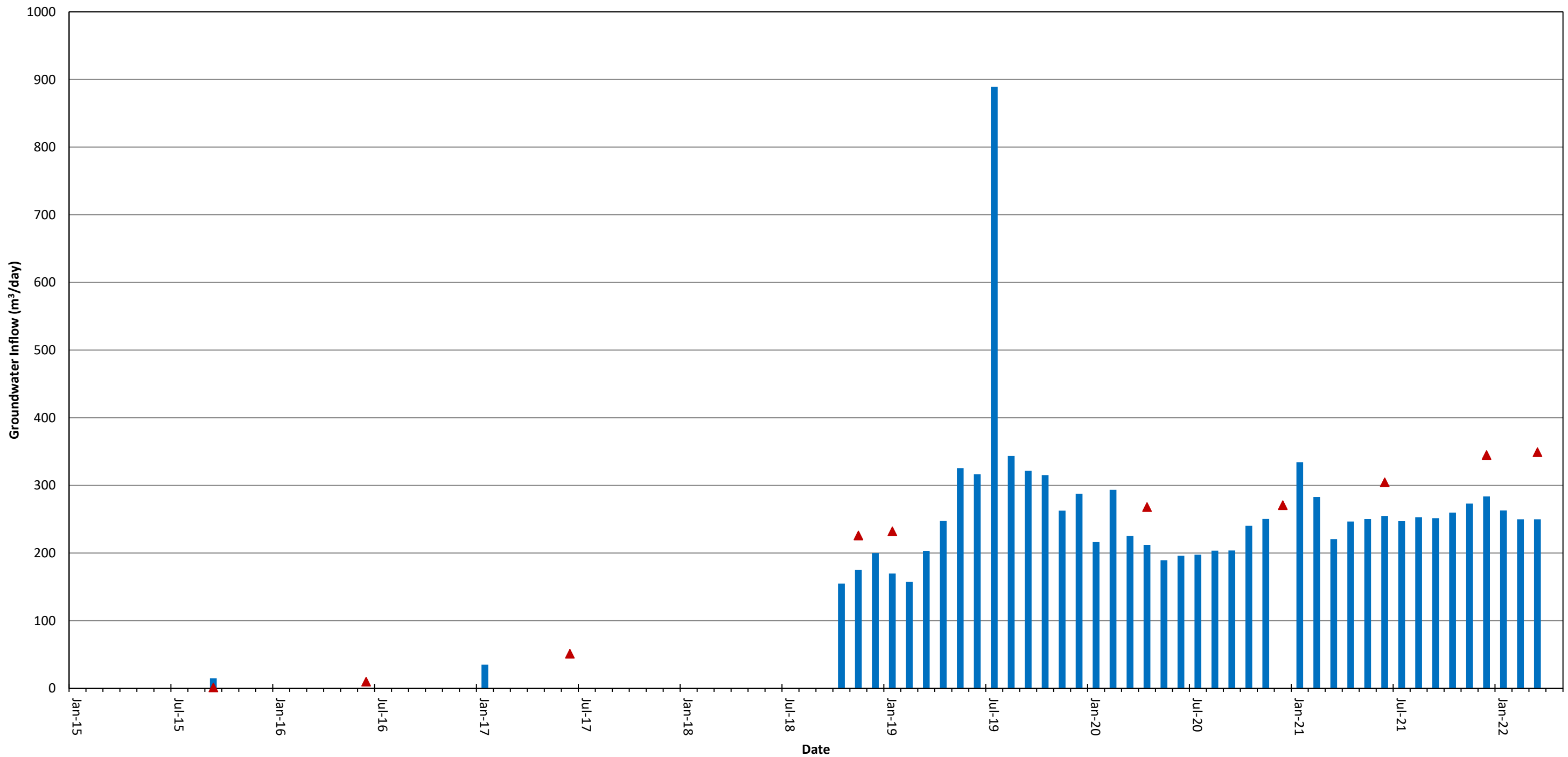
YYYY-MM-DD	2024-01-24
PREPARED	JL
DESIGNED	HG
REVIEWED	JL
APPROVED	DC

PROJECT  
AGNICO EAGLE MINES LIMITED  
MELIADINE MINE  
NUNAVUT

TITLE  
HYDRAULIC HEAD MONITORING CALIBRATION  
RESULTS - PZ-ML350-171 AND PZ-WH350-152

PROJECT NO.	PHASE	REV.	FIGURE
CA0020476.6818		0	25







▲ Predicted Groundwater Inflows

■ Measured Groundwater Inflows

CLIENT

  
**AGNICO EAGLE**

CONSULTANT



PROJECT

AGNICO EAGLE MINES LIMITED  
MELIADINE MINE  
NUNAVUT

TITLE

**MEASURED VERSUS PREDICTED  
GROUNDWATER INFLOW TO TIRIGANIAQ  
UNDERGROUND MINE**

PREPARED

JL

DESIGNED

HG

REVIEWED

JL

APPROVED

DC

PROJECT NO.

CA0020476.6818

PHASE

REV.

0

FIGURE

**26**

25 mm IF THIS MEASUREMENT DOES NOT MATCH WHAT IS SHOWN, THE SHEET SIZE HAS BEEN MODIFIED FROM A3S-B

## 5.0 BASE CASE MODEL PREDICTIONS

The Base Case Scenario represents the best estimate of groundwater inflow and groundwater TDS based on the measured data and the results of the model calibration. Model predictions were therefore undertaken using the base case calibrated model. Agnico Eagle is successfully implementing grouting, and it is a planned mitigation approach going forward. On this basis, grouting of the underground development is assumed to continue as part of future inflow predictions.

### 5.1 Base Case – Predicted Groundwater Inflow

Based on interpreted permafrost limits (WSP 2024a), three pits will intersect open taliks below lakes.

- WN01 is planned to be about 130 m deep with the ultimate base of the pit at -65 masl and is under a portion of Lake B5.
- PUM04 pit is planned to be about 40 m deep with the ultimate pit at -20 masl and is under the southern portion of Lake A8 West.
- Wes03 pit is planned to be about 120 m deep with the ultimate base of the pit at -55 masl and is partially under the north side of Lake A8 West.

Open pit mining commences after the dewatering of adjacent lakes. It is assumed that for one month of the year, dewatering outside of berm pit areas would not keep up with freshet inflows and standing water would be present in the lakes; the remaining 11 months of the year it is assumed that the lake is fully dewatered. With the lake dewatering and the underlying depressurization of the bedrock from mining at TM, inflow to the open pits is only predicted to occur during the one month where lake dewatering is not expected to keep up with freshet inflows. Predicted inflows to WN01 is expected to be less than 25 m<sup>3</sup>/day (average annual) and up to 50 m<sup>3</sup>/day (average annual) at Wes03 and Pum04. As this flow is predicted to occur in one month, the flow during that month will be approximately 12 times higher than the predicted average annual rate. This water would be relatively fresh (low TDS) in comparison to the more saline groundwater being intercepted by the underground. Overall, the predictions indicate that inflow to the pits will be largely controlled by how effectively the lake area is maintained in a dewatered state. If standing water is maintained in the lake footprint a high steady inflow of water to the open pits is likely possible.

Table 6 presents a summary of the predicted groundwater inflow to the TM development during operations for the Base Case, along with the predicted TDS and lake water contributions in the groundwater inflow. The predicted TDS and lake water contributions can be used in the Site Wide Water Quality Model to account for salinity loading from the groundwater, surface water, and other sources from the Project area.

Figure 27 presents the predicted hydraulic heads over the operations period. The predicted groundwater inflows incorporate the effects of grouting. Like the model set-up for calibration, an effective hydraulic conductivity of  $1 \times 10^{-9}$  was assigned to elements representative of grouted faults where the element size was approximately 10 m. In other areas of the model, where the element size increases from 10 m to approximately 25 m the assigned effective hydraulic conductivity was increased to approximately  $3 \times 10^{-9}$  m/s to reflect the larger element size.

Groundwater inflow to TM was predicted to increase from 400 m<sup>3</sup>/day in 2022 to a peak inflow of 1,625 m<sup>3</sup>/day in 2027 (Table 6). Inflows then decrease as storage effects diminish from 2027 to 2037, where the predicted inflow to the underground is 1,450 m<sup>3</sup>/day. Predicted TDS at TM is relatively stable between 50,500 and 58,000 mg/L, reflecting the low intersection of freshwater from the lakes and from shallow groundwater in the open taliks below these lakes. Figure 28 presents the predicted TDS near TM in the final year of mining.

Volcanic Rock Formation (Cryopeg)

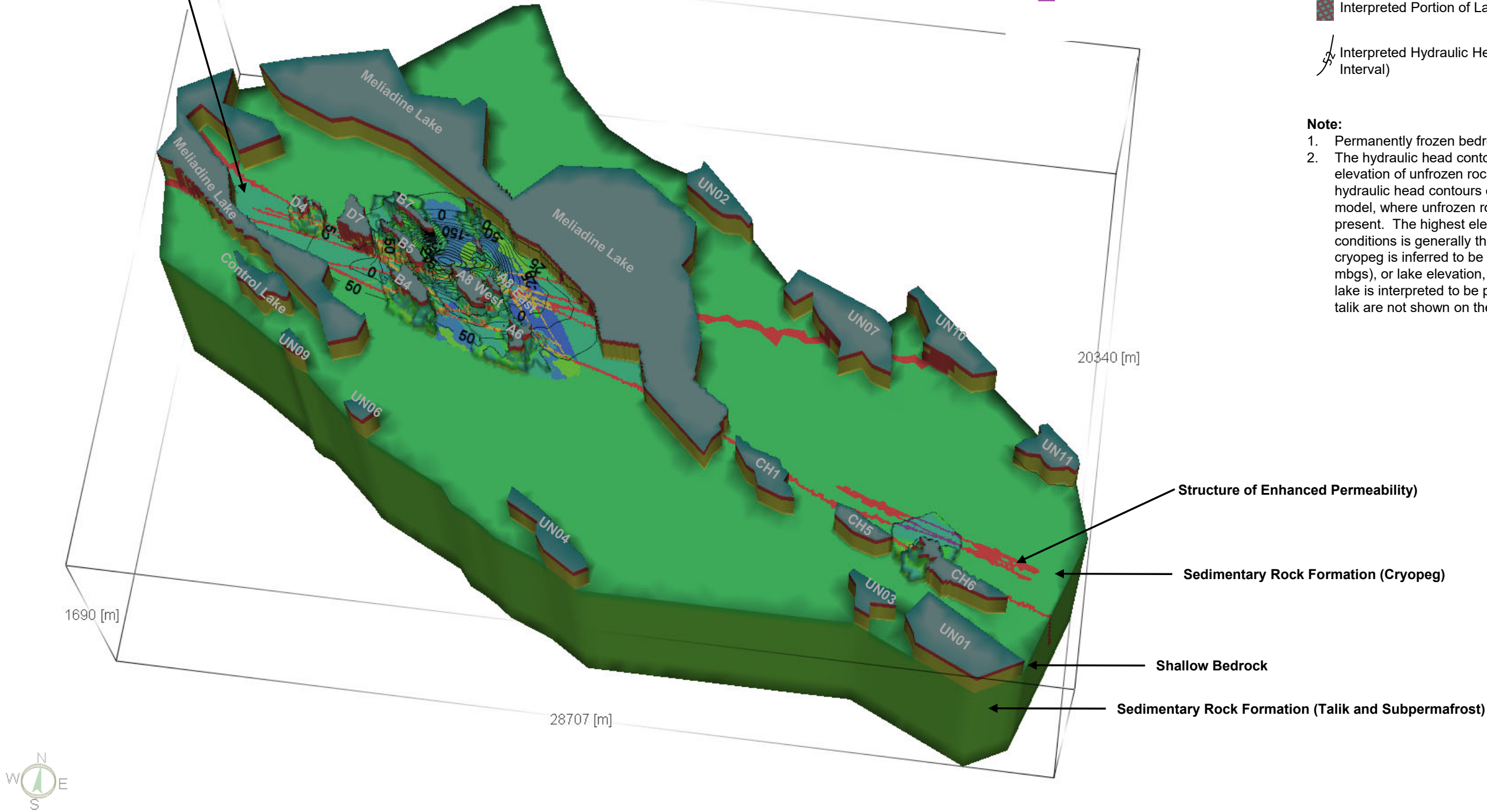
Conductivity: K<sub>xx</sub>  
- Patches -  
[m/s]  
3e-08  
3e-09  
3e-10  
3e-11

Legend

- Inferred Groundwater Flow Direction in Sub-permafrost
- Interpreted Portion of Lake Footprint with Open Talik
- Interpreted Hydraulic Head Contour (masl; 25 m Contour Interval)

**Note:**

1. Permanently frozen bedrock not shown.
2. The hydraulic head contours are shown for the highest elevation of unfrozen rock conditions, along with the hydraulic head contours on the perimeter of the model, where unfrozen rock conditions are present. The highest elevation of unfrozen rock conditions is generally the top of cryopeg where cryopeg is inferred to be present (approximately 280 mbgs), or lake elevation, where open talik below the lake is interpreted to be present. Lakes without open talik are not shown on these figures.



CLIENT  
**AGNICO EAGLE**

CONSULTANT  
**wsp**

YYYY-MM-DD	2024-01-24
PREPARED	JL
DESIGNED	HG
REVIEWED	JL
APPROVED	DC

PROJECT  
AGNICO EAGLE MINES LIMITED  
MELIADINE MINE  
NUNAVUT

TITLE  
**PREDICTED HYDRAULIC HEADS END OF YEAR 2031  
FINAL YEAR OF MINING AT TIRIGANIAQ UNDERGROUND  
MINE**

PROJECT NO.	PHASE	REV.	FIGURE
CA0020476.6818		0	27

5x Vertical Exaggeration

IF THIS MEASUREMENT DOES NOT MATCH WHAT IS SHOWN, THE SHEET SIZE HAS BEEN MODIFIED FROM A3S-B



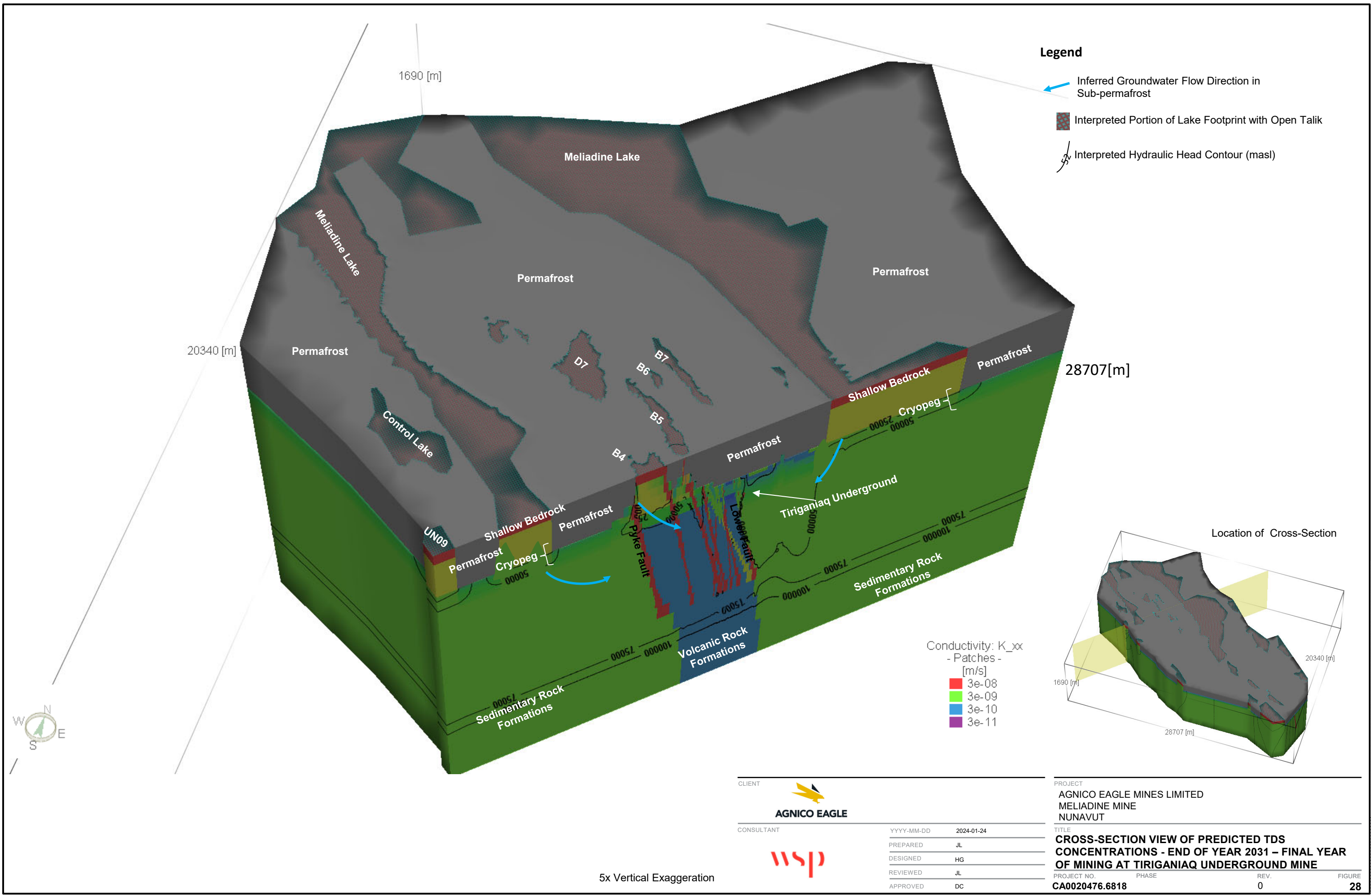


**Table 6: Predicted Groundwater Inflow and TDS Quality to Tiriganiaq Underground Mine – Base Case**

	Predicted Groundwater Inflow (m <sup>3</sup> /day)	Predicted TDS (mg/L)	Predicted Freshwater Lake Contribution (%)	Predicted B4 Contact Water Contribution (%)	Predicted B7 Saline Water Contribution (%)
2022	400	58,000	<1	<1	<1
2023	575	58,000	<1	<1	<1
2024	700	56,500	<1	<1	<1
2025	975	53,500	<1	<1	<1
2026	1,450	50,500	<1	<1	<1
2027	1,625	50,500	<1	<1	<1
2028	1,450	52,500	<1	<1	<1
2029	1,400	54,000	<1	<1	<1
2030	1,350	55,000	<1	<1	<1
2031	1,450	54,500	2	<1	<1



## 5.2 Base Case – Predicted Surface Water – Groundwater Interaction

Table 7 presents a summary of the predicted fluxes between lakes and the underlying groundwater flow system for pre-mining conditions to the end of operations. Predicted fluxes at post closure will be reported on under separate cover. Lakes evaluated in this assessment include:

- Lakes predicted by thermal modelling to have open talik (Lake B5, B5, B7, A6, A8 and CH6) (WSP 2024a).
- Lake D4. Closed talik was interpreted below Lake D4 based on the 0-degree isotherm predicted by thermal modelling (WSP 2024a). Predicted temperatures, however, suggest that the ground below the lake may not be fully frozen in consideration of the groundwater salinity and that the lake may be connected to the regional groundwater flow system through the cryopeg zone.
- Lakes outside of the thermal modelling domain but within the groundwater modelling domain that were interpreted to be potentially wide enough to support open talik (WSP 2024b). These lakes are presented on Figure 4.

Except for lakes near the underground workings (Lakes A6, A8, B4, B5, B7, D4, D7 and Meliadine Lake), the predicted changes in groundwater-surface water interaction are within 1 m<sup>3</sup>/day of pre-mining conditions. Of these lakes, D4, D7 and Meliadine Lake are not planned to be dewatered. The largest change in baseflow for these three lakes is D7 (reduction of 125 m<sup>3</sup>/day), followed by Meliadine Lake (reduction of 75 m<sup>3</sup>/day), located to the east, north and west of the underground workings, and D4 (reduction of 2 m<sup>3</sup>/day). In general, groundwater discharges to surface water in the Project area are expected to be a small component of the annual surface water budget. It is understood from AEM that this will be evaluated under separate cover using the surface water balance and water quality model.

Table 7: Predicted Groundwater-Surface Water Interaction

Simulated Period	Predicted Groundwater-Surface Water Exchange (m³/day); Positive Values = Surface Water Loss to Groundwater Flow System (Outflow); Negative Values = Groundwater Discharge to Surface Water (Inflow)																	
	Pre-Mining	Operations																
		2015	2016	2017	2018	2019	2020	2021	2022	2023	2024	2025	2026	2027	2028	2029	2030	2031
A6	1.4	1.3	1.3	1.3	1.4	1.5	1.6	1.7	1.9	2.0	2.1	2.3	2.7	3.2	-	-	-	-
A8 East	0.5	0.5	0.6	0.7	0.9	1.7	2.3	2.6	3.3	3.8	4.7	-	-	-	-	-	-	-
A8 West	4.6	4.6	4.8	5.7	7.5	12.6	16.1	18.0	23.9	31.1	41.1	-	-	-	-	-	-	-
B4	-0.7	-0.7	-0.7	-0.5	-0.1	1.0	2.0	2.5	4.4	7.2	22.8	34.5	43.0	49.6	55.1	59.4	62.9	66.3
B5	1.3	1.3	1.5	3.1	6.8	19.1	27.0	31.7	56.4	102.2	4.6	-	-	-	-	-	-	-
B6	0.5	0.5	0.5	0.5	0.5	0.6	0.7	0.8	0.0	0.0	0.0	-	-	-	-	-	-	-
B7	2.1	2.1	2.1	2.2	2.3	2.7	3.4	4.1	5.5	6.4	7.9	10.4	14.6	21.0	29.1	37.1	44.2	50.3
CH1	-2.0	-2.1	-2.1	-2.1	-2.1	-2.1	-2.1	-2.1	-2.1	-2.1	-2.1	-2.1	-2.1	-2.1	-2.1	-2.1	-2.1	-2.1
CH5	-0.3	-0.3	-0.3	-0.3	-0.3	-0.3	-0.3	-0.3	-0.3	-0.3	-0.3	-0.3	-0.3	-0.3	-0.3	-0.3	-0.3	-0.3
CH6	4.6	4.6	4.6	4.6	4.6	4.6	4.6	4.6	4.6	4.6	4.6	4.6	4.6	4.6	4.6	4.6	4.6	4.6
Control	0.8	0.8	0.8	0.8	0.8	0.8	0.8	0.8	0.8	0.8	0.8	0.8	0.8	0.8	0.8	0.8	0.8	0.8
D4	0.5	0.5	0.5	0.5	0.5	0.5	0.5	0.6	0.6	0.7	0.8	1.0	1.3	1.7	2.0	2.3	2.6	2.8
D7	1.4	1.4	1.4	1.6	2.2	4.1	6.2	7.4	10.9	15.3	30.6	53.0	70.2	86.0	99.7	110.5	119.3	126.7
Meliadine	-24.7	25.0	25.0	24.8	23.9	21.6	17.9	15.0	-9.8	-7.0	-3.6	0.7	5.5	10.8	17.3	26.2	37.2	49.6
UN01	-7.0	-7.2	-7.2	-7.2	-7.1	-7.1	-7.1	-7.1	-7.1	-7.1	-7.1	-7.1	-7.1	-7.1	-7.1	-7.1	-7.1	-7.1
UN02	2.0	2.0	2.0	2.0	2.0	2.0	2.0	2.0	2.1	2.1	2.1	2.1	2.1	2.1	2.1	2.1	2.1	2.1
UN03	0.3	0.3	0.3	0.3	0.3	0.3	0.3	0.3	0.3	0.3	0.3	0.3	0.3	0.3	0.3	0.3	0.3	0.3
UN04	0.5	0.2	0.2	0.2	0.2	0.2	0.2	0.2	0.2	0.2	0.2	0.2	0.2	0.2	0.2	0.2	0.2	0.2
UN05	0.0	0.0	0.0	0.0	0.0	0.0	0.0	0.0	0.0	0.0	0.0	0.0	0.0	0.0	0.0	0.0	0.0	0.0
UN06	0.8	0.7	0.7	0.7	0.7	0.7	0.7	0.7	0.7	0.7	0.7	0.7	0.7	0.7	0.7	0.7	0.7	0.7
UN07	-1.3	-1.3	-1.3	-1.3	-1.3	-1.3	-1.3	-1.3	-1.3	-1.3	-1.3	-1.3	-1.3	-1.3	-1.3	-1.3	-1.3	-1.3
UN09	1.9	1.8	1.8	1.8	1.8	1.8	1.8	1.8	1.8	1.8	1.8	1.8	1.8	1.8	1.8	1.8	1.8	1.8
UN10	7.1	7.1	7.1	7.1	7.1	7.1	7.1	7.1	7.1	7.1	7.1	7.1	7.1	7.1	7.1	7.1	7.1	7.1
UN11	5.9	5.9	5.9	5.9	5.9	5.9	5.9	5.9	5.9	5.9	5.9	5.9	5.9	5.9	5.9	5.9	5.9	5.9

Note: Lake A6, A8, B6, B6 are dewatered during operations. Flows are only provided for these lakes up the start of dewatering.

## 5.3 Sensitivity Analysis

### 5.3.1 Sensitivity Scenarios

Due to the inherent uncertainty in the subsurface conditions and parameters controlling groundwater flow, uncertainty exists in the model predictions such that the actual inflow could be higher or lower than the Base Case values. This uncertainty was evaluated using sensitivity analysis. As part of this analysis, selected model parameters were systematically varied from the Base Case values, and the results were used to identify the parameters to which predicted groundwater inflow is most sensitive. These included:

- **Bedrock Hydraulic Conductivity** – Hydraulic conductivity of shallow and deep competent bedrock were increased by a factor of two and three from Base Case Values.
- **Specific Storage** – Specific storage of the bedrock was increased by a factor of three from Base Case Values.
- **Presence of Enhanced Permeability Zones** – Hydraulic conductivity of the faults within the model were increased and decreased by a factor of two from Base Case Values.

**Model Boundaries** – Specified head boundaries assigned beneath the permafrost along the perimeter of the model were removed to verify the model limits are set sufficient far enough from the mine developments to not influence model predicted inflow.

### 5.3.2 Sensitivity Results and Selection of Upper Bound Scenario

Figure 29 and Figure 30 presents a summary of the sensitivity results and Table 8 presents a comparison of the total saline groundwater inflow for the peak year of total groundwater inflow (2027). Based on this analysis the following observations are noted:

- Removal of the specified head boundaries from the model perimeter did not alter the groundwater inflow predictions to the mine developments indicating the model boundaries are set sufficiently far enough from the mine developments.
- Groundwater inflow is somewhat sensitive to the assumed properties of the faults. For the peak year of inflow (2027), total saline groundwater inflow was approximately 14% higher than the Base Case assuming a factor of 2 increase in fault hydraulic conductivity. This sensitivity would be higher if grouting of the faults intersected by the underground did not occur. Changes in the fault properties are not recommended for development of an Upper Bound Scenario as the fault properties are already considered to be conservative based on supplemental testing in 2021 (WSP 2024b) and conceptual assumptions of their lateral extents and depths. The faults were also assumed to have enhanced permeability up to 2.5 km away from the TM and open pit developments, and the width of the Lower Fault was increased to between 15 to 20 m to account for potential additional low RQD corridors along its length. These assumptions are considered conservative since the permeability and width of a fault zone can be heterogeneous along strike (Gleeson and Novakowski 2009) resulting potentially in zones of greater hydraulic conductivity along strike over short distances; whereas over longer distances the presence of zones infilled with fault gouge will act to decrease hydraulic connectivity along strike.
- Groundwater inflows are somewhat sensitive to the specific storage of the bedrock. For the peak year of inflow (2027) and assuming a specific storage three times higher than the base case, total saline groundwater inflow was approximately 28% higher than the Base Case predictions. The majority of the development is located within the Mafic Volcanic Rock, for which specific storage has been set in consideration of site-specific testing (flow recession testing in 2015 and 2020; WSP 2024b).

- Total groundwater inflow is most sensitive to the hydraulic properties of the bedrock. For the peak year of inflow (2027) and a factor of 2 increase in bedrock hydraulic conductivity, total saline groundwater inflow was approximately 54% higher than the Base Case. For the peak year of inflow (2027) and a factor of 3 increase in bedrock hydraulic conductivity, total saline groundwater inflow was approximately 102% higher than the Base Case. Groundwater inflows in 2021 for the TM were predicted to be 560 m<sup>3</sup>/day for a factor of 3 increase in bedrock hydraulic conductivity (Figure 31). This flow is unrealistically high in comparison to observed groundwater inflow in 2021 (220 to 335 m<sup>3</sup>/day). This suggests that a factor of 3 increase in bedrock hydraulic conductivity near Tiriganiaq is not reasonable, and that a factor of 2 increase in bedrock hydraulic conductivity would be a more reasonable Upper Bound Prediction. For this sensitivity scenario, TM groundwater inflows were predicted to be 460 m<sup>3</sup>/day, relative to a measured inflow of between 220 to 335 m<sup>3</sup>/day.
- Predicted inflow to the open pits for the sensitivity scenarios ranged up to 50 m<sup>3</sup>/day (average annual) for WN01 and to 150 m<sup>3</sup>/day (average annual) to Wes03. Overall, inflow to the open pits will be most sensitive to the ability to maintain the lakes in a dewatered state, and the hydraulic conductivity of the shallow rock below the lake berms. The inflow is only predicted to occur in the one month of the year where dewatering efforts are assumed to not keep up with freshet inflows to the lake footprint. This water would be relatively fresh (low TDS) in comparison to the more saline groundwater being intercepted by the underground.

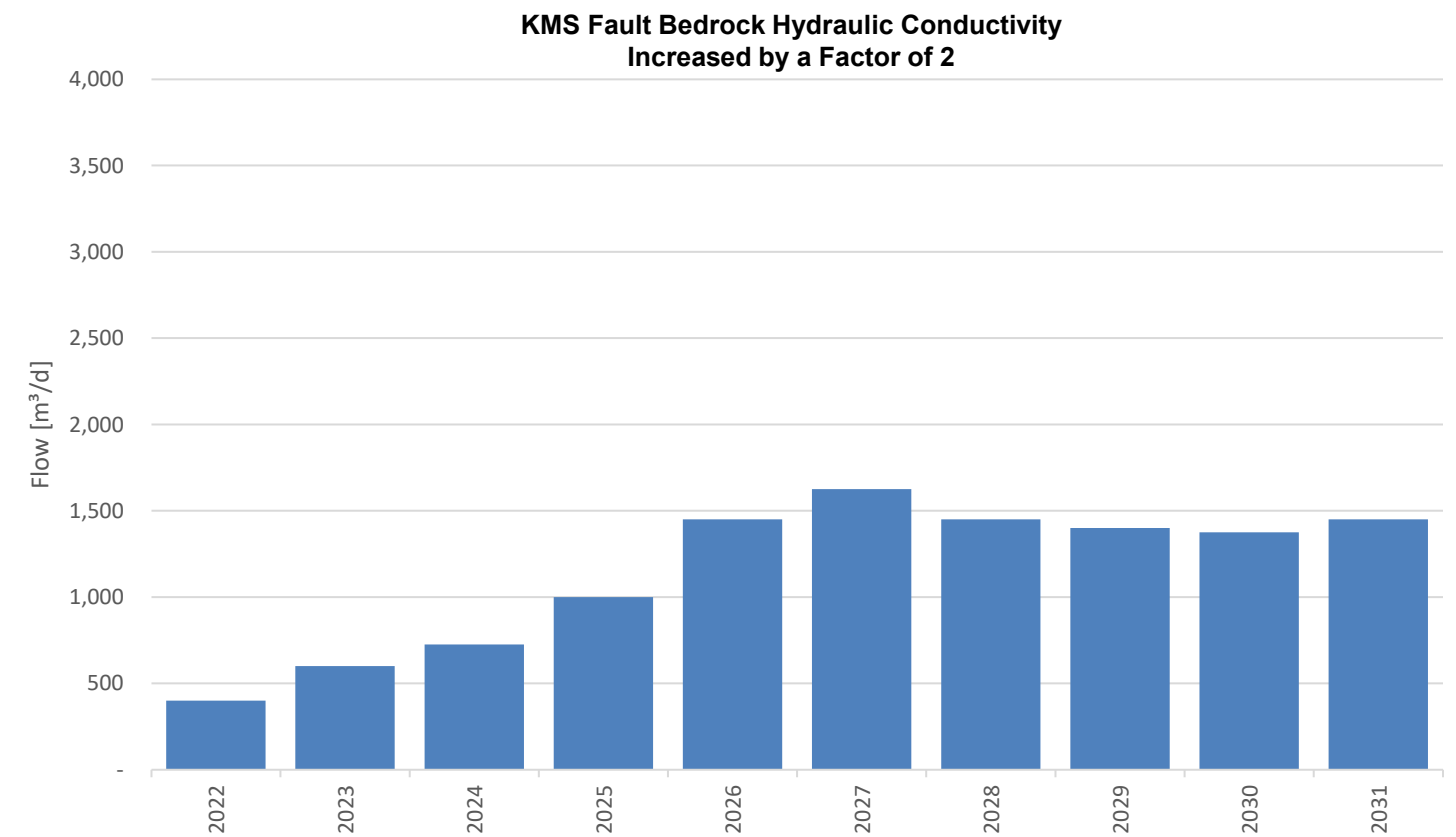
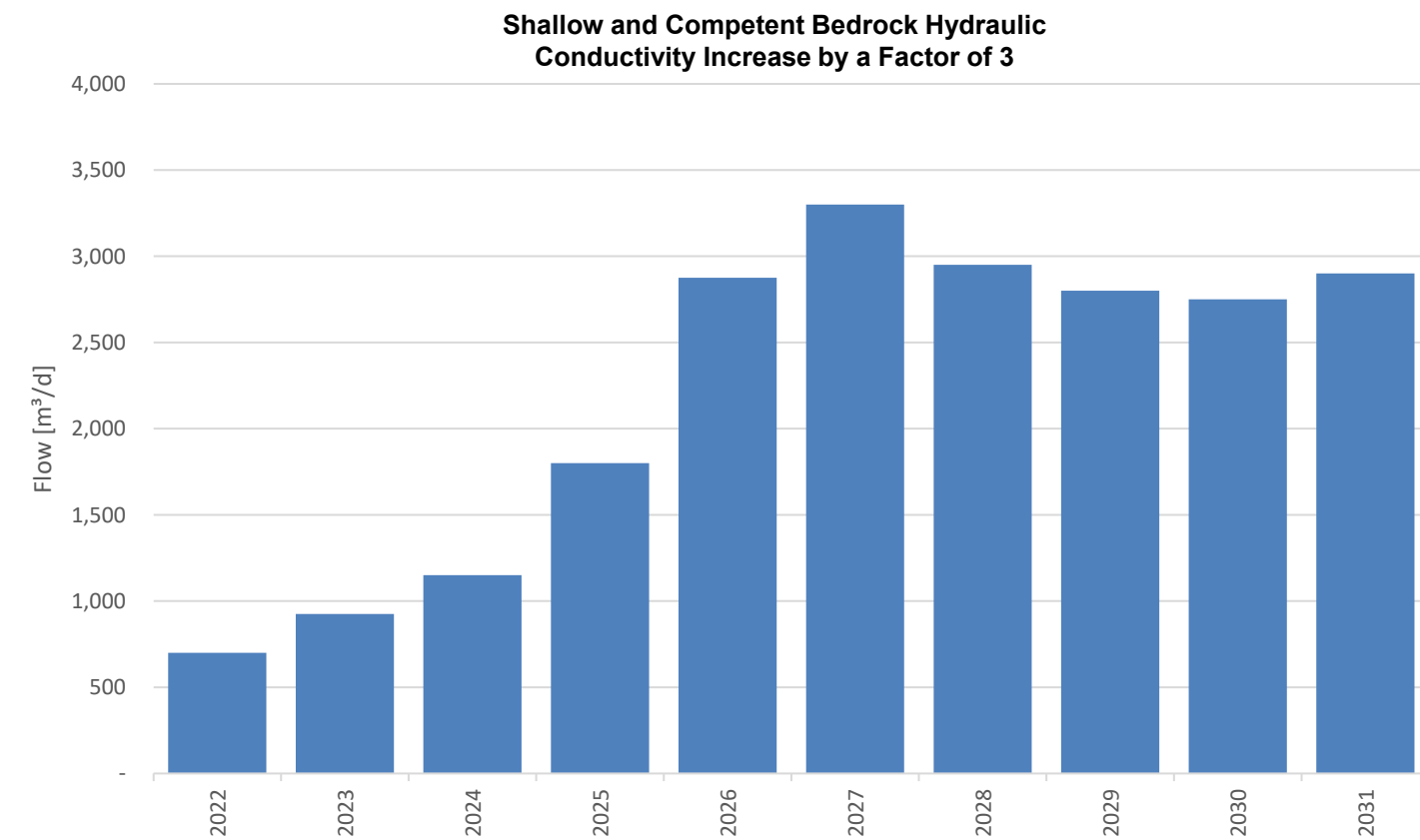
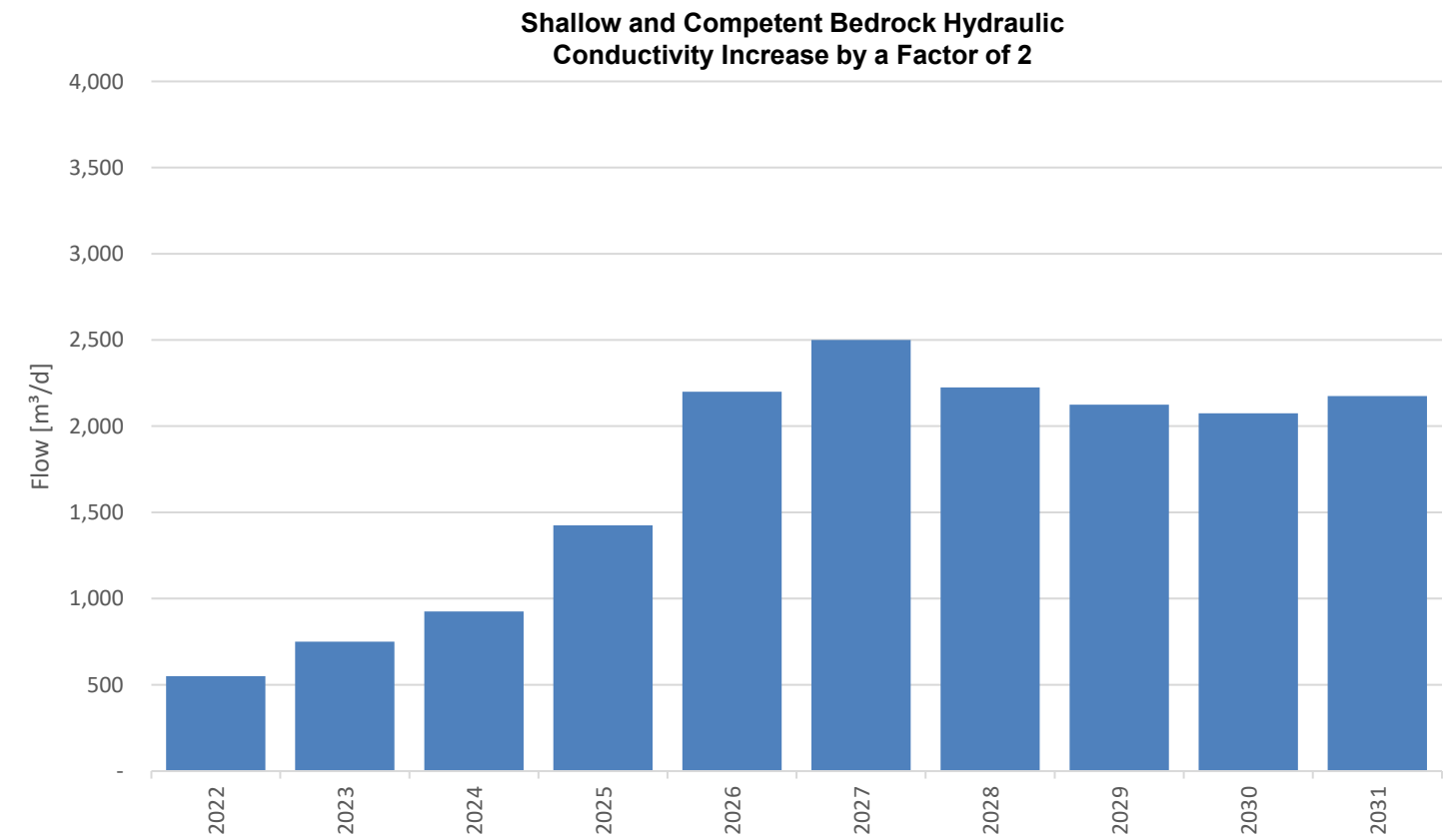
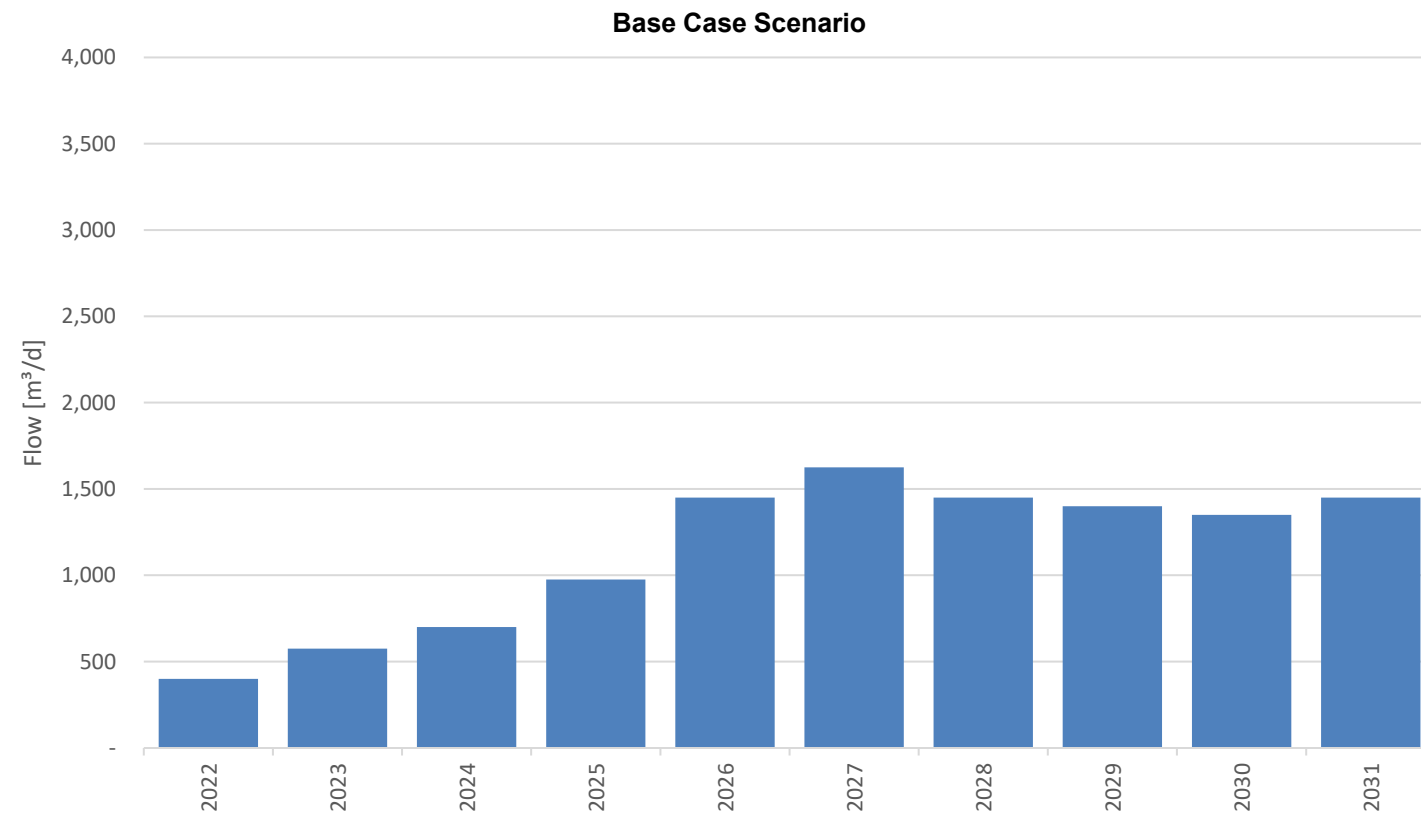
**Table 8: Comparison of Predicted Inflow to Tiriganiaq Underground Mine Year 2027**

Scenario	Change in Hydraulic Conductivity Relative to Base Case	Predicted Inflow Year 2027 (m <sup>3</sup> /day)	% Change from Base Case
Base Case	-	1625	-
Bedrock Hydraulic Conductivity	Factor of 2 Higher	2500	54
	Factor of 3 Higher	3,275	102
KMS Fault Hydraulic Conductivity	Factor of 2 Higher	1625	No Change*
Fault Hydraulic Conductivity	Factor of 2 Higher	1850	14
	Factor of 2 Lower	1475	-9
Specific Storage	Factor of 5 Higher	2075	28

\* Model predictions during the calibration period and in Years 2022 and 2024 had measurable changes in groundwater inflow relative to the Base Case.

Sensitivity results indicate the most sensitive parameter is the bedrock hydraulic conductivity. In consideration of the influence of this parameter on model calibration results, a factor of 2 increase in shallow and deep bedrock hydraulic conductivity was considered appropriate for selection of an Upper Bound Scenario for evaluation of water management at the Project.

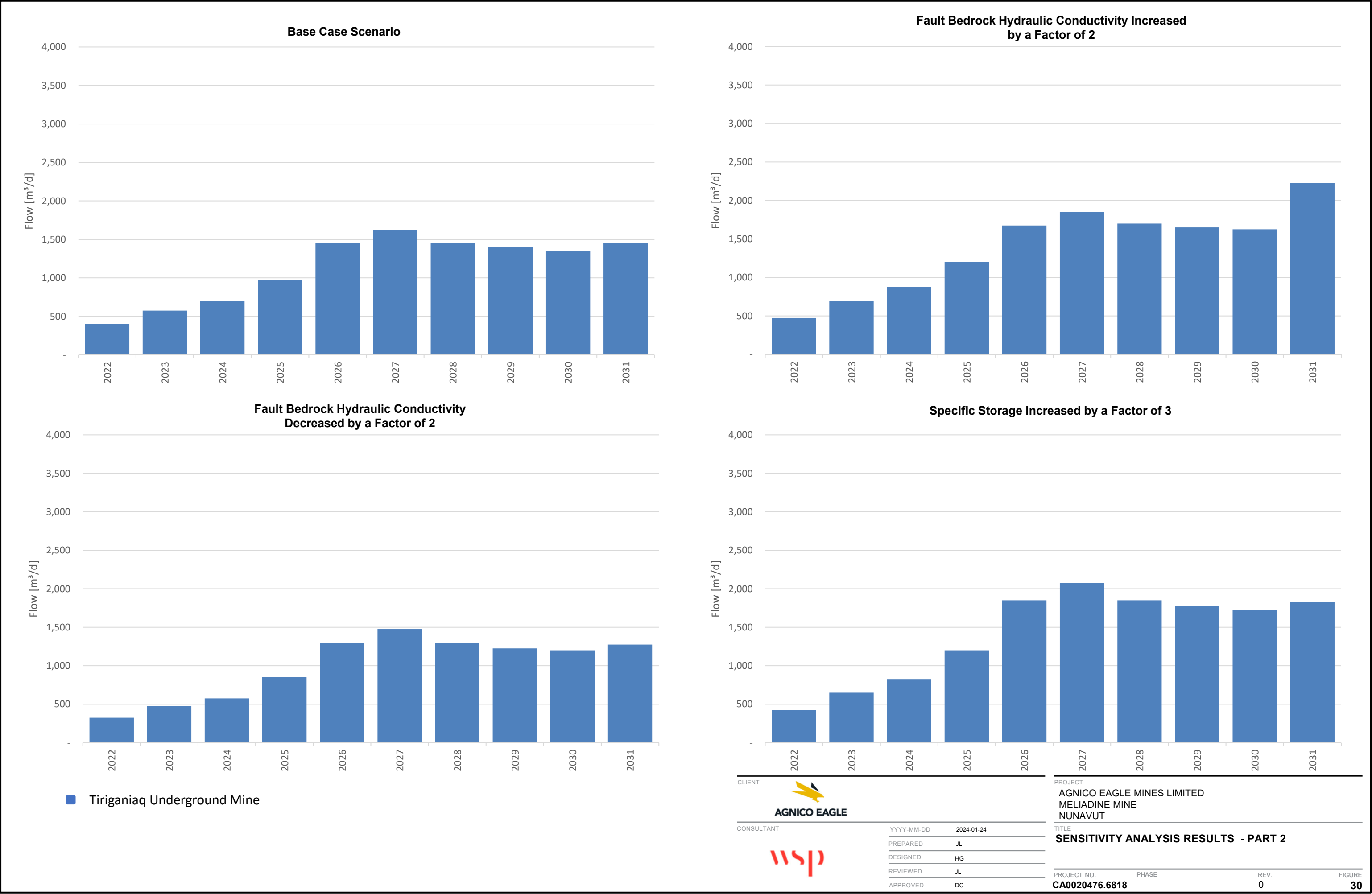
The Upper Bound Scenario is designed to be a reasonable, yet more conservative, assessment of potential groundwater inflow quantity and TDS quality than values that might be adopted for mine operation planning (i.e., Base Case Scenario).



- Tiriganiaq Underground Mine

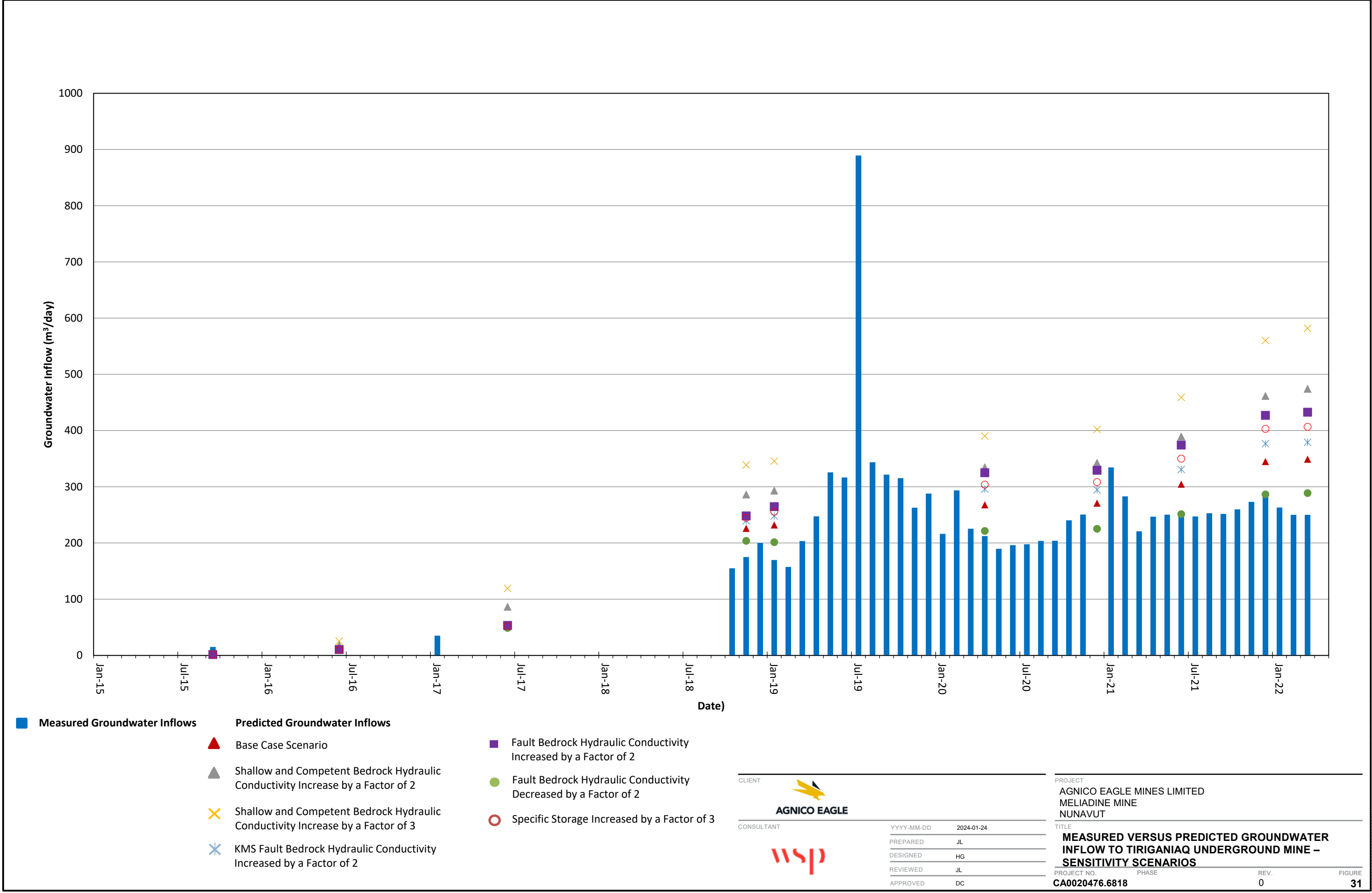






25 mm

IF THIS MEASUREMENT DOES NOT MATCH WHAT IS SHOWN, THE SHEET SIZE HAS BEEN MODIFIED FROM A3S-B



## 6.0 UPPER BOUND PREDICTIONS OF GROUNDWATER INFLOW

Table 9 presents a summary of the predicted groundwater inflow to TM during operations for the Upper Bound Scenario. The predicted groundwater inflows incorporate the effects of grouting.

Groundwater inflow to TM was predicted to increase from 550 m<sup>3</sup>/day in 2021 to a peak inflow of 2,500 m<sup>3</sup>/day in 2027 (Table 9). Inflows then decrease from 2027 to 2031, where the predicted inflow to the underground is 2,175 m<sup>3</sup>/day. Predicted TDS concentrations at TM is similar to the Base Case Scenario and range between 51,500 mg/L and 60,000 mg/L.

Table 9: Predicted Upper Bound Groundwater Inflows – Groundwater Inflow, TDS Quality and Lake Water Contributions

	Predicted Groundwater Inflow (m³/day)	Predicted TDS (mg/L)	Predicted Freshwater Lake Contribution (%)	Predicted B4 Contact Water Contribution (%)	Predicted B7 Saline Water Contribution (%)
2022	550	58,000	<1	<1	<1
2023	750	57,500	<1	<1	<1
2024	925	56,000	<1	<1	<1
2025	1,425	53,000	<1	<1	<1
2026	2,200	51,500	<1	<1	<1
2027	2,500	52,500	<1	<1	<1
2028	2,225	56,000	<1	<1	<1
2029	2,125	58,000	2	<1	<1
2030	2,075	60,000	2	<1	<1
2031	2,175	59,500	3	<1	<1

## 7.0 SUMMARY AND CONCLUSIONS

This report presents the development and calibration of an updated groundwater model for the Project, along with the prediction of groundwater inflow (quantity and TDS quality) for the mine developments located below the permafrost or in open taliks during operations. Relative to the model developed for the FEIS in 2014, the model incorporates supplemental data collection and thermal modelling completed in 2021 and 2022 to reduce uncertainty in model predictions. The model was calibrated to observed conditions since the completion of the FEIS (2015 – early 2022) and to pressure responses observed during a 72-hr flow recession test in 2020.

Base case predictions of total saline groundwater inflow to be managed at TM ranged from 400 m<sup>3</sup>/day in Year 2022, up to a peak inflow of 1,625 m<sup>3</sup>/day in Year 2027. For the Upper Bound predictions, the peak inflow is estimated to be up to 54% higher, with a predicted groundwater inflow of 2,500 m<sup>3</sup>/day.

Except for lakes near the underground workings (Lakes A6, A8, B4, B5, B7, D4, D7 and Meliadine Lake), the predicted changes in groundwater-surface water interaction are within 1 m<sup>3</sup>/day of pre-mining conditions. Of these lakes, D4, D7 and Meliadine Lake are not planned to be dewatered. The largest change in baseflow for these three lakes is D7 (reduction of 125 m<sup>3</sup>/day), followed by Meliadine Lake (reduction of 75 m<sup>3</sup>/day), located to the east, north and west of the underground workings, and D4 (reduction of 2 m<sup>3</sup>/day). In general, groundwater discharges to surface water in the Project area are expected to be a small component of the annual surface water budget. It is understood from AEM that this will be evaluated under separate cover using the surface water balance and water quality model.

Sensitivity analysis indicates that predicted inflows are most sensitive to the hydraulic conductivity of the bulk bedrock, and the upper bound scenario was selected in consideration of these results and model calibration. Conservative assumptions were made with respect to the fault extents and each fault was assumed to have enhanced permeability.

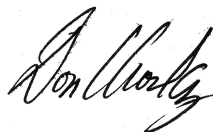
The predictions presented in this report represent the best estimate of the potential range of saline groundwater inflow to be managed at TM based on the conceptual model and data presented in the Updated Existing Conditions Report (WSP 2024b), which includes data up to early 2022. Groundwater inflow predictions should be reviewed as new hydraulic data is collected and as additional operational data is collected against which the model predictions can be verified.



## 8.0 CLOSURE

The reader is referred to the Study Limitations, which follows the text and forms an integral part of this report. We trust the above meets your present requirements. If you have any questions or require addition information, please contact the undersigned.

**WSP Canada Inc.**



Jennifer Levenick, M.Sc., P.Eng  
*Principal, Senior Hydrogeologist*

Don Chorley, P.Geo.  
*Senior Hydrogeology Specialist*

JL/DC/anr/jlb

[https://wsponlinecan.sharepoint.com/sites/ca-ca00204766818/shared documents/05. technical/1\\_gw model report/ca0020476.6818-mel2024\\_004-r-rev0 gw model/ca0020476.6818-mel2024\\_004-r-rev0 gw model\\_24\\_jan2024.docx](https://wsponlinecan.sharepoint.com/sites/ca-ca00204766818/shared%20documents/05.%20technical/1_gw%20model%20report/ca0020476.6818-mel2024_004-r-rev0%20gw%20model/ca0020476.6818-mel2024_004-r-rev0%20gw%20model_24_jan2024.docx)

## REFERENCES

- Agnico Eagle (Agnico Eagle Ltd.). 2014a. Volume 7.0 Freshwater Environmental, Final Environmental Impact Statement (FEIS) – Meliadine Gold Project. Report Number Doc 314-1314280007 Ver. 0. April 2014
- Agnico Eagle. 2014c. Follow-Up of Deep Ground Thermistor Cables at Meliadine – Compilation of the Data from 1998 to 2014. Revision A. October 2014.
- Blowes, D.W. and M.J. Logsdon. 1997. Diavik Geochemistry 1996-1997 Baseline Report. Prepared for Diavik Diamond Mines Inc.
- De Beers (De Beers Canada Inc.). 2010. Environmental Impact Statement for the Gahcho Kue Project. Volumes 1, 2, 3a, 3b, 4, 5, 6a, 6b, 7 and Annexes A through N. Submitted to Mackenzie Valley Environmental Impact Review Board. December 2010.
- Dominion Diamond (Dominion Diamond Ekati Corporation). 2014. Developer's Assessment Report Hydrogeology Baseline Report Annex IX. September 2014.
- Frape, S.K. and P. Fritz. 1987. Geochemical Trends for Groundwaters from the Canadian Shield; in Saline Water and Gases in Crystalline Rocks. Editors: Fritz, P. And Frape, S.K. Geological Association of Canada Special Paper 33.
- Gleeson, T. and K.S. Novakowski. 2009. Identifying watershed barriers to groundwater flow: Lineaments in the Canadian Shield. Geological Society of America Bulletin, 121:333-347.
- Golder (Golder Associates Ltd.). 2016a. Factual Report for Meliadine Project, Nunavut. Hydrogeological Investigation in Support of the Underground Mine Development at Tiriganiaq. Golder Doc. 547-1416135 Ver 0. 18 March 2016.
- Post, B., Kooi, H. and Simmons, C., 2007. Using hydraulic head measurements in variable-density ground water flow analyses. Ground Water, 45(6): 664-671.
- WSP. 2024a. Meliadine Mine – 2022 Thermal Assessment. WSP Doc. 20136436-938-R-Rev1. January 2024.
- WSP. 2024b. Updated Summary of Existing Conditions Meliadine Mine. WSP Doc. 22513890-942-R-Rev1-2000. January 2024.

## STUDY LIMITATIONS

WSP Canada Inc. (WSP) has prepared this document in a manner consistent with that level of care and skill ordinarily exercised by members of the engineering and science professions currently practising under similar conditions in the jurisdiction in which the services are provided, subject to the time limits and physical constraints applicable to this document. No warranty, express or implied, is made.

This document, including all text, data, tables, plans, figures, drawings and other documents contained herein, has been prepared by WSP Golder for the sole benefit of Agnico Eagle Mines Limited. It represents WSP's professional judgement based on the knowledge and information available at the time of completion. WSP is not responsible for any unauthorized use or modification of this document. All third parties relying on this document do so at their own risk.

The factual data, interpretations, suggestions, recommendations and opinions expressed in this document pertain to the specific project, site conditions, design objective, development and purpose described to WSP by Agnico Eagle Mines Limited and are not applicable to any other project or site location. In order to properly understand the factual data, interpretations, suggestions, recommendations and opinions expressed in this document, reference must be made to the entire document.

This document, including all text, data, tables, plans, figures, drawings and other documents contained herein, as well as all electronic media prepared by WSP are considered its professional work product and shall remain the copyright property of WSP. Agnico Eagle Mines Limited may make copies of the document in such quantities as are reasonably necessary for those parties conducting business specifically related to the subject of this document or in support of or in response to regulatory inquiries and proceedings. Electronic media is susceptible to unauthorized modification, deterioration and incompatibility and therefore no party can rely solely on the electronic media versions of this document.



[wsp.com](http://wsp.com)